


การแตกย่อยของนอร์มอลเฮกเซนบนตัวเร่งปฏิกิริยา Ce/ZSM-5



นาย ทศพล เมลืองนนท์

สถาบันวิทยบริการ  
จุฬาลงกรณ์มหาวิทยาลัย

วิทยานิพนธ์นี้เป็นส่วนหนึ่งของการศึกษาตามหลักสูตรปริญญาวิทยาศาสตรมหาบัณฑิต

สาขาวิชาเคมี ภาควิชาเคมี

คณะวิทยาศาสตร์ จุฬาลงกรณ์มหาวิทยาลัย

ปีการศึกษา 2546

ISBN 974-17-5184-2

ลิขสิทธิ์ของจุฬาลงกรณ์มหาวิทยาลัย

# CRACKING OF *n*-HEXANE OVER Ce/ZSM-5 CATALYSTS



**Mr. Tosapol Maluangnont**

สถาบันวิทยบริการ

**A Thesis Submitted in Partial Fulfillment of the Requirements  
for the Degree of Master of Science in Chemistry**

**Department of Chemistry**

**Faculty of Science**

**Chulalongkorn University**

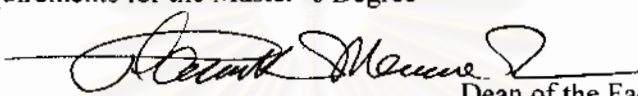
**Academic Year 2003**

**ISBN 974-17-5184-2**

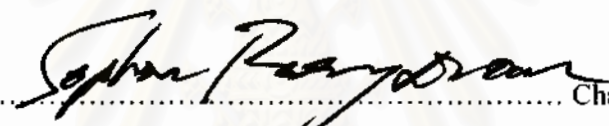
Thesis Title CRACKING OF *n*-HEXANE OVER Ce/ZSM-5  
CATALYSTS  
By Mr. Tosapol Maluangnont  
Field of Study Chemistry  
Thesis Advisor Aticha Chaisuwan, Ph.D.

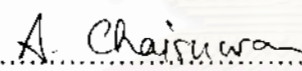
---

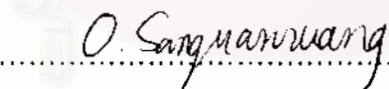
Accepted by the Faculty of Science, Chulalongkorn University in Partial  
Fulfillment of the Requirements for the Master 's Degree

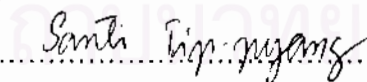
  
..... Dean of the Faculty of Science  
(Professor Piamsak Menasveta, Ph.D.)

THESIS COMMITTEE

  
..... Chairman  
(Professor Sophon Roengsumran, Ph.D.)

  
..... Thesis Advisor  
(Aticha Chaisuwan, Ph.D.)

  
..... Member  
(Oravan Sanguanruang, Ph.D.)

  
..... Member  
(Assistant Professor Santi Tip-pyang, Ph.D.)

นาย ทศพล เมลิองนนท์ : การแตกย่อยของนอร์มอลเฮกเซนบนตัวเร่งปฏิกิริยา Ce/ZSM-5 (CRACKING OF *n*-HEXANE OVER Ce/ZSM-5 CATALYSTS). อ. ที่ปรึกษา : ดร.อิริษา ฉายสุวรรณ. 94 หน้า. ISBN 974-17-5184-2.

ได้สังเคราะห์ซีโอไลต์ชนิด ZSM-5 ( $\text{SiO}_2/\text{Al}_2\text{O}_3$  เท่ากับ 40, หรือ  $\text{Si}/\text{Al}$  เท่ากับ 20) จากเจลที่มีอัตราส่วนโดยโมลเป็น  $1\text{SiO}_2 : 0.36\text{Na}_2\text{O} : 0.025\text{Al}_2\text{O}_3 : 0.10\text{TPABr} : 37.2\text{H}_2\text{O}$  ปรับค่าความเป็นกรดต่างของเจลเป็น 10.5 ด้วยกรดซัลฟิวริกเข้มข้น และตกผลึกที่ 170 องศาเซลเซียสเป็นเวลา 4 วัน ผลิตภัณฑ์ที่ได้เป็นของแข็งสีขาวที่มีพีคการเลี้ยวเบนลักษณะเฉพาะของโครงสร้างเอ็มเอฟไอ สามารถทำซ้ำวิธีสังเคราะห์ได้ในด้านความเป็นผลึกและองค์ประกอบทางเคมี ( $\text{Si}/\text{Al}$  เท่ากับ  $21.0 \pm 1.7$  และ  $\text{Na}/\text{Al}$  เท่ากับ  $1.0 \pm 0.3$ ) ได้ศึกษาเปรียบเทียบการเติม  $\text{Ce}^{3+}$  เข้าใน  $(\text{Na},\text{H})\text{ZSM-5}$  ให้ได้มากที่สุดโดยวิธีสองแบบซึ่งต่างกันในความแรง วิธีที่รุนแรงกว่า คือ มีความเข้มข้นของ  $\text{Ce}^{3+}$  ในสารละลายสำหรับการแลกเปลี่ยนไอออนมาก เวลาทำปฏิกิริยานาน และสภาพการกระตุ้นที่รุนแรงทำให้ซีเรียมเข้าไปในซีโอไลต์ได้มากกว่าอีกวิธีหนึ่ง เตรียม  $\text{HCeZSM-5}$  (หรือ  $\text{HZSM-5}$ ) จาก  $\text{CeNaZSM-5}$  (หรือ  $(\text{Na},\text{H})\text{ZSM-5}$ ) โดยการแลกเปลี่ยนแอมโมเนียมและการกระตุ้นในอากาศ วัสดุที่ได้ยังมีความเป็นผลึกสูง ทำการเร่งปฏิกิริยาการแตกย่อยของไอออนอร์มอลเฮกเซนด้วยตัวเร่งปฏิกิริยาเหล่านี้ที่ 500 องศาเซลเซียส, GHSV เท่ากับ 2000  $\text{h}^{-1}$  และเวลาในการทำปฏิกิริยาเป็น 30 นาที ศึกษาปฏิกิริยาที่เกิดจากความร้อนและที่เร่งด้วย  $\text{CeO}_2$  ด้วย พบว่าไพโรไลซิสของนอร์มอลเฮกเซนไม่มีนัยสำคัญ และโดยส่วนมาก  $\text{CeO}_2$  เปลี่ยนนอร์มอลเฮกเซนเป็นโค้ก  $\text{HZSM-5}$  ให้ค่าการเปลี่ยนแปลงที่สูง ให้ผลิตภัณฑ์โค้กต่ำ และให้ผลิตภัณฑ์โอเลฟินเบา (เอทิลีน โพรพิลีน และไอโซเมอร์ของบิวทิลีน) ในปริมาณที่ยอมรับได้ การปรับปรุงโดย  $\text{Ce}^{3+}$  แสดงว่าซีเรียมเพิ่มแอกติวิตีของ  $(\text{Na},\text{H})\text{ZSM-5}$  อย่างมาก ที่น่าพอใจคือความเลือกจำเพาะต่อโอเลฟิน และมีเอนเพิ่มขึ้นและลดลงตามลำดับโดย  $\text{CeMZSM-5}$  ( $M$  คือ  $\text{Na}^+$  หรือ  $\text{H}^+$ ) เมื่อเทียบกับ  $\text{HZSM-5}$  ได้ผลิตภัณฑ์แก๊ส ของเหลว และโค้กบน  $\text{CeMZSM-5}$  ใกล้เคียงกับบน  $\text{HZSM-5}$  นอกจากนี้สามารถติดตามการเปลี่ยนแปลงเลขออกซิเดชันของซีเรียมจากการสังเกตุสี ซึ่งขึ้นกับบรรยากาศที่ใช้ในการกระตุ้นในขั้นตอนการเตรียมด้วย ค่าการเปลี่ยนนอร์มอลเฮกเซนเพิ่มขึ้น 2 เท่าเมื่อเร่งปฏิกิริยาด้วย  $\text{Ce}^*\text{MZSM-5}$  ที่เผาในแก๊สไนโตรเจน พบว่า  $\text{Ce}^*\text{MZSM-5}$  ให้ผลิตภัณฑ์ของเหลวมากกว่า และผลิตภัณฑ์แก๊สและโค้กน้อยกว่าที่ได้จากทั้ง  $\text{CeMZSM-5}$  และ  $\text{HZSM-5}$  ได้ปริมาณผลิตภัณฑ์โอเลฟินเบาจาก  $\text{Ce}^*(40\%)\text{NaZSM-5}$  และ  $\text{HCe}(62\%)\text{ZSM-5}$  ผลที่ได้มากกว่าค่าที่ได้จาก  $\text{HZSM-5}$  การเกาะของโค้กบนตัวอย่างที่มีซีเรียมมีค่าน้อยกว่า  $\text{HZSM-5}$  (ยกเว้นเพียงตัวอย่างเดียวที่มากกว่า) พบว่าการเพิ่มผลิตภัณฑ์โอเลฟินโดยการแลกเปลี่ยนไอออนซีเรียมเป็นวิธีที่น่าสนใจ

ภาควิชา.....เคมี.....ลายมือชื่อนิสิต..... ทศพล เมลิองนนท์  
 สาขาวิชา.....เคมี.....ลายมือชื่ออาจารย์ที่ปรึกษา..... อิริษา ฉายสุวรรณ  
 ปีการศึกษา..... 2546.....

## 4472273323 : MAJOR CHEMISTRY

KEY WORD: Ce/ZSM-5/ MFI/ RARE EARTHS/ CATALYTIC CRACKING

TOSAPOL MALUANGNONT : CRACKING OF *n*-HEXANE OVER Ce/ZSM-5

CATALYSTS. THESIS ADVISOR : ATICHA CHAISUWAN, Ph.D. 94 pp.,

ISBN 974-17-5184-2.

ZSM-5 typed zeolite ( $\text{SiO}_2/\text{Al}_2\text{O}_3 = 40$ , or  $\text{Si}/\text{Al} = 20$ ) was synthesized from gel having molar composition of  $1\text{SiO}_2: 0.36\text{Na}_2\text{O}: 0.025\text{Al}_2\text{O}_3: 0.10\text{TPABr}: 37.2\text{H}_2\text{O}$ . The gel was subsequently pH-adjusted to 10.5 using concentrated  $\text{H}_2\text{SO}_4$  and was crystallized at  $170^\circ\text{C}$  for 4 days. The product was obtained as white solid having characteristic diffraction peaks of an MFI phase. The synthetic method was found highly reproducible in terms of crystallinity and chemical composition ( $\text{Si}/\text{Al} = 21.0 \pm 1.7$ ,  $\text{Na}/\text{Al} = 1.0 \pm 0.3$ ). Introduction of as high as possible  $\text{Ce}^{3+}$  into  $(\text{Na},\text{H})\text{ZSM-5}$  was comparatively investigated by two methods, which differ in severity. Method with higher severity, *i.e.*, high concentration of  $\text{Ce}^{3+}$  in exchange solution, long reaction time, and harsh activation condition, incorporated more cerium.  $\text{HCeZSM-5}$  (or  $\text{HZSM-5}$ ) was prepared by ammonium exchange plus air-activation of  $\text{CeNaZSM-5}$  (or  $(\text{Na},\text{H})\text{ZSM-5}$ ). The resulting materials still possess relatively high crystallinity. Catalytic cracking of *n*-hexane vapor was performed over these catalysts, at  $500^\circ\text{C}$ , GHSV of  $2000 \text{ h}^{-1}$ , and time-on-steam of 30 min. Thermal and  $\text{CeO}_2$ -catalyzed reactions were also studied. It is found that pyrolysis of *n*-hexane is insignificant, and  $\text{CeO}_2$  mainly converts *n*-hexane to coke.  $\text{HZSM-5}$  gives high conversion, low coke yield, and acceptable selectivity to light olefins (ethylene, propylene, and butenes). Modification by  $\text{Ce}^{3+}$  shows that activity of  $(\text{Na},\text{H})\text{ZSM-5}$  is greatly increased by cerium cations. Selectivity to olefins and methane are satisfactorily increased and decreased, respectively, by  $\text{CeMZSM-5}$  ( $M = \text{Na}^+$  or  $\text{H}^+$ ) better than by  $\text{HZSM-5}$ . Gas, liquid, and coke yields over  $\text{CeMZSM-5}$  are more or less similar to those over  $\text{HZSM-5}$ . Moreover, alternation of cerium oxidation state can be monitored by color change. An oxidation state of cerium depends on an atmosphere used for activation during preparation step. It is found that *n*-hexane conversion increases 2 times when catalyzed by  $\text{N}_2$ -calcined  $\text{Ce}^*\text{MZSM-5}$ . Additionally,  $\text{Ce}^*\text{MZSM-5}$  gives higher liquid yield, lower gas and coke yields compared to both  $\text{CeMZSM-5}$  and  $\text{HZSM-5}$ . An optimum light olefins yield is obtained over  $\text{Ce}^*(40\%)\text{NaZSM-5}$  and  $\text{HCe}(62\%)\text{ZSM-5}$ . These results are higher than those obtained over  $\text{HZSM-5}$ . Coke depositions over cerium-containing samples are (with one exception) lower than those over  $\text{HZSM-5}$ . Improvement of olefins yields by cerium ion exchange is found promising.

Department..... Chemistry..... Student's signature..... T. Maluangnont  
Field of study..... Chemistry..... Advisor's signature..... A. Chaisuwan  
Academic year..... 2003.....

## ACKNOWLEDGEMENTS

The author wishes to express his appreciation to Dr. Aticha Chaisuwan, the thesis advisor, for the assistance, encouragement, and patience during the time when this thesis was carried out. Thanks are also extended to Professor Dr. Sophon Roengsumran, Dr. Oravan Sanguanruang and Associate Professor Dr. Santi Tip-pyang for being members of the thesis committee whose comments are especially helpful. He would like to thank the Thai Silicate Company for supplying the sodium silicate solution, and the Thai Olefins Company for standard mixtures for GC analysis, respectively. Special discount of service cost of analysis from the Scientific and Technological Research Equipment Center, Petroleum and Petrochemical College, and the Metallurgy and Materials Science Research Institute, Chulalongkorn University, and the Department of Scientific Services, Ministry of Science and Technology, are acknowledged.

The author deeply appreciates the research grant from the Graduate School, Chulalongkorn University. The Department of Chemistry, Faculty of Science, Chulalongkorn University, and the Materials Chemistry and Catalysis Research Unit are thanked for granting a position of teaching and research assistants, respectively.

The author would also like to express his deepest gratitude to his parents and family members for their great support and enormous encouragement during the entire study. Finally, his thanks would be given to friends for their friendship and social support during the study.

# CONTENTS

	Page
ABSTRACT IN THAI.....	iv
ABSTRACT IN ENGLISH.....	v
ACKNOWLEDGEMENTS.....	vi
CONTENTS.....	vii
LIST OF FIGURES.....	x
LIST OF TABLES.....	xiii
LIST OF ABBREVIATIONS.....	xiv
<b>CHAPTER I INTRODUCTION</b>	
1.1 Statement of Problems.....	1
1.2 Objectives.....	4
1.3 Related work.....	4
<b>CHAPTER II THEORY</b>	
2.1 Zeolites.....	9
2.1.1 Composition of Zeolites.....	9
2.1.2 Structure of Zeolites.....	11
2.1.3 Shape Selectivity of Zeolites.....	11
2.1.4 Acid Sites of Zeolites.....	13
2.2 Zeolite Synthesis.....	14
2.2.1 Temperature and Time.....	15
2.2.2 Gross Composition.....	15
2.2.3 Hydroxide Concentration.....	17
2.2.4 Original Condition for ZSM-5 Synthesis.....	19

## CONTENTS (continued)

	Page
2.3 Ce <sup>3+</sup> Inside Zeolite: Nature and Catalytic Activity Structure of Zeolites.....	19
2.3.1 Hydroxide Complexes of Ce <sup>3+</sup> and Their Dissociation.....	20
2.3.2 Oxidation of Ce <sup>3+</sup> to Ce <sup>4+</sup> .....	22
2.4 Mechanisms of <i>n</i> -Hexane Transformation.....	24
2.4.1 Carbenium and Alkanium Ions.....	24
2.4.2 Classical (Bimolecular) Mechanism.....	26
2.4.3 Haag-Dessau (Monomolecular) Mechanism.....	26
2.4.4 Oligomeric Mechanism.....	28
<b>CHAPTER III EXPERIMENTS</b>	
3.1 Equipment and Apparatus.....	29
3.2 Chemicals and Gases.....	30
3.3 Synthesis of ZSM-5.....	31
3.4 Organic Template Removal.....	32
3.5 Cerium Ion Exchange.....	34
3.6 Ammonium Ion Exchange.....	35
3.7 Sample Preparation for ICP-AES.....	36
3.8 Catalytic Cracking of <i>n</i> -Hexane.....	36
<b>CHAPTER IV RESULTS AND DISCUSSION</b>	
4.1 As-Synthesized (TPA,Na)ZSM-5.....	38
4.2 Calcined (Na,H)ZSM-5.....	40
4.3 Elemental Analysis of (Na,H)ZSM-5.....	42
4.4 Preparation of HZSM-5.....	43
4.5 Quantitative Analysis of Cerium.....	44
4.6 Preparation of CeNaZSM-5.....	46



## CONTENTS (continued)

	Page
4.6.1 Si/Al and Sodium Content.....	47
4.6.2 Cerium Ion Exchange Level.....	48
4.7 Preparation of <i>H</i> CeZSM-5.....	50
4.7.1 Si/Al and Sodium Content.....	50
4.7.2 Cerium Ion Exchange Level.....	51
4.8 Crystallinity of Cerium-Containing ZSM-5.....	51
4.9 Catalytic Cracking of <i>n</i> -Hexane.....	53
4.9.1 Pyrolysis, CeO <sub>2</sub> and <i>H</i> ZSM-5.....	54
4.9.2 Air-Calcined Cerium-Containing ZSM-5.....	60
4.9.3 N <sub>2</sub> -Calcined Cerium-Containing ZSM-5.....	62
4.10 Active Sites in Ce <i>M</i> ZSM-5: H <sup>+</sup> vs Na <sup>+</sup> .....	64
4.11 Effect of Cerium Loading and Oxidation State (Ce <sup>3+</sup> vs Ce <sup>4+</sup> ).....	66
4.12 Reaction Mechanism.....	69
4.13 Effect of Catalyst Types on Olefins Yields.....	71
<b>CHAPTER V CONCLUSIONS.....</b>	<b>74</b>
<b>REFERENCES.....</b>	<b>76</b>
<b>APPENDICES.....</b>	<b>86</b>
<b>VITAE.....</b>	<b>94</b>

## LIST OF FIGURES

Figure	Page
1.1 Typical once-through pyrolysis yields for various feedstocks.....	2
2.1 Structure of a zeolite. (a) zeolite framework, (b) primary building unit, (c) 12-tetrahedral atoms SBU, (d) chain-type formed from (c), (e) ZSM-5 layer formed from (d), (f) channels system in ZSM-5, (g) straight-, and (h) zigzag channel.....	10
2.2 Three types of shape selectivity in zeolites: (a) reactant, (b) product, and (c) transition-state shape selectivity.....	12
2.3 Acidities in zeolites. (a) calcined zeolite, (b) Brønsted-, and (c) Lewis acid.....	14
2.4 Synthesis of ZSM-5 by different methods. (a) prepared according to Szostak and Thomas, pH: 3.5, Al source: $\text{Al}_2(\text{SO}_4)_3$ ; (b) pH: 10.5, Al source: $\text{Al}_2(\text{SO}_4)_3$ ; (c) pH: 10.5, Al source: $\text{NaAlO}_2$ .....	18
2.5 Hydrolysis of cerium inside a zeolite.....	20
(a) Luminescent excitation spectra of $\text{CeNaZSM-5}$ heated at different temperatures; (b) DRUV-Vis spectra of $\text{CeNaZSM-5}$ with different cerium ion exchange levels.....	23
2.6 Reaction of alkanes over acidic catalysts through (a) bimolecular, (b) monomolecular, and (c) oligomeric mechanism.....	27
3.1 Schematic diagrams of the catalytic apparatus for <i>n</i> -hexane cracking.....	31
3.2 Preparation diagram for the synthesis of ZSM-5.....	32
3.3 Heating programs for (a) template removal, (b) thermal treatment of $\text{Ce}^{3+}$ at a comparatively low temperature, (c) process (b) at high temperature and for ammonia removal, and (d) catalyst regeneration.....	33
4.1 A representative XRD pattern of (a) as-synthesized, and (b) calcined ZSM-5 zeolite.....	39

## LIST OF FIGURES (continued)

Figure	Page	
4.2	Elemental analysis result (wt%) of the different standards: (a) $\text{Al}_2\text{O}_3$ , (b) $\text{CeO}_2$ , and (c) $\text{SiO}_2$ . $\text{SiO}_2(\text{modified}) = 100 - \text{Al}_2\text{O}_3(\text{ICP}) - \text{CeO}_2(\text{XRF})$ .....	45
4.3	Elemental analysis of parent and cerium-containing ZSM-5: (a) Si/Al, (b) wt% $\text{Na}_2\text{O}$ , and (c) percentage cerium ion exchange level. (x1,Na is denoted for parent, calcined (Na,H)ZSM-5 ion exchanged once with $\text{Ce}^{3+}$ , and others are assigned similarly.).....	47
4.4	XRD pattern of (a) parent, calcined (Na,H)ZSM-5, (b) 3-time exchanged CeNaZSM-5, and (c) HCeZSM-5 prepared from (b). .....	52
4.5	<i>n</i> -Hexane conversion over various catalysts. Condition: 0.1 g of a catalyst, reaction temperature of $500^\circ\text{C}$ , GHSV of $2000 \text{ h}^{-1}$ , and time-on-steam of 30 min. Various ion exchange levels are shown in parentheses.....	54
4.6	Selectivity (wt%) to gaseous, liquid, and solid (coke) products over various catalysts: HZSM-5 and $\text{CeO}_2$ (a); and CeMZSM-5 ( $M=\text{Na}^+$ or $\text{H}^+$ ) with various $\text{Ce}^{3+}$ ion exchange levels calcined in air (b), or $\text{N}_2$ (c).....	55
4.7	Gaseous products selectivity (mol%) from various catalysts: thermal reaction, HZSM-5, $\text{CeO}_2$ (a); and CeMZSM-5 ( $M=\text{Na}^+$ or $\text{H}^+$ ) with various $\text{Ce}^{3+}$ ion exchange levels calcined in air (b), or $\text{N}_2$ (c). C <sub>n</sub> and C <sub>n</sub> = are, respectively, paraffin and olefin with n carbon atoms in a molecule.....	56
4.8	Liquid products selectivity (mol%) from various catalysts: thermal reaction, HZSM-5, $\text{CeO}_2$ (a); and CeMZSM-5 ( $M=\text{Na}^+$ or $\text{H}^+$ ) with various $\text{Ce}^{3+}$ ion exchange levels calcined in air (b), or $\text{N}_2$ (c). Key: C <sub>n</sub> and C <sub>n</sub> +: paraffin with n and more than n carbon atoms; Ar: aromatics, including benzene, toluene, xylene, ethylbenzene, 1,2,3-trimethylbenzene and 1,2,4,5-tetramethylbenzene.....	57

## LIST OF FIGURES (continued)

Figure	Page
4.9 Acidity of parent and cerium-containing ZSM-5. Change in pH value of the zeolite slurry. ( $x1, Na$ is denoted for parent, calcined ( $Na, H$ )ZSM-5 ion exchanged once with $Ce^{3+}$ , and others are assigned similarly.).....	65
4.10 Specific surface area (Langmiur) of air- and $N_2$ -calcined $CeMZSM-5$ ( $M = Na^+$ or $H^+$ ).....	67
4.11 Thermal or radical decomposition of $n$ -hexane.....	69
4.12 Catalytic or protolytic decomposition of $n$ -hexane.....	70
4.13 Light olefins yields over various catalysts studied.....	72
4.14 Coke deposition over various catalysts studied.....	73



สถาบันวิทยบริการ  
จุฬาลงกรณ์มหาวิทยาลัย

## LIST OF TABLES

Table	Page
2.1	Factors influencing zeolite crystallization.....14
2.2	The effects of variables in gross composition on the zeolite formation.....16
2.3	Reactant molar ratios claimed for ZSM-5 synthesis.....19
2.4	Lists of reactions of carbenium and alkanium ions.....25
3.1	Ce <sup>3+</sup> and NH <sub>4</sub> <sup>+</sup> ion exchange condition.....34
4.1	Selected 2θ of ZSM-5 with different treatment.....39
4.2	Chemical composition of (Na,H)ZSM-5 and HZSM-5.....43



สถาบันวิทยบริการ  
จุฬาลงกรณ์มหาวิทยาลัย

## LIST OF ABBREVIATIONS

Ar:	Aromatics
C <sub>n</sub> :	Paraffins with n carbon atoms
C <sub>n</sub> <sup>+</sup> :	Olefins with n carbon atoms
DRUV-vis:	Diffuse reflectance ultraviolet visible
EDX:	Energy dispersive X-ray
EXAFS:	Extended X-ray absorption fine structure
GHSV:	Gas-hourly space velocity
HAGO:	Heavy atmospheric gas oil
HVGO:	Heavy vacuum gas oil
ICP-AES:	Inductively coupled plasma-atomic emission spectroscopy
IR:	Infrared
LAGO:	Light atmospheric gas oil
MASNMR:	Magic angle spinning nuclear magnetic resonance
MTO:	Methanol-to-Olefin
NMR:	Nuclear magnetic resonance
RE:	Rare earth
SBU:	Secondary building unit
SEM:	Scanning electron microscopy
TPA <sup>+</sup> :	Tetrapropyl ammonium cation, (n-C <sub>3</sub> H <sub>7</sub> ) <sub>4</sub> N <sup>+</sup>
TPD:	Temperature programmed desorption
USY:	Ultra-stabilized Y zeolite
UV:	Ultraviolet visible
XPS:	X-ray photoelectron spectroscopy
XRD:	X-ray diffraction
XRF:	X-ray fluorescence

# CHAPTER I

## INTRODUCTION

### 1.1 Statement of Problems

High standard of living in the late twentieth century is due to the development in petroleum industries, of which products are utilized as fuels, transportation fuels, chemicals, and plastics.<sup>1</sup> Among them, light olefins are of considerable importance since they are raw materials for manufacturing chemicals and polymers. For example, ethylene is used for production of ethylene oxide, ethanol, ethylbenzene, and polyethylene;<sup>2</sup> and propylene is used for production of propylene oxide, propanol, cumene, and polypropylene.<sup>3</sup> They are, however, very rare or absent in natural sources and their preparations are needed.

The major industrial source of ethylene and propylene comes from pyrolysis (or thermal cracking) of either single- or multicomponent feedstocks based on a hydrocarbon complex mixture called petroleum.<sup>1,2</sup> In this process, hydrocarbons are broken down into smaller ones by thermal energy. High temperature (750-900°C), short residence time (0.1-0.6 s), and low hydrocarbon partial pressure are required for the highly selective production of olefins, together with minimum methane production and minimum deposition of carbonaceous materials called coke. The process is highly endothermic and occurs *via* free-radical mechanism. Selected results of once-through pyrolysis yields (wt%) for selected feedstocks are shown in Figure 1.1.<sup>2</sup>

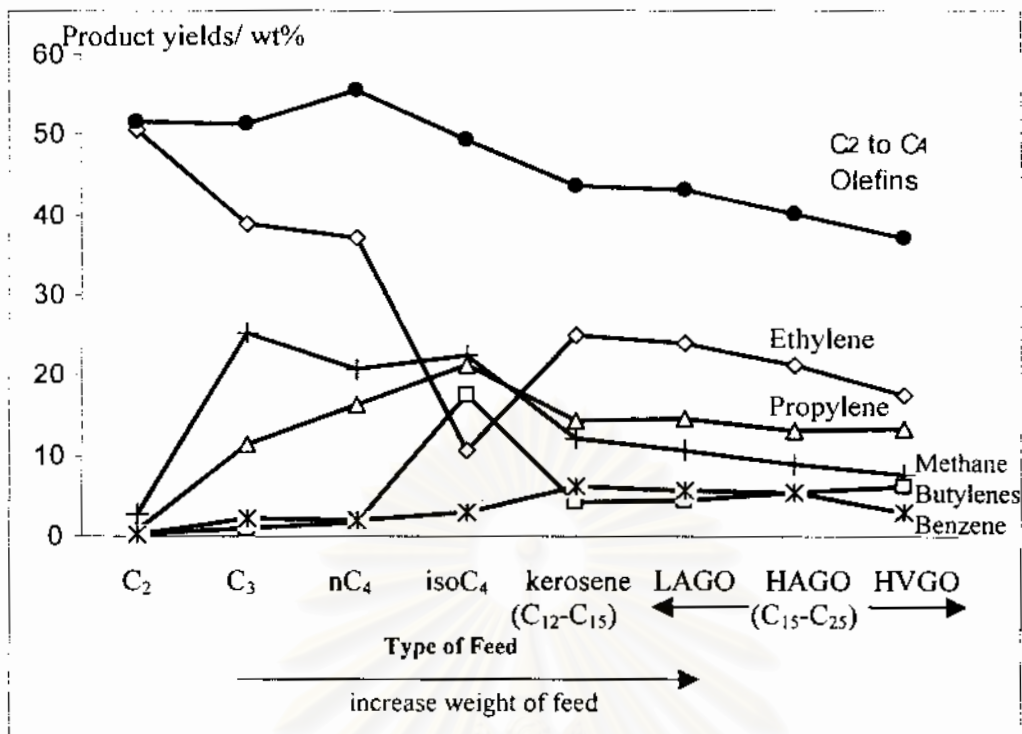


**Figure 1.1** Typical once-through pyrolysis yields for various feedstocks. Key: C<sub>2</sub>: ethane; C<sub>3</sub>: propane; nC<sub>4</sub>: *n*-butane; isoC<sub>4</sub>: isobutane; LAGO: light atmospheric gas oil; HAGO: heavy atmospheric gas oil; HVGO: heavy vacuum gas oil. See ref 2 for more complete product analysis.

For single-component feedstocks from ethane to isobutane, olefins yield (summation of ethylene, propylene, and butylenes) ranges from 51.5 to 49.4% by weight. Specifically, the amount of ethylene decreases, whereas those of propylene and butylenes increase. The undesired product, methane, ranges from 3-25 wt%. The amount of benzene is low. For multicomponent feedstocks, moving from light (kerosene, C<sub>12</sub>-C<sub>15</sub>) to heavy (HVGO) ones results in slightly lower olefins yield of 43.7 to 30.9 wt%. Less ethylene, propylene, and methane, and slightly higher benzene yield are observed in this case compared to single-component feedstocks (excluding isobutane feed which produces higher butylenes). The difference is due to the complexity of reaction network taking place during pyrolysis as a result of the diversity in the structure and chemistry of starting materials. Pyrolysis, however, has problems such as high energy input (hence high operation cost), and excessive coke generation (hence requiring frequent regeneration).<sup>1,2</sup> Solutions are therefore searched, and catalytic cracking is the answer.



From the above discussion, olefins production from single-component feedstocks is clearly preferred, because they provide large amount of light olefins. Cerium-based catalyst is one of the most promising systems for producing olefins from saturated hydrocarbons. However, few works appear regarding the use of cerium on shape-selective catalysts as zeolites, especially ZSM-5 type.<sup>4</sup> Therefore, in this work *n*-hexane is selected as a model compound, and its pyrolysis is studied and compared to catalytic cracking producing light olefins over cerium-containing ZSM-5 zeolites. The characteristic feature of ZSM-5 in favoring olefins formation was combined together with cerium. Catalytic activity and product distribution obtained from Ce<sup>III</sup>-ZSM-5 containing either Na<sup>+</sup> or H<sup>+</sup> as a co-counter cation will be compared.

Production of small olefins over CeO<sub>2</sub> was reported for ethane,<sup>5-7</sup> propane,<sup>8-10</sup> and isobutane.<sup>11</sup> However, there is no report concerning olefins production from larger hydrocarbons such as *n*-hexane. Relevant studies include *n*-hexane combustion over CeO<sub>2</sub>,<sup>12</sup> and over a cerium-containing mesoporous material CeMCM-41.<sup>13</sup> Transformation of *n*-hexane to its branched isomers, methylcyclopentane, benzene, and products with less than six carbon atoms, in which there were no olefins, was reported over Pt supported on CeO<sub>2</sub>.<sup>14</sup> Ce<sub>2</sub>O<sub>3</sub> is thermodynamically unstable toward air oxidation, and is progressively transformed to CeO<sub>2</sub> at O<sub>2</sub> partial pressure as low as 10<sup>-40</sup> atm.<sup>15</sup> Therefore direct comparison of Ce<sup>3+</sup>-ZSM-5 with Ce<sub>2</sub>O<sub>3</sub> is unavailable. The comparative study was carried out with commercial CeO<sub>2</sub> instead. Additionally, activation of the cerium-containing ZSM-5 was performed at both aerobic and anaerobic condition to compare the role of Ce<sup>3+</sup> and Ce<sup>4+</sup> species in a catalyst.

## 1.2 Objectives

1. To synthesize ZSM-5 typed zeolite with the Si/Al molar ratio of 20, and to convert it into a cerium-containing form.
2. To evaluate the developed Ce-containing ZSM-5 catalysts for catalytic cracking of *n*-hexane compared to commercial CeO<sub>2</sub> catalyst.
3. To optimize olefin yields obtained over these invented catalysts by investigating the following factors: content and oxidation state of cerium, and effects of cocations (H<sup>+</sup> vs Na<sup>+</sup>).

## 1.3 Related Work

Cerium has been used as a commercial catalyst, Ce/Fe/K oxide system, in production of styrene from ethylbenzene.<sup>15,16</sup> The C<sub>2</sub>H<sub>5</sub> fragment in ethylbenzene is dehydrogenated into the C<sub>2</sub>H<sub>4</sub> fragment in styrene. Two mechanisms were proposed.<sup>15,16</sup> In Ce<sup>4+</sup> mechanism, O<sup>2-</sup> of iron oxide abstracted β-hydrogen of ethylbenzene, forming adsorbed π-complex. As a result, Fe<sup>3+</sup> was reduced to Fe<sup>2+</sup>, which was oxidized to its original oxidation state by migration of lattice oxygen from CeO<sub>2</sub>. Partially reduced CeO<sub>2</sub>, *i.e.*, CeO<sub>2-x</sub>, was in turn oxidized by water in the feed. Therefore in Ce<sup>4+</sup> mechanism, this 4+ oxidation state is important because cerium in this state is able to supply its lattice oxygen to iron component. In Ce<sup>3+</sup> mechanism, on the other hand, the α-hydrogen of ethylbenzene attacked the acid site (Fe<sup>3+</sup>), while simultaneously the β-hydrogen directly attacked the basic site (Ce<sup>3+</sup>). Gaseous H<sub>2</sub> was liberated with the formation of styrene. Cerium with 3+ oxidation state was the active component itself.

A Ce-based material (Ce/O/F) is one of a catalyst providing best yields of propylene from dehydrogenation of propane *in the presence of O<sub>2</sub>* (oxidative dehydrogenation).<sup>8,17</sup> Zhang *et al.*<sup>8</sup> found that when a mixture of 1CeO<sub>2</sub>/2CeF<sub>3</sub> (mole ratio) was stirred to paste,

dried, calcined at 850°C for 2 h, and tested at reaction temperature of 500°C, the conversion of propane was 41.3%, the selectivity to propylene was 81.1%, giving propylene yield as high as 33.5%. This was one of the best yields reported in the literature.<sup>17</sup> In this system,<sup>8</sup> only cubic CeO<sub>2</sub> was found by X-ray diffraction measurement (XRD) in 1CeO<sub>2</sub>/2CeF<sub>3</sub> catalyst, though its lattice constant increased slightly. Solid state anion exchange of F<sup>-</sup> (r = 1.33 Å) with O<sup>2-</sup> (r = 1.32 Å) expanded CeO<sub>2</sub> lattice, since two larger F<sup>-</sup> anions were required to substitute for one smaller O<sup>2-</sup> anion. The melting of CeF<sub>3</sub> into CeO<sub>2</sub> changed the basicity of CeO<sub>2</sub>. However, the authors did not discuss the possibility that Ce<sup>3+</sup> in CeF<sub>3</sub> might migrate into, or exchange with Ce<sup>4+</sup> in, CeO<sub>2</sub>, and that it would be this Ce<sup>3+</sup> which was the active component.

However, in the oxidative dehydrogenation of propane catalyzed by Ce/Ni oxide studied by Jalowiecki-Duhamel *et al.*,<sup>9</sup> they found that besides characteristic peaks of Ce<sup>4+</sup>, those of Ce<sup>3+</sup> were detected by X-ray photoelectron spectroscopy (XPS) in a catalyst reduced *in situ*, along with an increase in propylene selectivity by a factor of 2 at the same conversion compared to the unreduced one. In oxidative dehydrogenation of ethane to ethylene, Sugiyama *et al.*<sup>5</sup> found that the conversion of ethane and the selectivity to ethylene were greatly enhanced over CeO<sub>2</sub> catalyst operated in the presence of CCl<sub>4</sub>, compared to that in the absence of CCl<sub>4</sub>. They suggested an existence of Ce<sup>3+</sup> in the form of CeOCl which was responsible for this enhancement. Similar improvement of Ce<sup>3+</sup> and Cl<sup>-</sup> was observed in SrCl<sub>2</sub>-promoted CeO<sub>2</sub>,<sup>6</sup> also in oxidative dehydrogenation of ethane. In all cases above, an exact conclusion cannot be drawn whether the improvement is due to Ce<sup>3+</sup> alone or to Ce<sup>3+</sup> in combination with Ce<sup>4+</sup>, since they coexist in all systems mentioned.

Zeolites have been used as catalysts for production of olefins through their cracking property.<sup>1</sup> To function as a cracking catalyst, a material must possess acidic properties (Brønsted or Lewis sites). Examples are AlCl<sub>3</sub>, acidic clays, amorphous silica-alumina, and since 1960 zeolites. The latter includes rare earth-containing X and Y (REX and REY), USY, and recently ZSM-5 in small amount, *i.e.*, up to 3%, in conjunction with zeolite Y. Catalytic cracking is of crucial importance primarily in gasoline (C<sub>4</sub>-C<sub>12</sub>) production.<sup>1</sup> The process

operates at 400-500°C, and slightly above atmospheric pressure. Conversions up to 80-90% with low gas and coke yield, and with better quality gasoline production are obtained.

Historically, a hydrogen form of USY zeolite (*HUSY*) produces large amount of olefins and is a low-coke selectivity catalyst.<sup>18</sup> Its disadvantage is the low cracking activity. Incorporation of 0.5-1 wt% (usually in the form of *mixed*) rare earth elements enhances the activity and hydrothermal stability, at the expense of olefins yield. For example, composition of alkenes in the C<sub>5</sub>-C<sub>10</sub> fraction of gasoline, from catalytic cracking of Arabian Heavy Flashed Distillate at 520°C, was reported to be 46.7 and 44.5 wt% for USY and *REUSY*, respectively.<sup>18</sup> Therefore, the gain in feed conversion must be kept in mind together with the loss in olefins selectivity. For all *RE*-containing USY zeolites, *RE* cations were often introduced as mixed cations with composition altered depending on commercial availability.

Addition of ZSM-5 into USY-based catalyst greatly increases yields of C<sub>3</sub>-C<sub>5</sub> olefins.<sup>19</sup> As an example, addition of 25% ZSM-5 into a pilot plant cracking unit resulted in an increase in ethylene, propylene, and butylenes yield of 0.84, 5.77, and 3.10 wt%, respectively.<sup>19</sup> Due to shape selectivity characteristics of ZSM-5, linear hydrocarbons are selectively transformed to alkanes and alkenes. Moreover, ZSM-5 has been shown to be one of the best catalyst in the Methanol-to-Olefin (MTO) process, yielding C<sub>2</sub>-C<sub>5</sub> alkenes with ~80% selectivity from methanol.<sup>1</sup>

Several reviews about the transformation of paraffins to smaller fragments are published.<sup>20-23</sup> The studies include the transformation over *HY*,<sup>24</sup> *KY*,<sup>25</sup> dealuminated *HY*,<sup>26,27</sup> *HUSY*,<sup>28</sup> *HZSM-5*,<sup>29-33</sup> or other molecular sieves such as SAPO-5,<sup>34,35</sup> MgAPO-5,<sup>35</sup> and CoAPO-5,<sup>35</sup> MCM-41,<sup>36</sup> and tungstophosphoric acid supported on MCM-41.<sup>36</sup> Even liquid phase isomerization of *n*-hexane over *HZSM-5*<sup>37</sup> and *H*-mordenite,<sup>38</sup> or gas phase aromatization<sup>39</sup> over *HZSM-5* have been reported.

However, works aiming at maximizing olefinic product contents are rare. Authors mainly concentrated on mechanisms instead. A sophisticated *in situ* spectroscopic study, such as <sup>13</sup>C cross-polarization magic angle spinning NMR, coupled with a flow reactor and a gas chromatograph, was carried out also for this purpose.<sup>31</sup> Otherwise, authors were not interested

in olefins. Antia *et al.*,<sup>32</sup> for example, reported selectivity to paraffins and olefins together in order to compare with selectivity to aromatic in their *n*-hexane cracking on binderless HZSM-5. Halik *et al.*<sup>34</sup> reported high selectivity to C<sub>2</sub>-C<sub>3</sub> olefins (59-62%) over SAPO-5 at very low conversion, *i.e.*, only 5%. In some cases, the material might be tested for its *n*-hexane cracking activity just only to show how active it was.

The following works presented high yield of olefins at a practical condition. Borade *et al.*<sup>40</sup>, though not intended to maximize light olefins yield from *n*-hexane, reported that at 500°C, HZSM-5 (Si/Al=18) gave C<sub>2</sub> to C<sub>3</sub> olefins selectivity of 15.3% at 84.3% conversion, hence light olefins yield of 12.9% was obtained. Wang *et al.*<sup>41</sup> reported that C<sub>3</sub> to C<sub>9</sub> paraffins can be transformed to light olefins. Selectivity to olefins as high as 53.7% was obtained at complete *n*-hexane conversion at 600°C over HZSM-5 (Si/Al=25) which was activated by air treatment at 750°C for 7.5 h. However, they did not report the amount of the undesired product methane, nor other products with carbon atoms greater than six. Recently, Talukdar *et al.*<sup>42</sup> showed that HZSM-5 (Si/Al=28) was superior to HMCM-22 of similar Si/Al ratio in *n*-hexane cracking, obtaining 31.8% yield of light olefins (74% conversion and 43% selectivity) at 530°C. This yield was higher than that obtained over HMCM-22 by a factor of 1.6. Therefore these results are clearly in agreement with the use of ZSM-5 as an olefin enhancement catalyst in commercial catalytic cracking process.

The detrimental effect of H<sup>+</sup> in commercial process for olefins formation is well known.<sup>17</sup> Alumina (Al<sub>2</sub>O<sub>3</sub>) which is used as a catalyst support can provide undesired deep catalytic cracking and coke formation, therefore its acid sites are often poisoned with an alkali ion dopant prior to use.<sup>17</sup> For example, Rombi *et al.*<sup>43</sup> reported the following propane conversion and propylene selectivity from propane dehydrogenation over Cr-supported  $\gamma$ -alumina: 19 and 98%; and 16 and 96% for a catalyst containing 1 and 0.5 wt% K, respectively. The values for a catalyst without K were considerably low. Moreover, there was a correlation between propylene selectivity and the ratio of strong to total acid sites. The higher this value (from heat of ammonia adsorption), the lower C<sub>3</sub>-olefin selectivity. Concerning propane conversion, the higher activity of K-containing catalysts was attributed

to the interplay of  $\text{Cr}^{6+}/\text{Cr}^{3+}$  couple. This concept, the interaction of a metal component of various oxidation states, will be utilized in this work as well.

The influence of acidity (and loss of acidity by alkali cation) in catalytic dehydrogenation over zeolites has also been studied, usually using  $\text{Na}^+$  form as a representative of alkali cations. In ethane oxidative dehydrogenation over various cation-exchanged *M*ZSM-5 (Si/Al=30) where  $M = \text{Na}^+$ ,  $\text{H}^+$ ,  $\text{Pt}^{2+}$  and  $\text{Ni}^{2+}$ , Chang *et al.*<sup>44</sup> found that at 550°C, *Na*ZSM-5 gave 42% ethane conversion and 54% selectivity to ethylene, whereas the values for *H*ZSM-5 were only 29 and 44%, respectively. Bulanek *et al.*<sup>45</sup> studied the propane oxidative dehydrogenation over various  $\text{Co}^{2+}$ -containing zeolites, including beta, ZSM-5, mordenite and ferrierite. They found that at 450°C for ZSM-5 (Si/Al=14), *CoNa*ZSM-5 gave 18.4% propane conversion with 12.8% selectivity of propylene, whereas *CoH*ZSM-5 gave the corresponding values of only 10.0 and 11.8%. The Co contents in *CoNa*- and *CoH*ZSM-5 were different, *i.e.* 1.59 and 2.10 wt%, respectively. Sodium cocation clearly has a beneficial effect in formation of olefins since the catalyst with even lesser cobalt content still provided higher propylene. In these two cases,<sup>44,45</sup> zeolites in Na-form exhibited not only higher feed conversion but also higher selectivity to the corresponding olefin compared to the H-form.

The advantage of containing  $\text{Na}^+$  as a co-counter cation was not limited to olefins formation in an aerobic condition only, but instead also extended to an anaerobic condition, which is the subject of this work. Katranas *et al.*<sup>46</sup> studied propane dehydrogenation to propylene over natural clinoptilolite zeolites. Over natural clinoptilolite containing, (apart from Si and Al), K, Na, Ca and Fe cations, propane conversion and propylene selectivity of 38 and 22.0%, respectively, were reported. When the natural zeolite was transformed into H-form where the amount of K, Na and Ca was reduced, propane conversion increased to 49% at the expense of propylene selectivity which dropped to 11.5%. Authors reported propylene yield of 8.4 and 5.6% for natural- and H-clinoptilolite, respectively. Wang *et al.*<sup>41</sup> reported light olefins yield from *n*-hexane cracking of 32.9 and 46.1% for *H*ZSM-5 without and with 0.5wt% K, respectively.

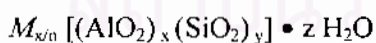
## CHAPTER II

### THEORY

#### 2.1 Zeolites

##### 2.1.1 Composition of Zeolites

Zeolites<sup>4,47,48</sup> are ordered, porous, and rigid crystalline aluminosilicates having a definite structure with a framework based on an extensive three-dimensional network of SiO<sub>4</sub> and AlO<sub>4</sub> tetrahedra. The tetrahedra are cross-linked by the sharing of oxygen atoms as shown in Figure 2.1(a). The electrovalance of the tetrahedral-containing aluminium is balanced by the inclusion in the crystal of *M'* cations. A representative unit cell formula for the composition of a zeolite is:



where *M* is the exchangeable cation of valence *n*; *y/x* is the Si/Al molar ratio, and is equal to or greater than 1 because Al<sup>3+</sup> does not occupy adjacent tetrahedral sites, otherwise the negatively charged units next to each other will be obtained; and *z* is the number of water molecules located in the channels and cavities inside a zeolite.

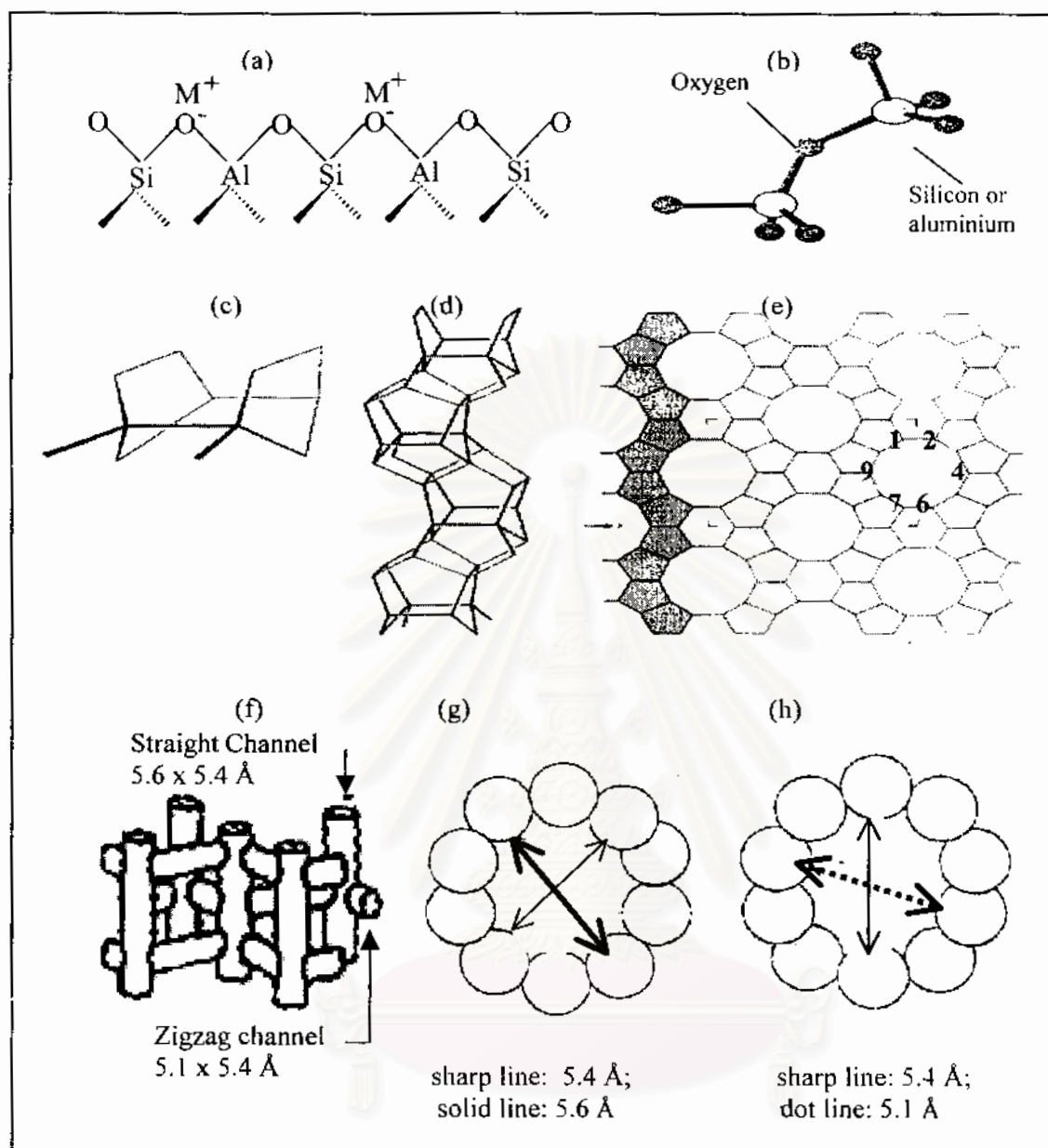


**Figure 2.1** Structure of a zeolite. (a) zeolite framework, (b) primary building unit, (c) 12-tetrahedral atoms SBU, (d) chain unit type formed from (c), (e) ZSM-5 layer formed from (d),<sup>49</sup> (f) channels system in ZSM-5, (g) straight-, and (h) zigzag channel.<sup>4,49</sup>



The Mobil oil company first synthesized ZSM-5 in 1972<sup>47</sup> and its structure code is later labeled MFI.<sup>4,48</sup> For hydrated NaZSM-5 zeolite, the typical unit cell is  $\text{Na}_n\text{Al}_n\text{Si}_{96-n}\text{O}_{192} \cdot 16\text{H}_2\text{O}$ ,<sup>48</sup> where the lowest Si/Al possible is 10, and originally the highest value is 60.<sup>47</sup> Nowadays, the highest Si/Al extends to infinity, *i.e.*, almost no aluminium in a zeolite at all.<sup>4,48</sup>

### 2.1.2 Structure of Zeolites

A common subunit used to describe the structure of zeolites is called primary building units, consisting of (Al,Si)O<sub>4</sub> tetrahedra as shown in Figure 2.1(b). These tetrahedra are linked together by corner sharing of Si or Al atoms in various ways, forming a secondary building unit (SBU).<sup>4</sup> For ZSM-5, its SBU comprises 12 tetrahedral atoms as shown in Figure 2.1(c).<sup>49</sup> In this notation, an oxygen atom situates at the middle of every line, whereas at every corner where two lines meet, or at the end of every line, situates Al or Si atom. Ring consisted of five oxygen atoms are evident in this structure; the name *pentasil zeolite* is therefore used to describe it. The SBUs form chains as shown in Figure 2.1(d), which in turn link to generate the structure through a center of inversion as shown in Figure 2.1(e).<sup>49</sup> A 10-membered ring aperture can be clearly seen in this figure.

ZSM-5 is a medium-pore zeolite having an orthorhombic symmetry.<sup>49</sup> It contains intersecting three-dimensional 10 ring channels system, a straight and a zigzag, as shown in Figure 2.1(f). The straight channel has a cavity of 5.4 x 5.6 Å free diameter, whereas the sinusoidal channel has a cavity of 5.1 x 5.4 Å free diameter. These two channels are compared also in Fig 2.1(g) and (h).<sup>4,49</sup>

### 2.1.3 Shape Selectivity of Zeolites

Zeolites are known as *molecular sieves* since they accept for adsorption molecules of certain dimensions while rejecting those of larger dimensions.<sup>4,47,48</sup> They possess

*shape selectivity*, which plays a very important role in zeolite catalysis. Shape selectivity is divided into 3 types: reactant, product, and transition-state shape selectivity, as shown in Figure 2.2.<sup>4</sup>

Reactant shape selectivity, Fig 2.2(a), results from the limited diffusivity of some of the reactants, *e.g.*, linear vs branched, which cannot effectively enter and diffuse inside the crystal. Product shape selectivity, Fig 2.2(b), occurs when slowly diffusing product molecules, for example *o*- and *m*-xylene, cannot rapidly escape from the crystal, and undergo secondary reactions, for example, to *p*-xylene. Restricted transition-state shape selectivity can be explained by the decrease of the rate constant for a certain reaction mechanism when the required transition state is too bulky to form readily, Fig 2.2(c).

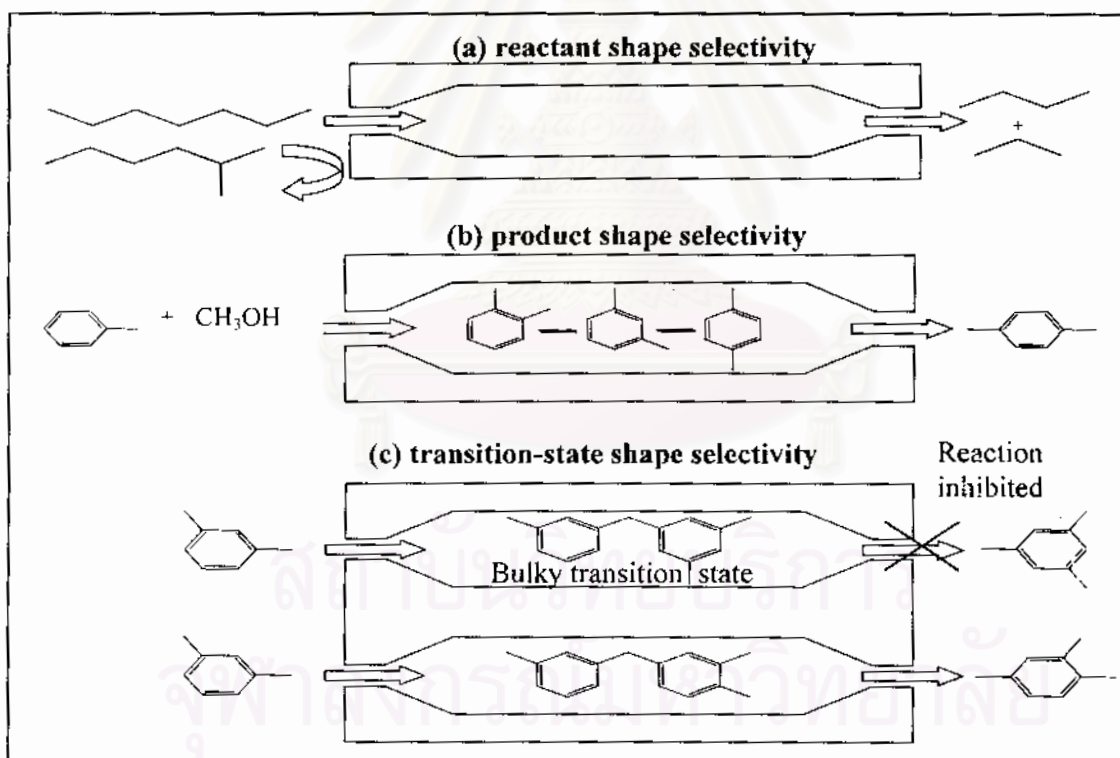


**Figure 2.2** Three types of shape selectivity in zeolites: (a) reactant, (b) product, and (c) transition-state shape selectivity.<sup>4</sup>

#### 2.1.4 Acid Sites of Zeolites

Classical Brønsted and Lewis acid models of acidity have been used to classify the active sites on zeolites.<sup>4</sup> Brønsted acidity is proton-donor acidity, and occurs when cations balancing the framework anionic charge of zeolites are protons ( $H^+$ ). Lewis acidity is electron acceptor acidity. An example is trigonally coordinated aluminium atom. Brønsted acidity is generally believed to be stronger than Lewis acidity,<sup>4</sup> and is almost solely responsible for alkanes, *e.g.*, *n*-hexane, transformation.

To produce the zeolite acid catalyst, a first step is to remove large organic quaternary amine cations occluded during synthesis by combustion in air or *calcination*. The obtained material contains alkali cations (*e.g.*  $Na^+$ ) and some protons as shown in Figure 2.3(a). Ammonium exchange of the alkali cations, followed by subsequent deammoniation, *i.e.*, thermal treatment releasing ammonia gas and leaving proton, results in the structure shown in Figure 2.3(b). Direct exchange with acid is also possible, but has to be done very carefully otherwise Al atoms will be extracted from the zeolite lattice.<sup>4</sup> Simultaneously, Brønsted acid sites are in equilibrium with Lewis acid if  $-OH$  groups are considered to bond totally to Si, leaving tricoordinated Al atoms (not shown in the Figure). Upon heating at high temperature, acid sites are transformed to Lewis acid sites by dehydration as shown in Figure 2.3(c). This process is reversible. Other cations such as rare earths can be introduced into zeolite by ion exchange method as well.

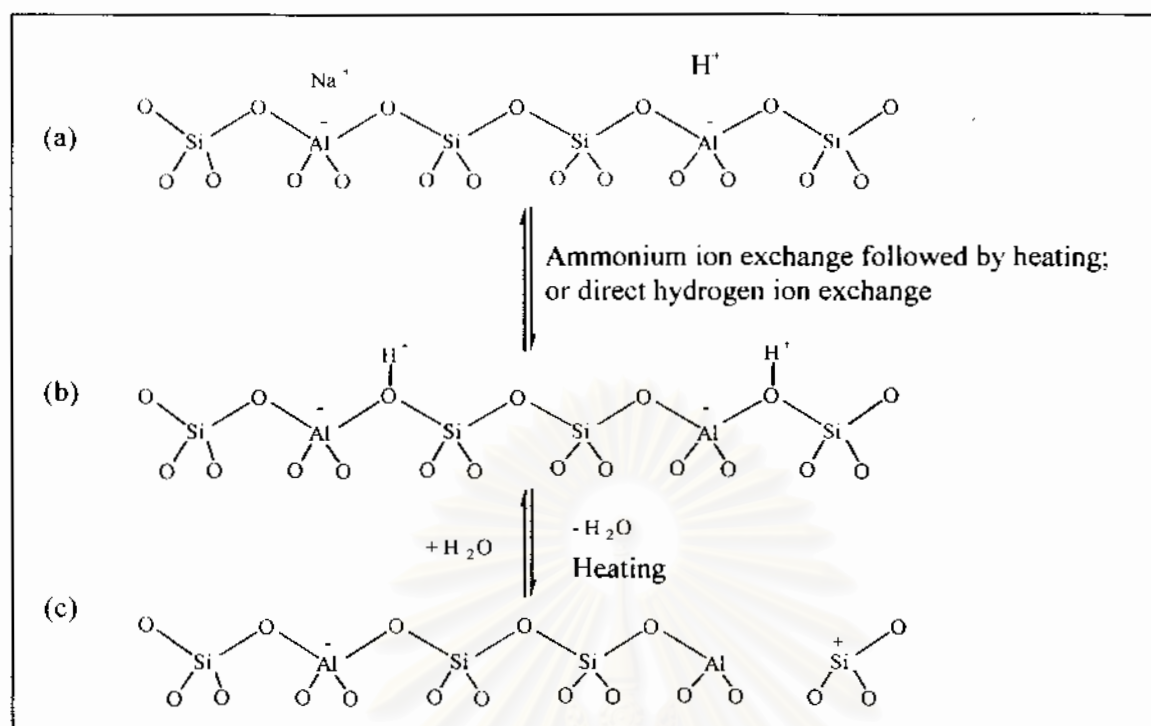


**Figure 2.3** Acidities in zeolites. (a) calcined zeolite, (b) Brønsted-, and (c) Lewis acid.

## 2.2 Zeolite Synthesis

Many factors have a major influence on the zeolite structure crystallized, *e.g.*, temperature, time, and gross composition. These factors are listed in Table 2.1 and are briefly discussed below.<sup>4</sup> A hydroxide concentration is found to be a crucial factor in forming ZSM-5 in this work, and therefore is discussed in a separate section.

**Table 2.1** Factors influencing zeolite crystallization.<sup>a,4</sup>

- |   |
|---|
| ▪ Temperature                           |
| ▪ Time                                  |
| ▪ Gross composition                     |
| 1. $\text{SiO}_2/\text{Al}_2\text{O}_3$ |
| 2. Cations                              |
| (a) Inorganic                           |
| (b) Organic                             |
| 3. $[\text{H}_2\text{O}]$               |
| 4. Anions (excluding $[\text{OH}^-]$ )  |
| 5. $[\text{OH}^-]$                      |

<sup>a</sup> other factors such as history-dependent factors, *e.g.*, aging, stirring, nature of mixture, and the order of mixing, are also existed.

### 2.2.1 Temperature and Time

To approximate their natural occurrence, zeolites are generally crystallized under high pressure and at moderately high temperatures (120-200°C).<sup>4</sup> High pressure can be usually achieved using a closed vessel called an autoclave. Concerning temperature, higher temperature yields more condensed but not zeolitic phases, whereas lower temperature prohibits convenient synthesis process. As an example for the influence of temperature on zeolite synthesis, ZSM-5 and ZSM-11 were reported to co-exist at temperatures of 130-180°C,<sup>4</sup> where percentage of ZSM-5 varied with temperatures as follows: <5% (130°C), 50-55% (145°C), 60-65% (160°C), and 75-80% (180°C).

Time is also important in systems where one phase is metastable with respect to another, as in the case of zeolite synthesis.<sup>4</sup> Generally, at constant temperature and initial mixture composition, the transformation proceeds from amorphous, to metastable, to more stable phase. Argauer and Landolt<sup>47</sup> claimed a wide range of temperature of 100-175°C at time ranging from six hours to sixty days for synthesis of ZSM-5 in an original patent. Clearly, time required varies widely, and is often optimized to yield the desired zeolitic phase in a reasonable period.

### 2.2.2 Gross Composition

The effects of variables in gross composition on the zeolite formation is shown in Table 2.2.<sup>4</sup>

Crystallization of a zeolite commonly occurs from a molecularly inhomogeneous system referred to as a gel. The alkali, sources of  $\text{AlO}_2$  and  $\text{SiO}_2$ , water, and other components are mixed in appropriate proportions and subjected to various temperatures. Note that sources of  $\text{AlO}_2$  and  $\text{SiO}_2$  strongly have influence on the crystalline phase obtained.  $\text{SiO}_2/\text{Al}_2\text{O}_3$  in the gel places a constraint on the framework composition of the zeolite produced. For example,<sup>4</sup> ZSM-5 is known to generally crystallize (in the presence of an

organic additive, discussed below) at  $\text{SiO}_2/\text{Al}_2\text{O}_3$  in the range of 20 to infinity. However, as this ratio decreases below 20, mordenite zeolite starts to form.

**Table 2.2** The effects of variables in gross composition on the zeolite formation.<sup>4</sup>

Variables	Primary influence
$\text{SiO}_2/\text{Al}_2\text{O}_3$	Framework composition
Inorganic cation(s)/ $\text{SiO}_2$	Structure, cation distribution, morphology, crystal purity, yield
Organic additives/ $\text{SiO}_2$	Structure, framework aluminum content
$\text{H}_2\text{O}/\text{SiO}_2$	Rate, crystallization mechanism
$\text{OH}^-/\text{SiO}_2$	Silicate molecular weight, $\text{OH}^-$ concentration

An example concerning some aspects of the influence of inorganic cations on zeolite formation is as follows. In the synthesis of high-silica ZSM-5,<sup>4</sup> addition of  $\text{Na}_2\text{O}$  or  $\text{K}_2\text{O}$  to the reaction mixture increased the crystal size to 20 and 26  $\mu\text{m}$  from the few- $\mu\text{m}$  size found in the  $\text{NH}_4^+$  system. Lithium cation encouraged the formation of large, lath-shaped ZSM-5 crystals over 100  $\mu\text{m}$  in length. The presence of  $\text{Na}^+$  in the crystallization of ZSM-5 zeolite was shown originally in the patent literature by Argauer and Landolt as well.<sup>47</sup> Other inorganic anions, excluding  $\text{OH}^-$ , have to be considered too. The presence of oxyanions such as  $\text{NO}_3^-$ ,  $\text{ClO}_4^-$ ,  $\text{PO}_4^{3-}$ ,  $\text{AsO}_4^{3-}$ ,  $\text{BrO}_3^-$  and  $\text{IO}_3^-$  is reported to enhance the nucleation and crystallization in ZSM-5 synthesis.<sup>50</sup>

Not only inorganic but also organic cations play important roles on zeolite formation. An organic cation is called crystal- or structure-directing agent, or *template*. Zeolite structure grows around the template, thus certain pores and subunits are stabilized. Crystallization of a specific zeolite structure is induced when a template is added. Template for ZSM-5 was originally reported to be tetrapropylammonium cation,  $\text{N}(n\text{-C}_3\text{H}_7)_4^+$ , or TPA.<sup>47</sup> Evidence supported its role as a channel-directing agent was found by crystallographic examination, since TPA<sup>+</sup> was trapped and oriented in the channel intersections with the alkyl arms extended into the straight and sinusoidal channels of ZSM-5

zeolite.<sup>4,48</sup> The broadness of <sup>13</sup>C-NMR signal of TPA<sup>+</sup> cations in the crystallizing gel in ZSM-5 synthesis, compared to that of TPA<sup>+</sup>-bromide was observed.<sup>4</sup> This was attributed to the interaction between the cation and the zeolite framework.

Water has been proposed to interact strongly with the cations present in the solution, thus itself becoming part of the template for structure directing.<sup>4</sup> It controls the rate of crystallization because transport properties within the gel and the viscosity of the reacting gel change with changing water concentration.

### 2.2.3 Hydroxide Concentration

The hydroxide ion is a moderately good complexing agent for Si and Al. The interaction between Si (or Al) with hydroxide ion is strong enough that these ions will dissolve in the aqueous alkali solutions; but the hydroxide complex of these ions is still weak enough that it does not prevent Si (or Al) from further reacting to produce the desired zeolite.<sup>4</sup>

In the synthesis of ZSM-5 (SiO<sub>2</sub>/Al<sub>2</sub>O<sub>3</sub>=80) zeolite conducted in this laboratory,<sup>51</sup> alternation of hydroxide concentration was found crucial. The preparation method according to Szostak and Thomas<sup>12</sup> (SiO<sub>2</sub>/Al<sub>2</sub>O<sub>3</sub>=55) yielded, at pH 3.5, amorphous plus trace of crystalline phase as shown in Fig 2.4(a). Addition of 6 M NaOH to increase the pH value to 10.5, *i.e.*, making reaction mixture more basic, resulted in the formation of zeolitic phases ZSM-5 and mordenite as shown in Fig 2.4(b). Hydroxide ions act as solvent, therefore increasing pH value resulted in much greater concentrations of reactants dissolved. They transport the silicate and aluminate species between the amorphous and the crystalline zeolite phase.<sup>4</sup> Crystal growth is consequently accelerated and crystallization time is consequently shorten, *i.e.*, products obtained changed from amorphous phase to crystalline phase at the very same condition. Similarly, Ahmed *et al.*<sup>53</sup> found that surface area and the ratio of 550-to-450 cm<sup>-1</sup> IR absorbance, which are indicative of crystallinity, gradually decreased as pH dropped from 10.0 to 8.0. On the other hand, too high pH redissolve the zeolite formed, hence reducing its crystallinity.<sup>4</sup> For example, van Grieken<sup>54</sup> found that at

very severe caustic condition, *e.g.*, pH > 14, crystallinity decreased to 74.1%, compared to 97.0% at a pH value of 14.

The synthesis of ZSM-5 was very sensitive to the starting materials, *e.g.*, Si sources, as Szostak and Thomas<sup>52</sup> used low-molecular weight silica and succeeded in ZSM-5 synthesis. On the contrary,<sup>51</sup> by using water glass instead while keeping other components the same, amorphous plus trace crystalline phase as shown in Figure 2.4(a) were obtained. Therefore it is not unexpected that Al sources also exert similar effects. Replacing an aluminium source  $\text{Al}_2(\text{SO}_4)_3$  by  $\text{NaAlO}_2$ , together with pH adjustment by addition of concentrated  $\text{H}_2\text{SO}_4$  to a value of 10.5, resulted in pure ZSM-5 as shown in Fig 2.4(c).

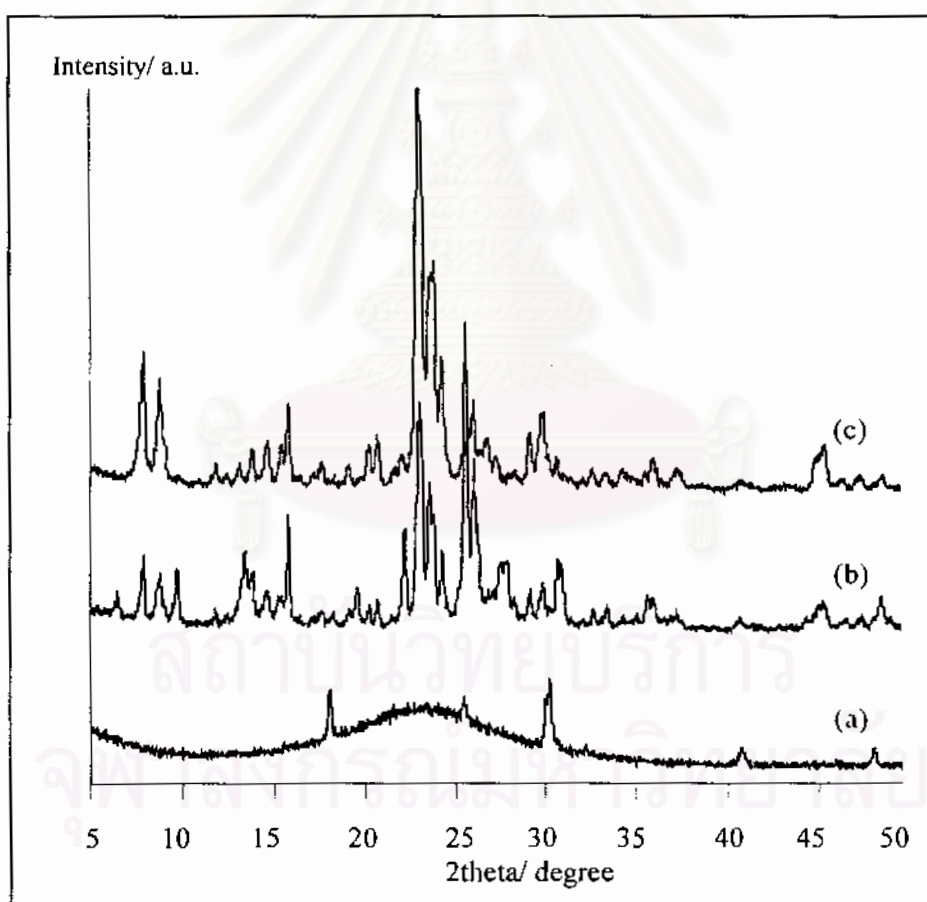


**Figure 2.4** Synthesis of ZSM-5 by different methods. (a) prepared according to Szostak and Thomas,<sup>52</sup> pH: 3.5, Al source:  $\text{Al}_2(\text{SO}_4)_3$ ; (b) pH: 10.5 (adjust by 6 M NaOH), Al source:  $\text{Al}_2(\text{SO}_4)_3$ ; (c) pH: 10.5 (adjust by concentrated  $\text{H}_2\text{SO}_4$ ), Al source:  $\text{NaAlO}_2$ .<sup>51</sup>



### 2.2.4 Original Condition for ZSM-5 Synthesis

ZSM-5 synthesis was first reported in the patent literature by Arguer and Landolt in 1972.<sup>47</sup> The ratios of various reaction components claimed for successful synthesis is shown in Table 2.3. Reaction mixture was heat at 100-150°C for 6 hours to 60 days. ZSM-5 was claimed to be able to catalyze the following reactions:<sup>47</sup> Cracking and hydrocracking of oils, isomerization of *n*-paraffins and naphthenes, polymerization of compounds containing an olefinic or acetylenic carbon, reforming, alkylation, isomerization of polyalkyl substituted aromatics, and disproportionation of aromatics.

**Table 2.3** Reactant molar ratios claimed for ZSM-5 synthesis.<sup>47</sup>

Reactant molar ratio	Broad	Preferred	Particularly preferred
OH/SiO <sub>2</sub>	0.07-10.0	0.1-0.8	0.2-0.75
$(n-C_3H_7)_4N^+ / \{(n-C_3H_7)_4N^+ + Na^+\}$	0.2-0.95	0.3-0.9	0.4-0.9
H <sub>2</sub> O/OH <sup>-</sup>	10-300	10-300	10-300
SiO <sub>2</sub> /Al <sub>2</sub> O <sub>3</sub>	5-100	10-60	10-40

### 2.3 Ce<sup>3+</sup> Inside Zeolite: Nature and Catalytic Activity

Usually in the literature, ion exchange of rare earth cations into zeolites, where cerium is hereafter mainly discussed as a representative, was done using a 3+ salt. The cation is not “naked” but instead there exists a hydration sphere around it. For example, Berry *et al.*<sup>55</sup> found that the extended X-ray absorption fine structure (EXAFS) spectra of Ce<sup>3+</sup>-exchanged HY zeolite was similar to that of Ce(NO<sub>3</sub>)<sub>3</sub>•6H<sub>2</sub>O, indicative of coordination by water to cerium in CeY.

### 2.3.1 Hydroxide Complexes of $Ce^{3+}$ and Their Dissociation

In high silica zeolite such as ZSM-5, it is generally agreed that a sparse distribution of negative charges cannot be effectively neutralized by trivalent cations. Instead, water ligand dissociation takes place, Figure 2.5, resulting in the reduction of the apparent charge of the cation. The distance between the framework negative charges and the balancing rare earth counter ions is also shorten.

As shown in Figure 2.5,  $Ce(H_2O)^{3+}$  dissociates to form  $Ce(OH)^{2+}$  and Bronsted acid,  $H^+$ . The divalent complex is able to dissociate more to  $CeO^+$  and another  $H^+$ . Note that  $Ce(OH)^{2+}$  also exist in aqueous solution.<sup>56</sup> There are many evidences supporting this reaction scheme, including IR spectroscopy,<sup>57-61</sup>  $NH_3$  temperature programmed desorption ( $NH_3$ -TPD),<sup>62</sup> neutron diffraction,<sup>63</sup> and elemental analysis.<sup>64</sup> These examples will be described below.

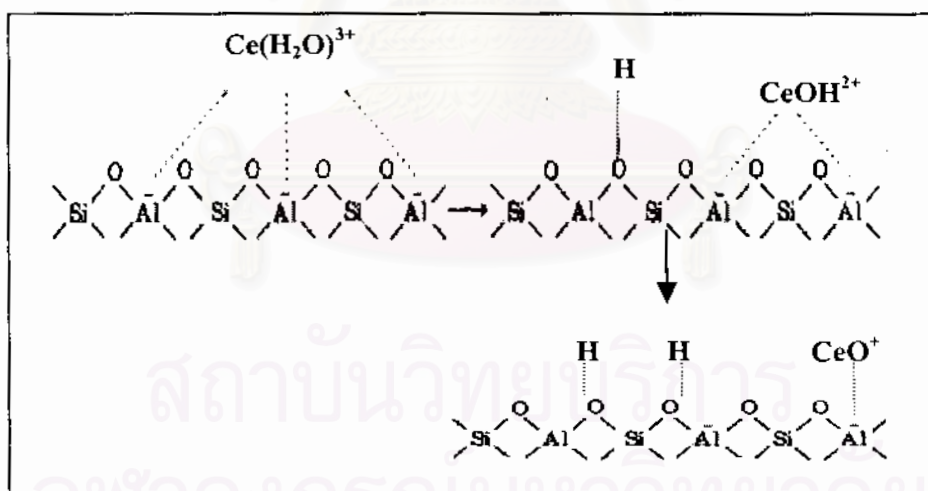


**Figure 2.5** Hydrolysis of cerium inside a zeolite.

Using IR spectroscopy, Christner *et al.*<sup>57</sup> was able to detect an absorption band of OH group connecting to cerium in  $NaCeY$  zeolite, *e.g.*,  $Ce(OH)^{2+}$ , which appeared as a result of dissociation reaction in Figure 2.5, at  $3555\text{ cm}^{-1}$ . Others reported the same band at a slightly shifted position, *e.g.*,  $3530\text{ cm}^{-1}$  in  $CeHY$  zeolite,<sup>58</sup> and  $3500\text{ cm}^{-1}$  for  $CeNaX$  zeolite.<sup>59</sup> Konya *et al.*<sup>60</sup> recently published a comparative IR studies of  $NaMOR$ ,  $Ce^{3+}$ -

exchanged *NaMOR*, and *HMOR*. There was an absorption band at  $3735\text{ cm}^{-1}$  in *NaMOR*, which was ascribed vibration of to Si-OH moieties. When *NaMOR* was exchanged with  $\text{Ce}^{3+}$ , new absorption band ascribed to bridging Si(OH)Al of Brønsted acid character occurred at  $3611\text{ cm}^{-1}$ . *HMOR* showed an absorption band characteristic of Brønsted acid at the same position. The authors<sup>60</sup> proposed cerium hydrolysis as a source for proton in *CeNaMOR*.

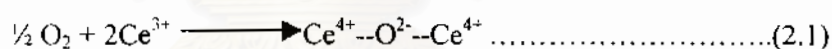
Generation of Brønsted acid by ion exchange of  $\text{Ce}^{3+}$  into zeolite was also shown by IR spectroscopy using pyridine as a probe molecule. Weyrich and Holderich<sup>61</sup> found that pyridine sorbed into *NaZSM-5* zeolite resulted in the absorption band at  $1445\text{ cm}^{-1}$ , which was due to the Lewis acidity, and no absorption band belonged to Brønsted acid could be observed in the same sample. However, when pyridine was absorbed into  $\text{Ce}^{3+}$ -exchange *NaZSM-5*, an absorption band at  $1545\text{ cm}^{-1}$  characteristic of Brønsted acid-bound pyridine was present. The appearance of this band was also explained by cerium hydrolysis.

Supporting result by Ito *et al.*<sup>62</sup> using  $\text{NH}_3$ -TPD on  $\text{Ce}^{3+}$ -exchanged *NaMOR* is as follows. Three desorption peaks were observed in their work. The lowest temperature peak at  $200\text{-}300^\circ\text{C}$  was ascribed to weakly adsorbed ammonia on the mordenite matrix. The peak at  $400\text{-}500^\circ\text{C}$  was ascribed to  $\text{NH}_3$  coordinated to cerium cations. And the peak at highest temperature ( $\geq 600^\circ\text{C}$ ) was ascribed to  $\text{NH}_3$  interacted with the Brønsted acid site. The very direct observation of  $\text{H}^+$  as a result of rare earth hydrolysis inside a zeolite was reported by Cheetham *et al.*<sup>63</sup> Using neutron diffraction, they were able to detect attachment of proton to framework oxygen in  $\text{La}^{3+}$ -exchanged *NaY* zeolite, though no  $\text{H}^+$  was not detected in *NaY* before ion exchange.

Besides these techniques,  $\text{Ce}^{3+}$  hydrolysis was indirectly observed by elemental analysis also. Li and Flytzani-Stephanopoulos<sup>64</sup> found by ICP that in  $\text{Ce}^{3+}$ -*NaZSM-5* samples prepared, the sum of cation concentration, *i.e.*,  $3\text{Ce}+\text{Na}$ , was less than the molar concentration of Al, implying loss of balancing cations not detected by ICP. They attributed this charge imbalance to protons.

### 2.3.2 Oxidation of Ce<sup>3+</sup> to Ce<sup>4+</sup>

In some cases, transformation into the different oxidation state is possible. Ce<sup>3+</sup> in zeolite is easily oxidised to Ce<sup>4+</sup> by air oxidation. Dyer *et al.*<sup>65</sup> reported an observation that CeX and CeY zeolites attained the yellow/cream colour attributable to Ce<sup>4+</sup> when the samples were heated in air, whereas the samples which were dried carefully in a N<sub>2</sub> steam did not show this colour. Yellow colour is widely accepted as characteristic of Ce<sup>4+</sup>.<sup>15</sup> In another study, Tempere *et al.*<sup>59</sup> proposed an oxidation reaction shown in Equation (2.1), and stated that the Ce<sup>3+</sup> oxidation was complete when the temperature was higher than 450°C at O<sub>2</sub> partial pressure of 36 torrs (0.047 atm). The same authors also showed by XPS spectroscopy,<sup>66</sup> that in air oxidized Ce<sup>3+</sup>NaY, the intense peaks characteristics of Ce<sup>4+</sup> were also observed in addition to the characteristic peaks of Ce<sup>3+</sup> obtained originally before oxidation.



Other techniques such as luminescence and diffused reflectance UV-Vis spectroscopy were utilized to study air oxidation of Ce<sup>3+</sup> inside zeolites as well. The former technique is based on the fact that Ce<sup>3+</sup> is luminescent active, whereas Ce<sup>4+</sup> is luminescent silent. Hong<sup>67</sup> studied air oxidation of various Ce<sup>3+</sup>-containing zeolites, including A, X, Y, ZK-4, chabazite, rho, EMC-2, mordenite, and ZSM-5. Ce<sup>3+</sup>NaZSM-5 (Si/Al=13.5) sample that did not receive any treatment, *i.e.*, at 25°C, showed two peaks in the excitation spectra typical of Ce<sup>3+</sup> in zeolites. When the sample was heated at different temperatures ranging from 100-500°C for 4 h under flowing air, signal due to Ce<sup>3+</sup> was progressively lost, indicative of transformation of Ce<sup>3+</sup> to Ce<sup>4+</sup>. The spectra are shown in Fig 2.6(a). Though air oxidation occurred, only part of cerium was oxidized, but *not* all.

Li and Flytzani-Stephanopoulos<sup>64</sup> studied the DRUV-Vis spectra of Ce<sup>3+</sup>NaZSM-5 (Si/Al=13.8) of various ion exchange level, *e.g.*, 9, 24, 42, and 54%, prepared

by repeating ion exchange *plus* heat treatment at 500°C in air for 2 h. The following signals were observed as shown in Fig 2.6(b). The first and second were that at 210 and 260 nm, attributable to the  $4f-5d$  interconfiguration transition of  $Ce^{3+}$ . The last one appeared at 294 nm, attributable to  $Ce^{4+} \leftarrow O^{2-}$  charge transfer of  $CeO_2$  cluster. All three peaks were observed even in  $Ce(9\%)NaZSM-5$  which was subjected to 500°C heat treatment in air only once. Unfortunately, the  $Ce^{3+}$  peaks (210 and 260 nm) appeared quite unresolved, and were overlapped with the  $Ce^{4+} \leftarrow O^{2-}$  peak (294 nm). Despite the uncertainty of  $Ce^{3+}/Ce^{4+}$  peak separation in the DRUV-vis spectra by Li and Flytzani-Stephanopoulos,<sup>64</sup> the results still provided an evidence supporting the luminescent results of Hong<sup>67</sup> quite well. The presence of 294-nm band in the DRUV-Vis spectra agreed with the decrease of luminescent  $Ce^{3+}$  signals. Surprisingly, samples from these two groups accidentally had the same ion exchange level (9%) and similar Si/Al ratio.

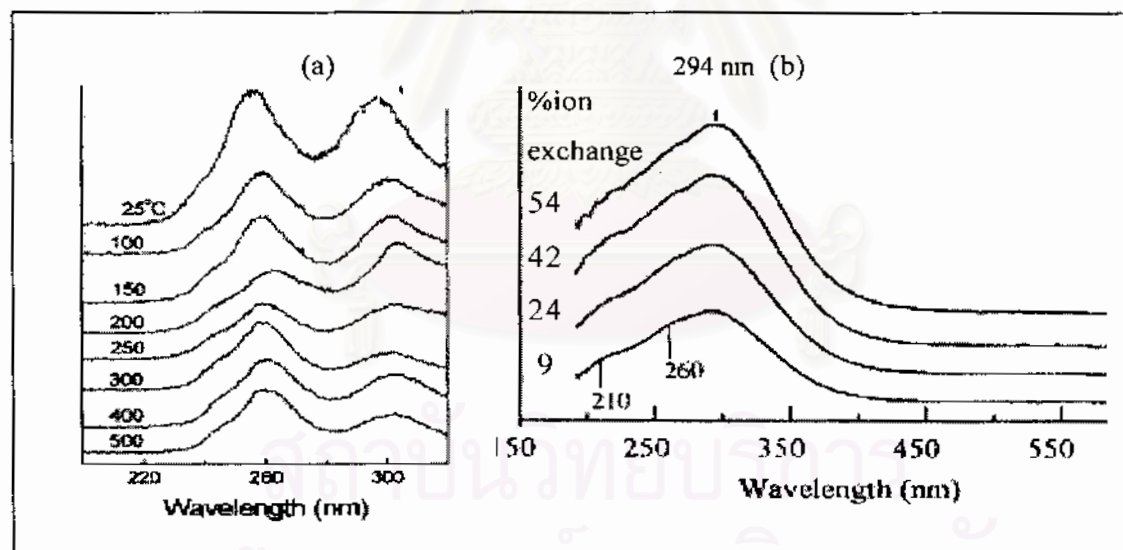
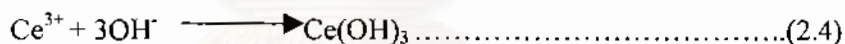
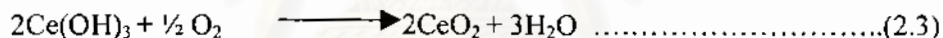
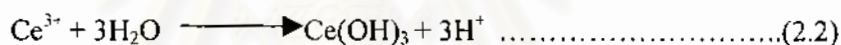


**Figure 2.6** (a) Luminescent excitation spectra of  $Ce^{3+}NaZSM-5$  heated at different temperatures;<sup>67</sup> (b) DRUV-Vis spectra of  $Ce^{3+}NaZSM-5$  with different cerium ion exchange levels.<sup>64</sup>

Moreover, Zhang and Flytzani-Stephanopoulos<sup>68</sup> found by scanning electron microscopy (SEM) couple with energy dispersive X-ray (EDX) analysis that in  $Ce^{3+}(60\%)NaZSM-5$ , two types of cerium were observed. The first was well distributed in the

ZSM-5 zeolite crystal and was suggested to associate with framework, *i.e.*, a counter ion. The second enriched the crystal surface and was thought to be in an oxidic form.

In some cases the ion exchange-induced oxidation is reported. Van Kooten *et al.*<sup>69</sup> monitored ion exchange process of  $\text{Ce}^{3+}$  and NaZSM-5 by elemental analysis. They found that the decrease in the cerium concentration of the exchange solution was not fully compensated for by the increase in the sodium concentration. They suggested the possibility that  $\text{Ce}^{3+}$  ions might enter the zeolite without ion exchange as shown in Equation (2.2), *i.e.*, formation of  $\text{Ce}(\text{OH})_3$  gel and proton. When calcination,  $\text{Ce}(\text{OH})_3$  was transformed to  $\text{CeO}_2$  and  $\text{H}^+$  as shown in Equation (2.3). Solution becomes more acidic as a result of  $\text{H}^+$ . Formation of  $\text{Ce}(\text{OH})_3$  gel was also suggested by Weyrich *et al.*,<sup>70</sup> but in basic condition, as shown in Equation (2.4).



## 2.4 Mechanisms of *n*-Hexane Transformation

### 2.4.1 Carbenium and Alkanium Ions

Reaction of alkanes on acidic catalysts such as zeolites proceeds *via* heterolytic bond cleavage involving carbocations. Brønsted acid sites are believed to responsible solely in this reaction.<sup>20-23</sup> Carbocations include *carbenium ions* and *alkanium ions* (these names are recommended by IUPAC).<sup>23</sup> Carbenium ions are tricoordinated, whereas alkanium ions are pentacoordinated.

**Table 2.4** Lists of reactions of carbenium and alkanium ions.<sup>23</sup>

A. Reactions of carbenium ions	B. Reactions of alkanium ions
(1a) Rearrangement	(1b) $\beta$ -Scission
(2a) Hydride shift	(2b) Loss of proton to Brønsted site
(3a) Alkyl shift	
(4a) $\beta$ -Scission	
(5a) Hydride transfer	

Carbenium ions undergo various reactions as shown in Table 2.4.<sup>23</sup>

Rearrangements are often facile, especially those forming more stable carbenium ions, *i.e.*, primary to secondary to tertiary, *etc.* This type of rearrangement results in the modification of carbon skeleton. Nonbranching rearrangements, where the degree of chain branching remains the same, proceeds by hydride shift and alkyl shift, *e.g.*, methyl shift.  $\beta$ -Scission, or  $\beta$ -elimination, is the fragmentation of carbenium ions into smaller carbenium ions and alkenes at  $\beta$  position with respect to the carbon bearing the positive charge. During this process the formation of primary carbenium ions should be avoided. This scission requires at least three carbon atoms in the carbenium ions that undergo cleavage. Besides these intramolecular reactions, there is also an intermolecular reaction called hydride transfer. This reaction proceeds by transfer of hydride from an alkane to a carbenium ion, resulting in another carbenium ion and a new alkane, *i.e.*,  $R^+ + HR' \rightarrow RH + R'^+$ .

Alkanium ions undergo much limited reactions. When  $\beta$ -scission occurs at a C-C bond, carbenium ions and alkenes are formed. If the C-H bond is cleaved, carbenium ions and  $H_2$  are formed. The former is cracking whereas the latter is dehydrogenation. Loss of protons back to a counteranion of the catalyst surface results in an alkane molecule with identical carbon skeleton. These reactions constitute for a fundamental of a classical (bimolecular), Haag-Dessau (monomolecular), and oligomeric mechanism discussed below.

### 2.4.2 Classical (Bimolecular) Mechanism

This reaction mechanism is depicted in Fig. 2.7(a).<sup>21</sup> Hydride transfer from an alkane RH to a carbenium ion  $R_1^+$  takes place. Another alkane,  $R_1H$ , is formed together with a new carbenium ion  $R^+$ . This  $R^+$  cracks by  $\beta$ -scission to produce an alkene with carbon number always less than the original RH alkane. Products from the bimolecular mechanism include alkanes and alkenes, both with at least three carbon atoms. Formation of light products such as methane, ethane, and  $H_2$  would require  $\beta$ -scission giving high-energy primary carbenium ions, and is therefore inhibited. Isobutane is characteristic of bimolecular mechanism.<sup>71</sup> Bimolecular mechanism plays an important role in catalytic cracking.

Note that there must be alkenes available in this mechanism for initiation, and their origins are proposed by several pathways.<sup>20-23</sup> Alkenes may (1) present as impurities in the feed stream; (2) present in small amounts by thermal reaction; or they may be formed as a result of (3) hydride abstraction by Lewis acid sites in a catalyst; or as a result of (4) feed protonation by Brønsted acid, resulting in alkanium ions which subsequently undergo further reactions as described in Table 2.4 and below. However, nowadays the fourth pathway is the most widely recognized.

### 2.4.3 Haag-Dessau (Monomolecular) Mechanism

This recent mechanism, originally proposed by Hagg and Dassau and also known as protolytic mechanism, is shown in Fig. 2.7(b).<sup>21</sup> The Brønsted acid,  $H^+$ , protonates an alkane RH to give an alkanium ion  $RH_2^+$ . This ion in turn collapses to give the cracking products, e.g., an alkane  $R_1H$  and a carbenium ions  $R_2^+$ . The latter subsequently undergo further  $\beta$ -scission to other products, and lose proton back to the catalyst's surface. The difference in carbon number  $R$ , i.e.,  $R=R_1+R_2$ , should be noted. If the protonation occurs at a C-H bond, followed by the decomposition of the resulting  $RH_2^+$  to  $H_2$ ,  $H^+$ , and an alkene,  $R$ ,



with the same carbon number, this is called *protolytic dehydrogenation*. This mechanism provides an explanation for the formation of  $H_2$ , methane, and ethane (or ethylene), which cannot be accounted for by the classical  $\beta$ -scission mechanism. Methane formation is characteristic of monomolecular mechanism.<sup>23,71</sup>

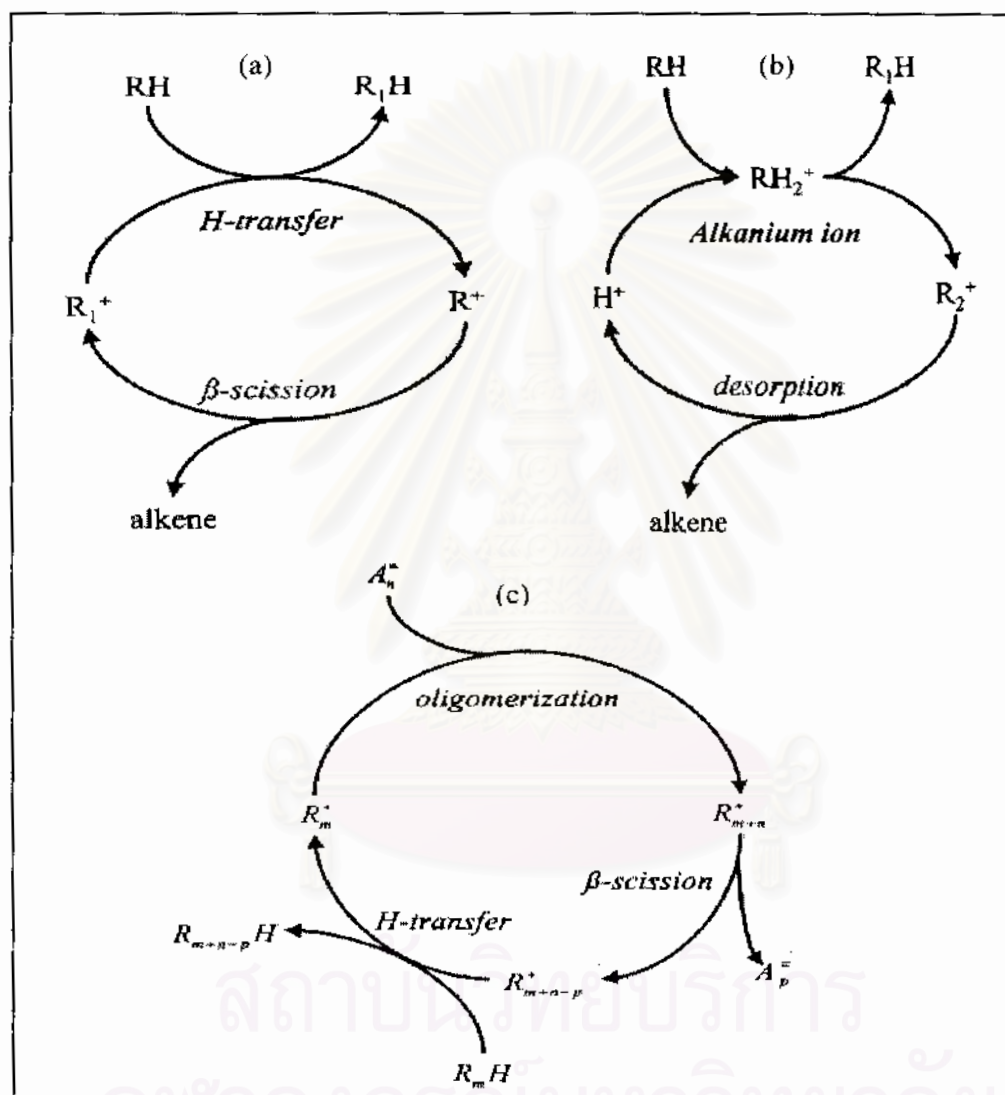


**Figure 2.7** Reaction of alkanes over acidic catalysts through (a) bimolecular, (b) monomolecular, and (c) oligomeric mechanism.<sup>21</sup>

The monomolecular mechanism differs from the classical mechanism since proton donation by the catalyst is necessary for each turnover. In contrast, formation of one carbenium ion in classical mechanism can lead to many turnovers of the cycle. The former is kinetically significant only at high temperatures and at low alkene concentrations, *i.e.*, at low

conversions of pure alkane, and at low alkane partial pressure. This is because the alkenes produced are much better proton acceptors than the alkanes. Alkenes therefore increasingly win the competition for the protons as the conversion increases. Once bimolecular mechanism is initiated, this pathway may be up to 800 times faster than monomolecular mechanism.<sup>71</sup> This feature is called “autocatalytic”.

#### 2.4.4 Oligomeric Mechanism

This mechanism, illustrated in Fig. 2.7(c),<sup>21</sup> is proposed to account for the appearance of carbonaceous materials called coke, and the formation of products larger in carbon number than the feed.<sup>71</sup> An alkene  $A_n$  is oligomerized, or alkylated with, a carbenium ion  $R_m^+$  originates from feed molecule. The resulting carbenium ion  $R_{m+n}^+$  undergoes  $\beta$ -scission as usual to produce an alkene  $A_p$  and another carbenium ion  $R_{m+n-p}^+$ . Hydrogen transfer step occurs between the reactant alkane ( $R_mH$ ) and an oligomeric carbenium ion  $R_{m+n-p}^+$ . As a result, an alkane  $R_{m+n-p}H$  with carbon number larger than the feed is produced, together with a carbenium ion  $R_m^+$  which continues to enter into the reaction cycle.

The alkylation or the oligomerization step is favored by high alkene partial pressures and high surface carbenium ions concentrations, *i.e.*, high conversions. Coke deposition occurs when oligomerization is faster than  $\beta$ -scission, such that the size of the oligomer continues to grow and eventually cyclizes to form coke.<sup>71</sup>

## CHAPTER III

### EXPERIMENTS

#### 3.1 Equipment and Apparatus

##### Ovens and Furnace

The catalysts were crystallized at a desired temperature using a Memmert UM-500 oven. The solid samples were typically calcined in a Carbolite RHF 1600 muffle furnace in an air atmosphere. When a N<sub>2</sub> atmosphere is required, the solid samples were calcined instead in a split-tube furnace made in a laboratory.

##### X-ray Powder Diffractometer

XRD measurement was performed using a Rigaku D/Max-2200 X-ray powder diffractometer at Petroleum and Petrochemical College, Chulalongkorn University, with nickel filtered CuK<sub>α</sub> radiation (30kV, 30mA) at an angle of 2θ ranged from 5 to 50°. The scan speed was 5°/min, and the scan step was 0.02°. Scattering, divergent and receiving slits were fixed at 0.5°, 0.5° and 0.3 mm, respectively.

##### ICP-AES Spectrometer

Aluminum and sodium contents in the catalysts were analyzed using a Perkin Elmer Plasma-1000 inductively coupled plasma atomic emission spectrometer at the Scientific and Technological Research Equipment Center, Chulalongkorn University.

##### XRF Spectrometer

Cerium contents in the catalysts were determined using a SISON ARL 8410 X-ray fluorescence spectrometer at the Department of Scientific Services, Ministry of Science and Technology.

### **Surface Area Analyzer**

Specific surface area of a catalyst was determined using a Micromeritics adsorptometer, model Flowsorb 2300, at the Metallurgy and Materials Science Research Institute, Chulalongkorn University.

### **Gas Chromatograph**

Hydrocarbon gases were analyzed using a Shimadzu GC-9A gas chromatograph equipped with a 30-m long and 0.53-mm outer diameter Alumina-PLOT column. Liquid samples were analyzed using a Shimadzu GC-14A gas chromatograph equipped with 30-m long and 0.32-mm outer diameter HP-5 (0.25  $\mu\text{m}$  film thickness) column. All GC detectors are flame ionization detectors (FID).

### **The Catalytic Apparatus**

The catalytic apparatus for *n*-hexane cracking assembled in this laboratory comprises of a borosilicate tube reactor of 0.54-cm internal diameter, a laboratory-made split-tube furnace, a K-type thermocouple connected to a temperature programming assemble, a gas manifold, a gas-liquid saturator and a nitrogen gas cylinder. The catalytic apparatus was shown in Figure 3.1.

## **3.2 Chemicals and Gases**

Nitrogen gas of high purity grade were purchased from Thai Industrial Gases (TIG) and were additionally dehydrated by passing through a 40 cm x 2.5 cm tube of molecular sieve 4A. Cerium nitrate hexahydrate (99%+), cerium(IV) oxide (99.9%+), and tetrapropyl ammonium bromide, TPABr (98%+) were products of Aldrich. Sodium silicate solution (10.13 wt.%  $\text{Na}_2\text{O}$ , 29.71 wt.%  $\text{SiO}_2$ , 59.80 wt.%  $\text{H}_2\text{O}$ ) was kindly provided from Thai Silicate. Sodium aluminate was a product of Riedel-de Haën. *n*-Hexane (99%+) was from Aldrich. Standard solutions (1000 ppm) of cerium and sodium were obtained from Fluka. Standard gas mixture and liquid mixture for GC analysis was kindly obtained from Thai

Olefins. Other chemicals were from Merck, Fluka, or J. T. Baker, otherwise specifically identified.

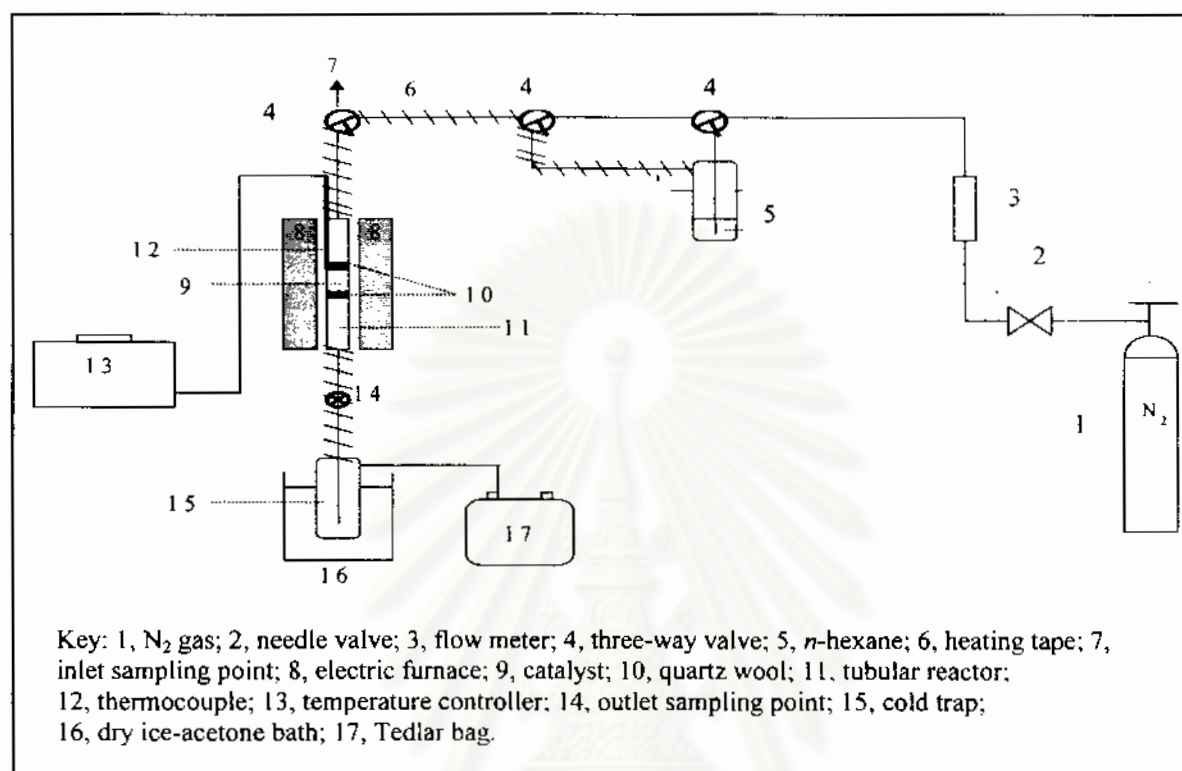


**Figure 3.1** Schematic diagrams of the catalytic apparatus for *n*-hexane cracking.

### 3.3 Synthesis of ZSM-5

The synthesis of ZSM-5 was developed in this work. It is a hydrothermal synthesis in a basic solution using a gel composition similar to that reported in an acidic solution developed by Szostak and Thomas.<sup>52</sup> The starting materials are different. Preparation diagram is shown in Figure 3.2. Two portions of solution were prepared. Solution A was obtained by dissolving 5.11 g of TPABr in 52.63 g of water. Simultaneously, solution B was prepared by dissolving 0.79 g of NaAlO<sub>2</sub> in 52.63 g of water. These two portions were stirred separately for an hour before dropwise addition of solution A into solution B using an addition funnel. The mixture was stirred additionally for one hour before it was added dropwise into a 4-neck round bottom flask containing 38.79 g of water glass. The resulting gel with molar composition of 1SiO<sub>2</sub>: 0.36Na<sub>2</sub>O: 0.025Al<sub>2</sub>O<sub>3</sub>: 0.10TPABr: 37.2H<sub>2</sub>O (SiO<sub>2</sub>/Al<sub>2</sub>O<sub>3</sub> molar ratio of 40, or Si/Al molar

ratio of 20), is mechanically stirred for 2 hours at 500 rpm. After that, pH of the gel is adjusted using concentrated  $\text{H}_2\text{SO}_4$  to a value of 10.5. The gel was statically crystallized in a  $150\text{-cm}^3$  Teflon lined stainless-steel autoclaveable vessel and heated under its autogenic pressure at  $170^\circ\text{C}$  for 4 days. For calculation see Appendix 1.

The solid product was separated from the solution by centrifugation and washed with deionized water until pH value of a centrifugate is equal to that of deionized water. The final product yields 11.09 g, *i.e.*, 96% yield based on weight of silica used initially.

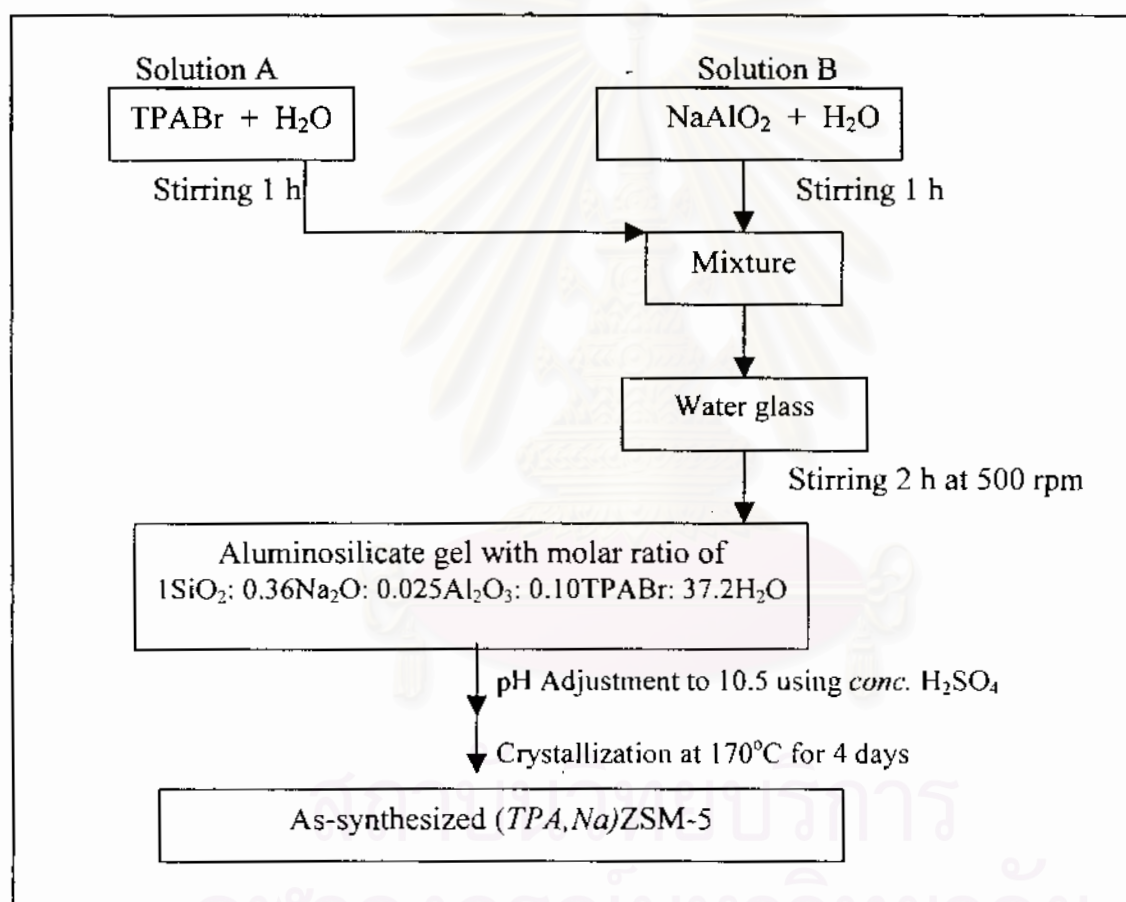


**Figure 3.2** Preparation diagram for the synthesis of ZSM-5.

### 3.4 Organic Template Removal

TPABr used in the preparation step of the catalysts as a template (or structure directing agent) was removed from the catalysts pores by converting to carbon dioxide at high temperature. The as-synthesized ZSM-5 was calcined in an muffle furnace from room

temperature to 600°C in a muffle furnace, and the temperature was maintained at 600°C for 12 h. The calcined zeolite obtained was denoted as (Na,H)ZSM-5. Heating programs for template removal and other purposes are shown in Figure 3.3.

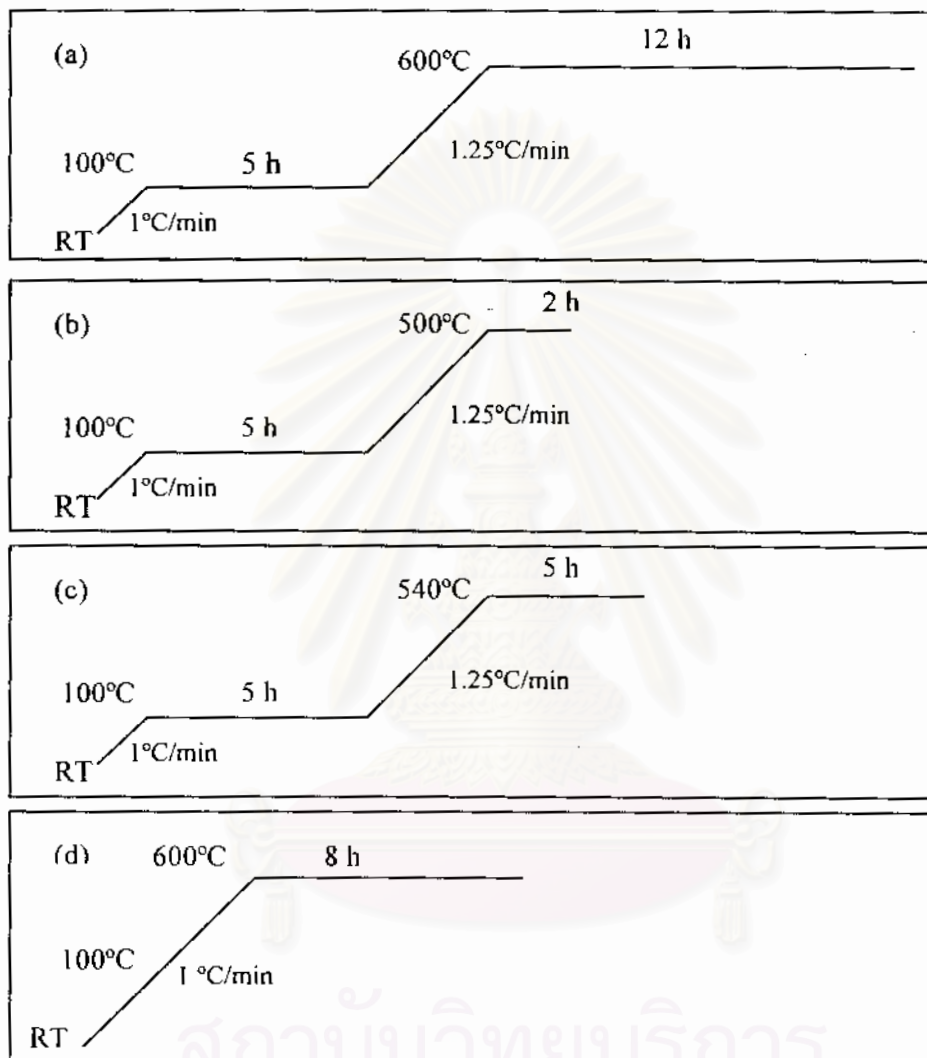


**Figure 3.3** Heating programs for (a) template removal, (b) thermal treatment of  $\text{Ce}^{3+}$  at a comparatively low temperature, (c) process (b) at high temperature and for ammonia removal, and (d) catalyst regeneration.

### 3.5 Cerium Ion Exchange

There are two  $Ce^{3+}$  ion exchange procedures conducted in this work. Each procedure is a two-step method comprising of a conventional aqueous ion exchange and thermal treatment. The ion exchange details are summarized in Table 3.1.

**Table 3.1**  $Ce^{3+}$  and  $NH_4^+$  ion exchange condition.<sup>a</sup>

Parameter	$Ce^{3+}$ (L) <sup>68</sup>	$Ce^{3+}$ (H)	$NH_4^+$
Cation source	$Ce(NO_3)_3 \cdot 6H_2O$	$Ce(NO_3)_3 \cdot 6H_2O$	$NH_4Cl$
Mol cation/ mol $Na^+$	0.9	5.0	50.0
[Cation]/ M	0.009	0.05	0.10
Duration/ h	2	24	1
Calcination program: Temp/ °C	500	540	540
Calcination program: Time/ h	2	5	5
Total times of two-step treatment	3	3	2

<sup>a</sup>1g zeolite/ 75mL  $H_2O$ ; reflux at boiling temperature.

The first one, hereafter referred to as low-loading (L) method, is as follows. Into a 1000-mL Erlenmeyer flask, 4.01 g of calcined (Na,H)ZSM-5 was added with 150 mL of water. A solution of 1.27 g of  $Ce(NO_3)_3 \cdot 6H_2O$  in 150 mL of water was subsequently added into the flask. The zeolite:water volume ratio was kept constant at 1:75, molar concentration of  $Ce^{3+}$  was 0.009 M,  $Ce^{3+}/Na^+$  molar ratio was kept constant at 0.9, i.e., 2.7 equivalent. For calculation see Appendix 2. A reflux of the resulting solution was carried out at boiling temperature for 2 hours. Slight difference from the reported method of Zhang and Flytzani-Stephanopoulos<sup>68</sup> was that refluxing temperature was raised from 85°C, and  $Ce^{3+}$  molar concentration was raised from 0.007 M. After completion of ion exchange, the treated zeolite was separated from the mother liquor by centrifugation, and was washed with deionized water until  $NO_3^-$  was not detected by a brown ring method utilizing  $FeSO_4$  and  $H_2SO_4$ . See Appendix 3 for details. The zeolite was air-dried overnight and, in order to activate the movement of  $Ce^{3+}$  cations into inner cavities of ZSM-5, was calcined at 500°C for 2 hours by



a heating program shown in Fig 3.3(b) in air using a muffle furnace. If an inert ( $N_2$ ) atmosphere was required, a sample was calcined in a quartz boat using a split-tube furnace made in this laboratory. The whole ion exchange procedure, aqueous ion exchange *plus* heat treatment, was repeated twice more.

Because the first method does not yield a cerium ion exchange level high enough, the second method has been invented and is hereafter referred to as high-loading (H) method. An amount of  $Ce(NO_3)_3 \cdot 6H_2O$  was increased such that molar concentration of  $Ce^{3+}$  was 0.05 M, and  $Ce^{3+}/Na^+$  molar ratio equaled 5.0, *i.e.*, 15 equivalent, and reflux time was lengthened to 24 hours. Moreover, the more severe activation condition was employed, *i.e.*, 540°C for 5 hours, as shown in Figure 3.3(c). The whole procedure was repeated twice as described above.

### 3.6 Ammonium Ion Exchange

Ammonium ion exchange details are summarized also in Table 3.1, and calculation is shown in Appendix 2. Into an Erlenmeyer flask, 3.75 g of calcined (Na,H)ZSM-5 was added with 140 mL of water. A solution of 7.65 g of  $NH_4Cl$  in 140 mL of water was subsequently added into the flask. The zeolite:water volume ratio was kept constant also at 1:75, molar concentration of  $NH_4^+$  was 0.50 M, and  $NH_4^+/Na^+$  molar ratio was 50.0. The resulting solution was refluxed at boiling temperature for an hour. The zeolite was then separated from the mother liquor by centrifugation, and was washed with deionized water until free from  $Cl^-$  as detected by silver nitrate. The treated zeolite was air-dried overnight and was calcined at 540°C for 5 hours by a program shown in Fig 3.3(c) in air atmosphere. The two-step treatment, *i.e.*, ion exchange plus calcination, was repeated once to give  $H^+$ -containing ZSM-5.

When Ce-containing NaZSM-5 in previous section was used as a starting material, proton form of Ce-containing ZSM-5 was obtained.

### 3.7 Sample Preparation for ICP-AES

In a 100-mL Teflon beaker, 0.0400 g of a calcined catalyst was soaked with 10 mL of 37% HCl and subsequently with 10 mL of 48% hydrofluoric acid to get rid of silica in the form of volatile SiF<sub>4</sub> species. The solid was heated, but not boiled, to dryness on a hot plate. The fluoride treatment was repeated twice more. An amount of 10 mL mixture of 6 M HCl: 6 M HNO<sub>3</sub> at a volume ratio 1:3 was added and further heated to dryness. An amount of 10 mL deionized water was added to the beaker and warmed for 5 minutes to complete dissolution. The solution was transferred to a 50-mL polypropylene volumetric flask and made to the volume by adding deionized water. The flask was capped and shook thoroughly. If the sample was not analyzed immediately, the solution would be then transferred into a plastic bottle with a treaded cap lined with a polyethylene seal.

### 3.8 Catalytic Cracking of *n*-Hexane

An amount of 0.1 g of each ground catalyst was pressed into a 0.7-mm thick self-supporting wafer using a stainless steel die of a 13-mm inner diameter, in the same manner as making KBr samples for IR measurement. The pressing force of 5 tons was held on a catalyst wafer for 4 min and then it was crushed into tiny pellets of a size 2 x 2 x 0.7 mm<sup>3</sup> approximately. A 0.1000-g portion of the tiny pellets ZSM-5 catalyst was loaded into the middle of a borosilicate tubular reactor having a diameter of 0.54 cm, and hold in place by a plug of quartz wool. The catalyst portion was also covered with small amount of quartz wool. The height of the loaded catalyst was 0.8 mm, resulting in a catalyst volume of 0.18 mL. A catalyst was then activated in the tubular reactor at the temperature of 500°C for 1 h under the nitrogen flow at 4.7 mL/min. Feed of 25% *n*-hexane in nitrogen was passed from the top through the catalyst at a gas-hourly space velocity (GHSV) of 2000 h<sup>-1</sup> (or 6.78 mL/min). For calculation of these values see Appendix 4. After the time on stream of 30 min, a 3- $\mu$ L portion of gaseous products was withdrawn from the catalytic line, at the septum point below

the catalyst location, by a gas tight syringe and was analyzed for *n*-hexane remained using a GC equipped with an Al<sub>2</sub>O<sub>3</sub>-PLOT column. At the same time liquid products were collected in a cold trap sunk in a dry ice/acetone bath, while gaseous products were collected in a Tedlar bag. Subsequently, liquid products in the cold trap were evacuated. The volatile liquid was analyzed. Coke content was determined by weight loss of a catalyst after catalyst regeneration by calcination program shown in Figure 3.3(d).

Catalysts were varied in order to investigate the effects of, for example, content and oxidation state of cerium, acidity (Na<sup>+</sup> vs. H<sup>+</sup>), *etc.*, in catalytic cracking of *n*-hexane. Blank experiment was performed without a catalyst, *i.e.*, having only quartz wool inside a tube reactor. Commercial CeO<sub>2</sub> was also tested in similar manner.



สถาบันวิทยบริการ  
จุฬาลงกรณ์มหาวิทยาลัย

## CHAPTER IV

### RESULTS AND DISCUSSION

#### 4.1 As-Synthesized (TPA,Na)ZSM-5

ZSM-5 zeolite ( $\text{SiO}_2/\text{Al}_2\text{O}_3$  molar ratio of 40, or Si/Al of 20) was synthesized by the recipe described in Section 3.3. An *as-synthesized* product possessing TPA<sup>+</sup> and Na<sup>+</sup> at nonframework position is labeled (TPA,Na)ZSM-5. It was a white solid having X-ray diffraction pattern characteristic of an MFI phase<sup>47</sup> as shown in Table 4.1 and Figure 4.1(a). Prominent peaks are, for example, those at  $2\theta$  of 7.92, 8.82, 23.10, 23.66, 23.92, and 24.38°. The method was found successful and was highly reproduced. Eleven attempts in this work all yield an MFI phase. Crystallinity of ZSM-5 synthesized from different batches, calculated by summing the intensity at  $2\theta$  of 23.0 to 25.0° (not shown), differs within 10%. The difference was acceptable considering the limitation of quantitative analysis by an XRD technique.

During synthesis the gel pH was originally, on average, 11.8. After pH adjustment to 10.5 and subsequent crystallization at 170°C for 4 days, the mother liquor had a pH value of 11.2 to 12.4. Change in pH value was observed earlier in the literature.<sup>4</sup> The pH of the gel does not relate directly to the total OH content of the system. Instead, it dictates the presence of free OH in the system. Silica in the gel mixture can exist in various forms<sup>4</sup> such as orthosilicates  $\text{SiO}_4^{4-}$ , dimeric silicates  $\text{Si}_2\text{O}_7^{6-}$ , and larger silicates with cyclic  $(\text{SiO}_3)_n^{2n-}$ . The rise in pH is attributed to the incorporation of  $\text{SiO}_2$  unit into the zeolite framework. As the

crystals grow, the ratio of free OH/SiO<sub>2</sub> rises. This reason can be accounted for an increase in pH value after crystallization, *i.e.*, 10.5 to a range from 11.2 to 12.4.

**Table 4.1** Selected  $2\theta$  of ZSM-5 with different treatment.

Sample	2theta/ degree						
(a) Effect of calcination							
(TPA,Na)ZSM-5	7.92,	8.82,	23.10,	23.66,	23.92,	24.38	
(Na,H)ZSM-5	7.90,	8.78,	23.02,	23.24,	23.66,	23.90,	24.36
(b) Effect of ion exchange							
(Na,H)ZSM-5	7.90,	8.80,	23.02,	23.26,	23.68,	23.90,	24.38
3-time exchanged CeNaZSM-5	7.90,	8.78,	23.02,	23.24,	23.66,	23.90,	24.36
HCeZSM-5	7.90,	8.78,	23.02,	23.26,	23.68,	23.90,	24.36

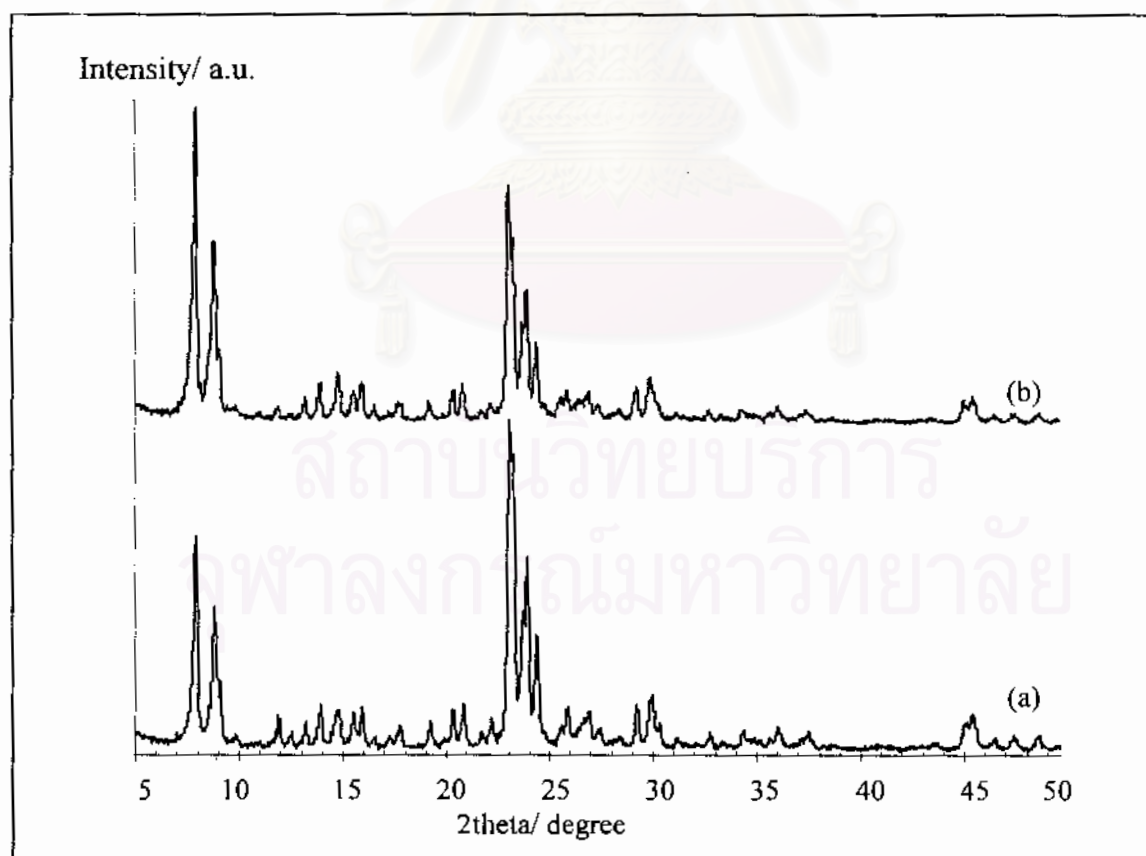


**Figure 4.1** A representative XRD pattern of (a) as-synthesized, and (b) calcined ZSM-5 zeolite.

The synthetic recipe developed in this work will be compared to that reported in the patent by Arguer and Landolt<sup>47</sup> as follows. The ratio  $\text{OH}^-/\text{SiO}_2$  is 0.66,  $\text{H}_2\text{O}/\text{OH}^-$  is 56, and  $\text{SiO}_2/\text{Al}_2\text{O}_3$  is 40. These values are within the particularly preferred range for formation of ZSM-5, see Table 2.3. Using the recipe for ZSM-5 synthesis developed in this work, the fraction of template over total cationic species,  $(n\text{-C}_3\text{H}_7)_4\text{N}^+/\{(n\text{-C}_3\text{H}_7)_4\text{N}^+ + \text{Na}^+\}$ , is 0.12. This value is lower than that reported by Arguer and Landolt<sup>47</sup> (0.4-0.9). The developed method has an advantage that it employs less amount of expensive tetrapropyl ammonium bromide.

Starting from 38.79 g of water glass (10.13 wt.%  $\text{Na}_2\text{O}$ , 29.71 wt.%  $\text{SiO}_2$ , 59.80 wt.%  $\text{H}_2\text{O}$ ) as described in Section 3.3, the solid obtained was 11.09 g. The (as-synthesized) solid yield was 96% based on weight of silica used initially. Van Grieken<sup>54</sup> found that  $\text{SO}_4^{2-}$  from  $\text{Al}_2(\text{SO}_4)_3$  yield 90.8% of ZSM-5 product, whereas a yield of 82.9 and 75.1% were obtained from  $\text{Al}(\text{NO}_3)_3$  and  $\text{Al}(\text{iso-OC}_3\text{H}_7)_3$ , respectively. Effect of anions other than  $\text{OH}^-$  was discussed before in Section 2.2.2. It may be possible that  $\text{SO}_4^{2-}$  from  $\text{H}_2\text{SO}_4$  in this work exerts a similar effect.

The ZSM-5 zeolite synthesized has Si/Al molar ratio in product close to the value in the gel, *i.e.*,  $20.1 \pm 1.7$  vs 20.

#### 4.2 Calcined (Na,H)ZSM-5

The template molecules entrapped in the pores of the zeolite must be removed such that there is free space available for various applications, *e.g.*, ion exchange and catalysis.  $\text{TPA}^+$  cations used in the ZSM-5 synthesis, Section 3.3, were removed by calcination at  $600^\circ\text{C}$  for 12 h as shown in Figure 3.3(a). The zeolite was first heated from room temperature to  $100^\circ\text{C}$  and held at  $100^\circ\text{C}$  for 5 h in order to *gently* remove water adsorbed. Low heating rate ( $1^\circ\text{C}/\text{min}$ ) prevented water from reacting with an active  $\text{AlO}_2^-$ . The zeolite was further heated to  $600^\circ\text{C}$  ( $1.25^\circ\text{C}/\text{min}$ ), and the heating was held at this temperature for 12 h to oxidatively burned out the organics inside. Careful heating at  $600^\circ\text{C}$  as conducted in this work would not

affect the crystallinity of ZSM-5, since Arguer and Landolt<sup>47</sup> has shown that 100% crystallinity was still attained after 927°C calcination in air for 10 h.

Characteristic  $2\theta$  and the XRD pattern of calcined ZSM-5 are shown in Table 4.1 and Figure 4.1(b), respectively. The calcined material is labeled  $(Na,H)ZSM-5$ . Some of the prominent changes of calcined  $(Na,H)ZSM-5$  compared to the as-synthesized  $(TPA,Na)ZSM-5$  are (1) diffraction peaks shifted to the lower  $2\theta$  value, for example, 7.92 to 7.90, 8.82 to 8.78, 23.92 to 23.90, and 24.38 to 24.36°; (2) the peak at  $2\theta$  of 23.10 split into two peaks at 23.02 and 23.24°; and (3) *relative* intensity at  $2\theta$  of 7.9 and 23.1 (or 23.0°) changed apparently. The first peak gained in intensity whereas the last peak loss.

XRD peak shift after calcination was observed earlier. Wu *et al.*<sup>72</sup> showed that the XRD pattern of the as-synthesized sample, originally belong to an orthorhombic symmetry (Section 2.1.2), changed to a monoclinic symmetry when calcined,  $NH_4^+$  ion exchange, and calcined again. The simulated *monoclinic* diffraction pattern, including the doublet nature and the change in relative intensity, item (2) and (3) above respectively, fit well with the observed for  $HZSM-5$ . Wu *et al.*<sup>72</sup> computed that lattice parameter  $a$  increased from 20.07 to 20.11–20.17 Å. For monoclinic symmetry, an increase in the parameter  $a$  resulted in an increase in interplanar spacing  $d$ . Therefore, according to Bragg's equation ( $n\lambda = 2d\sin\theta$ ),  $2\theta$  can shift to lower position.

This symmetry change involves minor displacements of atomic positions and is controlled either by the presence of extraframework species such as template, water,  $Na^+$ , or by framework species such as Al.<sup>72</sup> Wu *et al.*<sup>72</sup> did not observed a symmetry change in  $NaZSM-5$  (Si/Al=800) because of inhibition by too high sodium content (2.2 wt%  $Na_2O$ ). However, they stated that when the sodium oxide content was reduced to below 0.03 wt%  $Na_2O$ , such a symmetry change was observed. Such a change was observed in this work, *i.e.*, for  $(Na,H)ZSM-5$  (Si/Al=20) with 1.8wt%  $Na_2O$  content, Figure 4.1(b).

### 4.3 Elemental Analysis of (Na,H)ZSM-5

Composition of a zeolite was determined by acid digestion using HCl, HF, and HNO<sub>3</sub> as described in Section 3.7. The aluminum and sodium contents were determined by inductively-coupled plasma atomic emission spectroscopy (ICP-AES). Silicon content cannot be determined upon this sample preparation, because it was transformed to a volatile SiF<sub>4</sub> species during digestion. Therefore concentration of Si was determined by subtraction of the weight of freshly calcined zeolite with that of AlO<sub>2</sub> and Na<sub>2</sub>O.

According to ICP-AES, ZSM-5 zeolites synthesized from different batches (Section 4.1) had Si/Al molar ratio of  $20.1 \pm 1.7$ . This compares well with the value in the gel (Si/Al=20). Elemental analysis, together with XRD results in Section 4.1, give evidence that this developed method was able to synthesize ZSM-5 reproducibly. Even with Si/Al molar ratio of 40 can be synthesized using this procedure.<sup>51</sup>

Concerning Na/Al ratio, values of  $1.0 \pm 0.3$  were found. However, this ratio depended either on the history, *i.e.*, ZSM-5 from different batches may naturally exhibited different Na/Al, or on the number of washing during the work up step. Washing a zeolite thoroughly to eliminate excess sodium cations is crucial, since excess sodium in the form of Na<sub>2</sub>O, Na/Al > 1, may block the entrance for ion exchange or catalysis. Na<sub>2</sub>O may make the exchange solution basic. As a result, Ce<sup>3+</sup> cations may not undergo ion exchange into the zeolite, but instead precipitate out at the external surface, see Equation 2.4.

An explanation which can be accounted for the case of Na/Al < 1 is as follows. TPA<sup>+</sup> cations may not transform solely to CO<sub>2</sub> and H<sub>2</sub>O, but also to H<sup>+</sup>, Section 2.1.4.<sup>4</sup> In a review by Szostak,<sup>4</sup> the calcined ZSM-5 was reported to contain about 17% H<sup>+</sup>, with the remainder of the cations being sodium. Since moles of Na<sup>+</sup> (0.124) greatly exceed those of TPA<sup>+</sup> (0.01919), after calcination, the zeolite should *largely* have Na<sup>+</sup> as a counter ion. The notation for calcined ZSM-5, *e.g.*, (Na,H)ZSM-5, was used earlier in Section 4.2.



#### 4.4 Preparation of HZSM-5

HZSM-5 was prepared by  $\text{NH}_4^+$  ion exchange of the parent calcined (Na,H)ZSM-5 using the method in Section 3.6. Elemental analysis of HZSM-5 and the parent (Na,H)ZSM-5 from the same synthetic batch is shown in Table 4.2.

**Table 4.2** Chemical composition of (Na,H)ZSM-5 and HZSM-5.

Sample	Si/Al	Wt%Na <sub>2</sub> O
(Na,H)ZSM-5	21.7	1.81
HZSM-5	20.5	0.11

From Table 4.2, Si/Al ratio of the zeolite remains fairly constant, *i.e.*, 20.5 to 21.7. The difference is herein considered insignificant. However, sodium content is greatly decreased by this process as shown by wt%Na<sub>2</sub>O which drops from 1.81 to 0.11%. Hydrogen content cannot be determined directly by ICP-AES, but can be calculated by the decrease of sodium content. An ion exchange level of 94% is achieved.

This result agrees quite well with that for zeolite Y reported by Occelli and Ritz.<sup>73</sup> They showed that a 1-h  $\text{NH}_4^+$ -exchange resulted in a decrease of wt% Na<sub>2</sub>O in zeolite REY from 3.30 to 0.41%, *i.e.*, 88% ion exchange level. A prolong treatment, 10-h ion exchange, gave the same sodium content to that of 1-h. Similarly, another sample in this work (not shown in the table) where a 24-h  $\text{NH}_4^+$ -ion exchange was done three times without any intermediate calcination, a level of only 86% was achieved. According to Occelli and Ritz, when zeolite REY containing 0.41 wt%Na<sub>2</sub>O was calcined at 500°C for 2h *prior to* the second exchange, the sodium content was further reduced to 0.11, *i.e.*, 97% ion exchange. The same calcination temperature was utilized in this work. As mentioned in Section 2.1.4, high temperature results in thermal decomposition of  $\text{NH}_4^+$  to  $\text{NH}_3$  and proton. In addition, the sodium ions, by thermal activation, migrate from the constrained sites to the more available

sites which exchanging ions like  $\text{NH}_4^+$  ions can be accessible. The same explanation should also hold true for ZSM-5 zeolite in this present work.

#### 4.5 Quantitative Analysis of Cerium

It was soon realized in this work that quantitative analysis of cerium using ICP-AES described in Section 4.3, which worked well for Al, Na (and also Si), gave values quite low from those expected. A comparative study for cerium determination was therefore conducted between two techniques: ICP-AES and X-ray fluorescence spectroscopy (XRF). ICP-AES was able to determine Al, Na, and Ce directly from the acid-digested solution. Silicon concentration was determined as described in Section 4.3 above. XRF analysis was able to detect all interested elements, *i.e.*, Al, Na, Ce, including Si.

Silica gel  $\text{SiO}_2$  (Merck), activated  $\text{Al}_2\text{O}_3$  (Aldrich), and  $\text{CeO}_2$  (99.9+%, Aldrich), were separately placed in a  $200^\circ\text{C}$ -preheated oven for 2 h in order to expel adsorbed water. After that they were mixed in a desired proportion and ground thoroughly. Three standards (I, II, and III) having composition (wt%) as shown by the black bar in Figure 4.2(a) to (c) were prepared with concentrations of  $\text{SiO}_2$ ,  $\text{Al}_2\text{O}_3$ , and especially  $\text{CeO}_2$ , as close as possible to the concentration speculated in the samples, *i.e.*, 91.27-93.92 % $\text{SiO}_2$ , 4.38-4.87 % $\text{Al}_2\text{O}_3$ , and 1.28-3.89 % $\text{CeO}_2$ . Results are shown in Figure 4.2.

Concerning aluminum content, Figure 4.2(a), results obtained by ICP-AES corresponded well to the value prepared. On the contrary, XRF gave low Al content. This may be due to the limitation of light atom analysis by the XRF machine. For quantitative analysis of cerium, Figure 4.2(b), values from XRF were similar to those prepared, whereas those from ICP were very low. Note that the difference was apparently highlighted in Standard I with high  $\text{CeO}_2$  content (3.86 wt%).

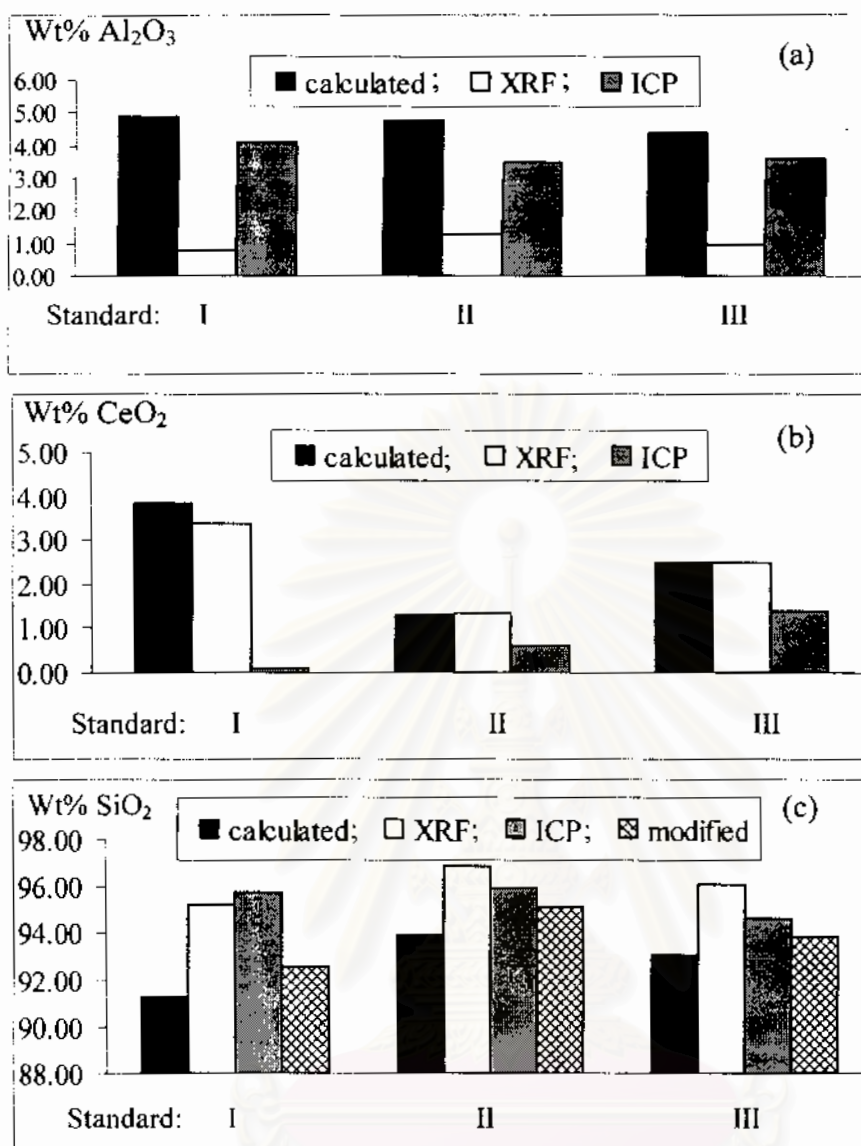


**Figure 4.2** Elemental analysis result (wt%) of the different standards: (a) Al<sub>2</sub>O<sub>3</sub>, (b) CeO<sub>2</sub>, and (c) SiO<sub>2</sub>. SiO<sub>2</sub>(modified) = 100 - Al<sub>2</sub>O<sub>3</sub>(ICP) - CeO<sub>2</sub>(XRF).

Figure 4.2(c) illustrates the Si content. For XRF this value can be determined directly from the fluorescence intensity, and the results are far from the values calculated. For ICP-AES, however, Si was determined by subtracting a value of 100% with Al<sub>2</sub>O<sub>3</sub> and CeO<sub>2</sub> content. Since cerium contents were found very low by ICP-AES, Si content was therefore relatively high. Moreover, the assumption that there were only Al, Na, Si, and Ce in Ce<sup>3+</sup>-exchanged zeolite now seemed less acceptable. Ce(NO<sub>3</sub>)<sub>3</sub>·6H<sub>2</sub>O used also contained 1-2% La as an impurity. Taken into account that analysis of Al and Ce from ICP-AES and XRF,

respectively, gave reasonable results, calculation of Si content can be modified by subtracting 100% with these values. Figure 2.4(c) showed that this calculation indeed was acceptable.

The last component to be mentioned was sodium. The question arose whether XRF can determine Na<sup>+</sup> concentration accurately or not. In one sample having 62.1% Ce<sup>3+</sup> ion exchange level (found by XRF), wt%Na<sub>2</sub>O was found by ICP-AES, and XRF to be 1.04 and 1.00%, respectively. However, when the same sample was repeated for XRF analysis, Na<sub>2</sub>O cannot be detected. It was therefore decided to use sodium content from ICP-AES analysis.

In conclusion, for quantitative analysis of catalysts in this work, aluminum and sodium contents were determined by ICP-AES. Cerium content was determined by XRF. Si content, *in case of (Na,H)ZSM-5*, was evaluated by subtraction of 100 with Al<sub>2</sub>O<sub>3</sub> and Na<sub>2</sub>O content found from ICP-AES. For *Ce<sup>3+</sup>-exchanged ZSM-5*, however, subtraction of 100 with Al<sub>2</sub>O<sub>3</sub> and Na<sub>2</sub>O (both from ICP-AES) *and* CeO<sub>2</sub> (from XRF) should be performed instead. This type of calculation was used throughout this study.

#### 4.6 Preparation of CeNaZSM-5

A reflux of a slurry of parent *(Na,H)ZSM-5* in aqueous solution of Ce<sup>3+</sup> with various concentrations was carried out at various periods of time as shown by Method L and H in Table 3.1. Condition of method H was more severe than that of method L. Values of Si/Al, wt%Na<sub>2</sub>O, and %cerium ion exchange of both parent calcined *(Na,H)ZSM-5* and *CeNaZSM-5* are shown in Figure 4.3. Values for *HCeZSM-5*, which will be mentioned in Section 4.7, are also shown for comparison.

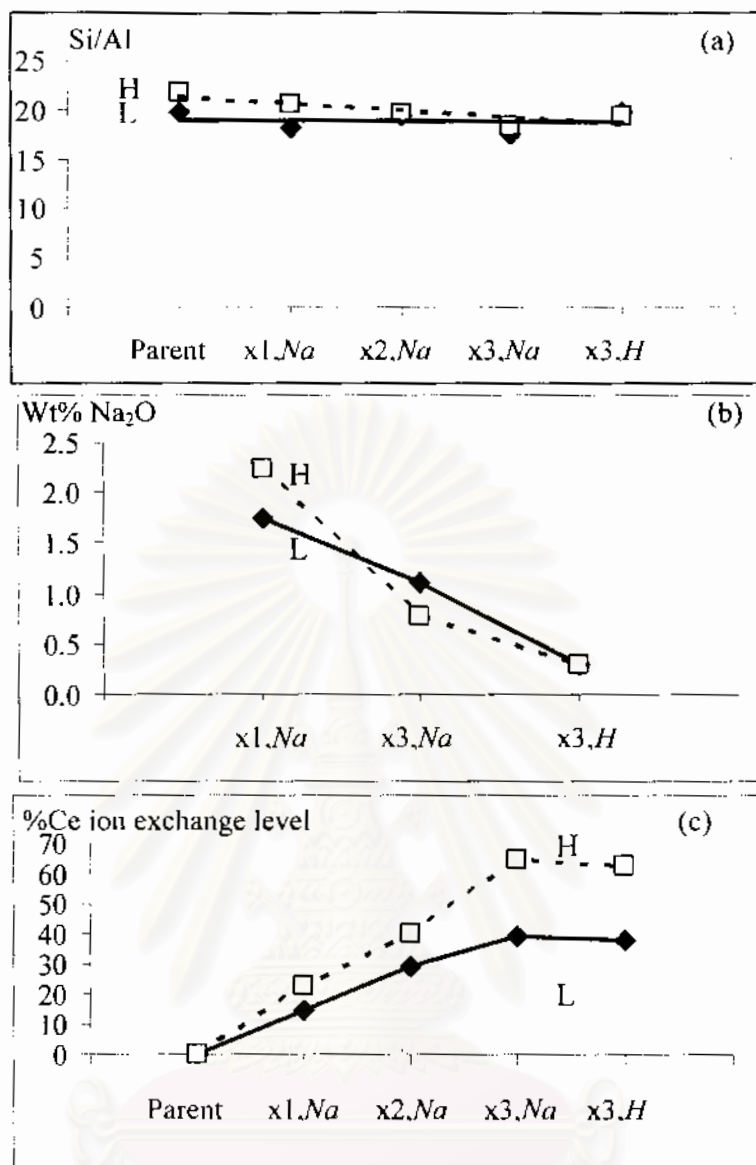


**Figure 4.3** Elemental analysis of parent and cerium-containing ZSM-5: (a) Si/Al, (b) wt%Na<sub>2</sub>O, and (c) percentage cerium ion exchange level. (x1.Na is denoted for parent, calcined (Na,H)ZSM-5 ion exchanged once with Ce<sup>3+</sup>, and others are assigned similarly.)

#### 4.6.1 Si/Al and Sodium Content

The Si/Al molar ratio, Figure 4.3(a), was found relatively constant throughout the ion exchange process. For H and L series, Si/Al range from 17.5 to 19.9, and 18.4 to 21.8, respectively. The deviation from one to another point within the same series was considered

insignificant. The starting zeolite was from different batch; therefore, Si/Al varied inherently as already mentioned in Section 4.3.

In  $\text{Ce}^{3+}$  ion exchange, aqueous  $\text{Ce}^{3+}$  will substitute for  $\text{Na}^+$  inside (Na,H)ZSM-5. As a consequence, sodium content should decrease as ion exchange process progresses. This decrease was indeed observed and is shown in Figure 4.3(b). For example, 1- and 3-time exchanges give wt% $\text{Na}_2\text{O}$  of 2.24 and 0.77, respectively, for method H, and 1.75 and 1.12, respectively, for method L. Similarly to the case of Si/Al, wt% $\text{Na}_2\text{O}$  of a given zeolite varies from batch to batch. However, sodium content in a zeolite treated by method H decreases at a faster rate than that by method L. This is reasonable since introduction of  $\text{Ce}^{3+}$  by method H is more effective than method L.

#### 4.6.2 Cerium Ion Exchange Level

The most important value certainly was the cerium ion exchange level. Theoretically if all Al atoms were at tetrahedral position in a zeolite and possessed negative charges, complete  $\text{Ce}^{3+}$  ion exchange would result in Ce/Al ratio of 1/3, *i.e.*, 33% based on aluminum. For convenience, however, the value was calculated by  $3 \times (\text{Ce}/\text{Al}) \times 100\%$ , such that a complete  $\text{Ce}^{3+}$  ion exchange would yield  $3 \times (1/3) \times 100\%$ , or 100%. This exchange level was utilized throughout the study.

As shown in Figure 4.3(c), ion exchange level increased steadily as a function of times of exchange. Method L was slightly modified from the reported method of Zhang and Flytzani-Stephanopoulos<sup>68</sup> such that the refluxing temperature was raised from 85°C to boiling temperature, and  $\text{Ce}^{3+}$  molar concentration was raised from 0.007 to 0.009 M. Values for 1, 2, and 3 times of ion exchange from method L and from Zhang and Flytzani-Stephanopoulos<sup>68</sup> were 14, 29, and 39%, and of 11, 26, and 60%, respectively. Generally with one exception, the present work yields higher  $\text{Ce}^{3+}$  level because it employs a slightly more severe condition.

For 3-time ion exchange where less  $\text{AlO}_2^-$  tetrahedra were available, it may be possible that washing, which varies from one laboratory to another, is the source for this discrepancy. Exhaustive washing of a zeolite *in this work*, until free from  $\text{NO}_3^-$  as described in Section 3.5, washes out loosely bound  $\text{Ce}^{3+}$ . As a result, cerium ion exchange level of 39%, compared to the value by Zhang and Flytzani-Stephanopoulos<sup>68</sup> of 60%, was found. Indeed, based on ICP-AES, SEM/EDX, and XPS results, Zhang and Flytzani-Stephanopoulos<sup>68</sup> believed that the higher uptake of Ce in the third exchange must be due to surface deposition rather than true ion exchange. Cerium leaching was also reported by Berry *et al.*<sup>55</sup> They showed that EXAFS amplitude of  $\text{Ce}^{3+}$ -exchanged Y zeolite was reduced by *ca.* 20% when the zeolite was washed with  $\text{NH}_4\text{Cl}$ , compared with that of the freshly prepared sample.

Because a level of only 39% was achieved by method L, method H was introduced. The latter differs from the former in several manners. Firstly, there existed higher concentration of  $\text{Ce}^{3+}$  in method H, *i.e.*,  $\text{Ce}^{3+}/\text{Na}^+$  molar ratio of 5.0 was used instead of 0.9 as in method L. Secondly, refluxing time was lengthen from 2 to 24 hours. Finally, a zeolite was calcined at higher temperature and at a longer time, *i.e.*,  $540^\circ\text{C}$  for 5 h instead of  $500^\circ\text{C}$  for 2 h. See Figure 3.3(c) and (b) respectively. Using method H, levels of 23, 40, and 65% were achieved for 1, 2, and 3-time ion exchange. Method H provided 1.5 times higher cerium content than the reported<sup>68</sup> method *which was reproduced* in this work.

Enhancement of cerium content by an increase in  $\text{Ce}^{3+}/\text{Na}^+$  molar ratio, and of reflux time, can be easily understood. The former provides more  $\text{Ce}^{3+}$  available in the solution, whereas the latter provides more time for a reaction to take place. It is well known that heat treatment of a zeolite can activate  $\text{Na}^+$  to migrate from the constrained sites to the accessible sites. As a result, cerium ions were then ion exchanged with  $\text{Na}^+$  ions located at the accessible sites. Berry *et al.*<sup>55</sup> found that EXAFS spectra of  $\text{Ce}^{3+}$ -exchanged Y zeolite heated *in vacuo* at  $300^\circ\text{C}$  differed from that of the parent sample. Fitting parameters showed the appearance of a new shell of Si atoms, suggesting that the cerium ions were more strongly bound to the zeolite framework. Heat treatment and repeated ion exchange are generally used

to obtained high cerium-loading zeolite, for example, in zeolite ZSM-5,<sup>61,64,68-70</sup> and zeolite Y.<sup>55,74</sup>

Fully exchanged CeZSM-5 was difficult to prepare, although various attempts described above have been done. Van Kooten *et al.*<sup>69</sup> gave three reasons to explain this observation. Firstly, the hydrated  $\text{Ce}^{3+}$  cation has large radius (5.8 Å) compared to the channel of ZSM-5 (5.4 x 5.6 and 5.1 x 5.4 Å, Section 2.1.2). Secondly, the water ligands have a strong affinity to cerium. Finally, the trivalent  $\text{Ce}^{3+}$  cation is not able to effectively neutralize the negative charges far apart from each other on the framework (which is in this case ZSM-5 with Si/Al ~ 20).

Additionally, Weyrich *et al.*<sup>70</sup> proposed cerium hydrolysis as another source of incomplete exchange. The hydrolysis, Figure 2.5, produces proton and cerium species with an effective charge of less than 3. For example,  $\text{Ce}(\text{H}_2\text{O})^{3+}$  dissociates to  $\text{Ce}(\text{OH})^{2+}$  and  $\text{H}^+$ . The hydroxo complex  $\text{Ce}(\text{OH})^{2+}$  is able to dissociate more to  $\text{CeO}^+$  and another  $\text{H}^+$ . Proton produced participates in ion exchange also, resulting in only a fraction of Ce that is truly ion-exchanged for  $\text{Na}^+$  in the zeolite.

#### 4.7 Preparation of HCeZSM-5

HCeZSM-5 zeolite was prepared by  $\text{NH}_4^+$ -ion exchange of the 3-time ion exchanged CeNaZSM-5 by the method described in Section 3.6. The notation implies that ZSM-5 was first exchange with  $\text{Ce}^{3+}$  before the remaining  $\text{Na}^+$  counter ions were further exchanged and converted to  $\text{H}^+$ .

##### 4.7.1 Si/Al and Sodium Content

Similar to CeNaZSM-5 (Section 4.6.1), Si/Al molar ratio of HCeZSM-5 did not considerably change from that of the parent zeolite, Figure 4.3(a). Considering sodium content in Figure 4.3(b), wt% $\text{Na}_2\text{O}$  greatly decreased from 3-time exchanged CeNaZSM-5 to



*HCeZSM-5*. For example, it dropped from 1.12 to 0.31, and 0.77 to 0.30 wt%Na<sub>2</sub>O for 3-time exchanged *CeNaZSM-5* prepared by method L and H, respectively. Although there were originally different amounts of sodium content left (1.12 vs 0.77), finally there existed an upper limit of ammonium exchange by this method, resulting in *ca.* 0.30 wt%Na<sub>2</sub>O unexchanged. However, this content is considered low and is adequate for use in catalytic study.

#### 4.7.2 Cerium Ion Exchange Level

Cerium content in *HCeZSM-5* was shown in Figure 4.3(c). Ion exchange levels for L and H series of *HCeZSM-5* were 38 and 62%, respectively. These values were nearly identical to those of the respective 3-time exchanged *CeNaZSM-5*, 39 and 65%. As mentioned above, ammonium ion exchange was effective in reducing sodium content, but it hardly affected cerium content. The first explanation is that cerium ions, which move to inner positions,<sup>73</sup> cannot be back-exchanged due to its large *hydrated* size. Another possible explanation is that Ce<sup>3+</sup> cations have higher charge, therefore binding the negative framework strongly, whereas Na<sup>+</sup> cations with less charge were forced to leave the zeolite.

#### 4.8 Crystallinity of Cerium-Containing ZSM-5

Selected two theta of a parent, calcined (*Na,H*)ZSM-5, 3-time exchanged *CeNaZSM-5*, and *HCeZSM-5* are shown in Table 4.1. The XRD patterns are shown in Figure 4.4.

Peak positions of (*Na,H*)ZSM-5 in Table 4.1(b) correspond quite well to those cited in Table 4.1(a) synthesized from different batches. See also Figure 4.4(a) and 4.1(a). This finding further supports the validity of the present ZSM-5 synthesis developed in this work.<sup>51</sup> Features described before in Section 4.2 for calcined (*Na,H*)ZSM-5, *i.e.*, shifted peak position to the lower 2θ value, splitting of the peak at 2θ of 23.10°, and change in *relative* intensity at

$2\theta$  of 7.9 and 23.1 (or  $23.0^\circ$ ) are all observed. Summation of peak intensity at  $2\theta$  of  $23.0$ - $25.0^\circ$  was calculated and was relatively assigned as the zeolite crystallinity of 100%.

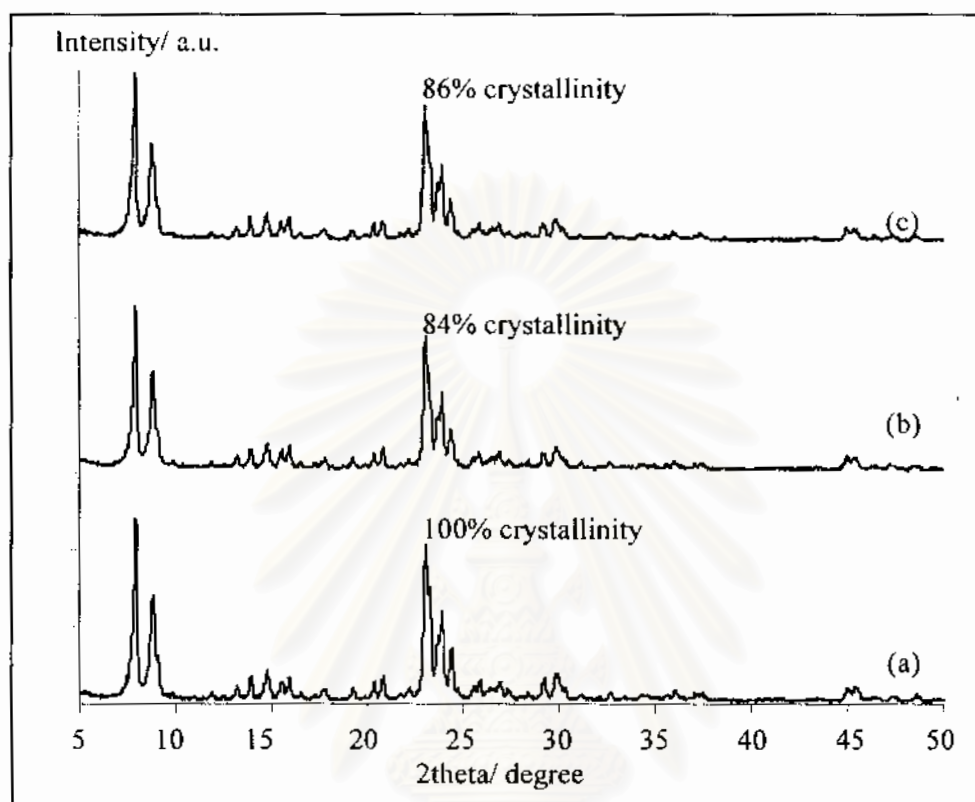


**Figure 4.4** XRD pattern of (a) parent, calcined ( $Na,H$ )ZSM-5, (b) 3-time exchanged  $CeNaZSM-5$ , and (c)  $HCeZSM-5$  prepared from (b).

For 3-time exchanged  $CeNaZSM-5$  sample, some of its peak positions further shifted to lower two theta compared to the untreated one. For example, those at  $8.80$  shifted to  $8.78$ ,  $23.26$  to  $23.24$ ,  $23.68$  to  $23.66$  and  $24.38$  to  $24.36^\circ$ . A reduction in peak position, or equivalently an increase in  $d$  spacing, of the  $RE$ -exchanged ZSM-5 was observed before by Argauer and Landolt.<sup>47</sup> A prolong treatment for this sample, 3 times 24-h  $Ce^{3+}$  ion exchange plus 3 times 5-h heat treatment at  $540^\circ C$ , does not severely affect the crystallinity (84%).

The last sample to be described was  $HCeZSM-5$ . Some of the peaks in  $HCeZSM-5$  shifted back to the original position in ( $Na,H$ )ZSM-5 when  $Na^+$  was replaced by  $H^+$ . For example, those at  $2\theta$  of  $23.24$  shifted to  $23.26$ , and  $23.66$  to  $23.68^\circ$ . Similar observation was

reported before in H- and rare earth ion-exchanged ZSM-5.<sup>47</sup> In this study, treatment of the parent zeolite for 3 times of 24-h  $Ce^{3+}$  exchange, 2 times of 5-h heat treatment at 540°C, 2 times of 1-h  $NH_4^+$  exchange, and finally 2 times of 2-h heat treatment at 500°C was performed to obtain HCeZSM-5. However, it still possesses rather high crystallinity up to 86% as shown in Figure 4.4(c). Decrease in crystallinity after multivalent ion exchange is well known in zeolites. For example, van Kooten *et al.*<sup>69</sup> found a linear decrease in intensity of CeNaZSM-5 as a function of cerium content found in the exchanged zeolite. CeNaZSM-5 at 70% exchange level was found to have 80% crystallinity compared to the parent ZSM-5.<sup>69</sup> Approximately, it is in agreement with the present results, *i.e.*, CeNaZSM-5 at 65% exchange level has 84% crystallinity compared to the parent (Na,H)ZSM-5.

In both CeNaZSM-5 and HCeZSM-5, no other crystalline phases was detected though cerium ion exchange degree as high as ~ 65%, *i.e.*, 3.30 wt%  $CeO_2$ , was achieved. This was as expected, since  $Ce^{3+}$  was introduced in cation forms. The cations with positive charges should be stabilized by an interaction with framework negative charges, thus preventing them to bind to each other and form cerium-containing *crystalline* phases, *e.g.*,  $Ce_2O_3$  or  $CeO_2$ . The absence of these phases in CeNaZSM-5 was reported by others as well.<sup>64,68,69</sup> On the contrary, Yokoyama and Misono<sup>75</sup> observed very weak broad peaks of  $CeO_2$  in Ce(60%)NaZSM-5, together with the decrease in peak intensity of the ZSM-5 to one third of the parent material. Clearly their zeolite was severely destroyed. The discrepancy should be due to different procedures. Yokoyama and Misono<sup>75</sup> performed  $Ce^{3+}$  ion exchange at 150°C and 4 atm in an autoclave, whereas this work and others<sup>64,68,69</sup> did at temperature not higher than boiling temperature and at 1 atm.

#### 4.9 Catalytic Cracking of *n*-Hexane

*n*-Hexane was catalytically transformed to light olefins over various catalysts, *e.g.*,  $CeO_2$ , Na- and HZSM-5 containing cerium in various amounts. Ce-containing catalyst is given a code as Ce(*X*%)NaZSM-5, where *X* is the Ce ion exchange level. For CeZSM-5

possessing  $H^+$  as a counter ion, the code will be  $HCe(X\%)Z$ . The notation  $CeNa$  and  $HCe$ , are used to identify the sequence of ion exchange step, *i.e.*, Na to Ce, and (Na, Ce) to (H, Ce), respectively. Additionally, the variation in preparation procedure, whether the materials were calcined in air or  $N_2$  during the heat treatment step, is also studied.  $N_2$ -calcined samples contain an asterisk in their name, *e.g.*,  $Ce^*(X\%)NaZSM-5$ .

#### 4.9.1 Pyrolysis, $CeO_2$ and $HZSM-5$

Fraction of *n*-hexane converted thermally and catalytically over  $CeO_2$  and  $HZSM-5$  are shown in Figure 4.5. Distributions of products obtained in gas, liquid, and solid states are shown in Figure 4.6. Selectivity to various gaseous products is shown in Figure 4.7. Liquid products are categorized by carbon number as shown in Figure 4.8.

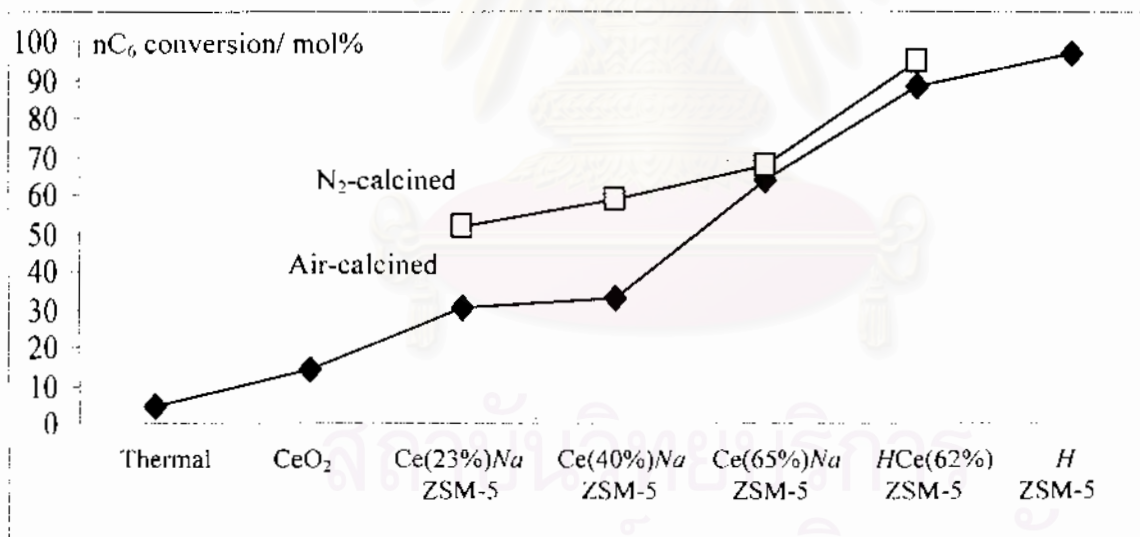


**Figure 4.5** *n*-Hexane conversion over various catalysts. Condition: 0.1 g of a catalyst, reaction temperature of 500°C, GHSV of 2000 h<sup>-1</sup>, and time-on-stream of 30 min. Various ion exchange levels are shown in parentheses.

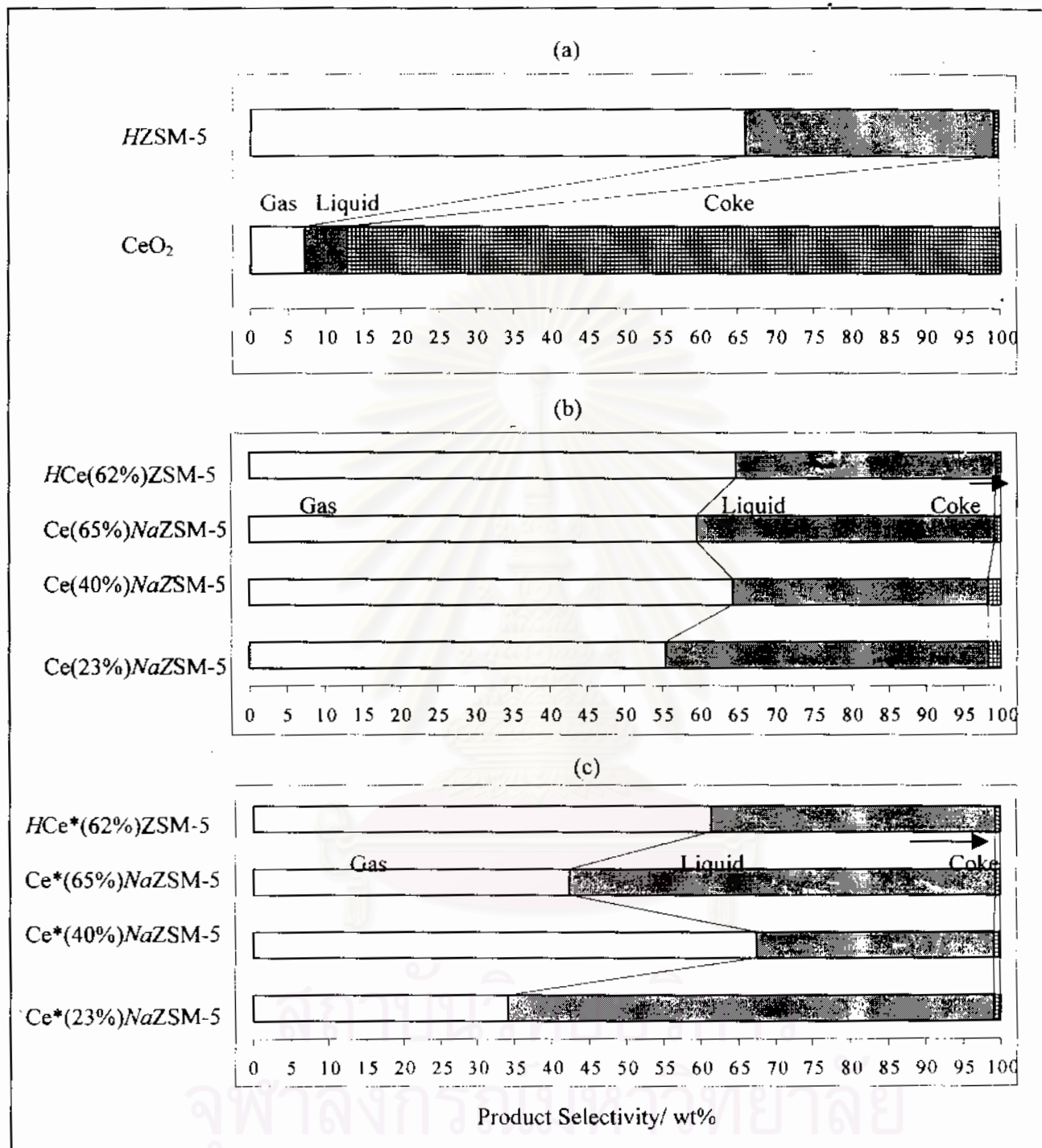


**Figure 4.6** Selectivity (wt%) to gaseous, liquid, and solid (coke) products over various catalysts: HZSM-5 and CeO<sub>2</sub> (a); and CeM ZSM-5 ( $M=Na^+$  or  $H^+$ ) with various Ce<sup>3+</sup> ion exchange levels calcined in air (b), or N<sub>2</sub> (c).

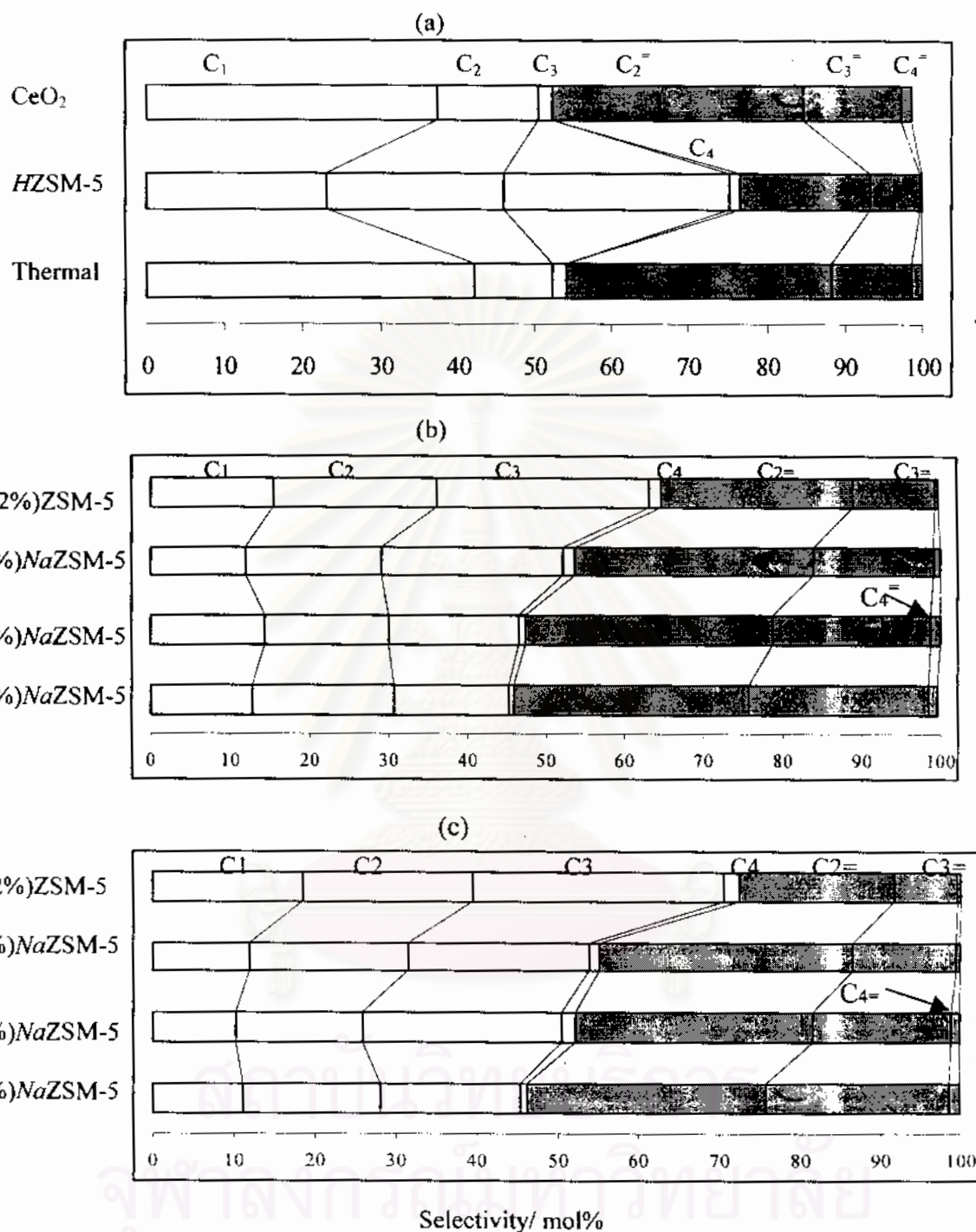


**Figure 4.7** Gaseous products selectivity (mol%) from various catalysts: thermal reaction, HZSM-5, CeO<sub>2</sub> (a); and CeMZSM-5 ( $M=Na^+$  or  $H^+$ ) with various Ce<sup>3+</sup> ion exchange levels calcined in air (b), or N<sub>2</sub> (c). C<sub>n</sub> and C<sub>n</sub>= are, respectively, paraffin and olefin with n carbon atoms in a molecule.

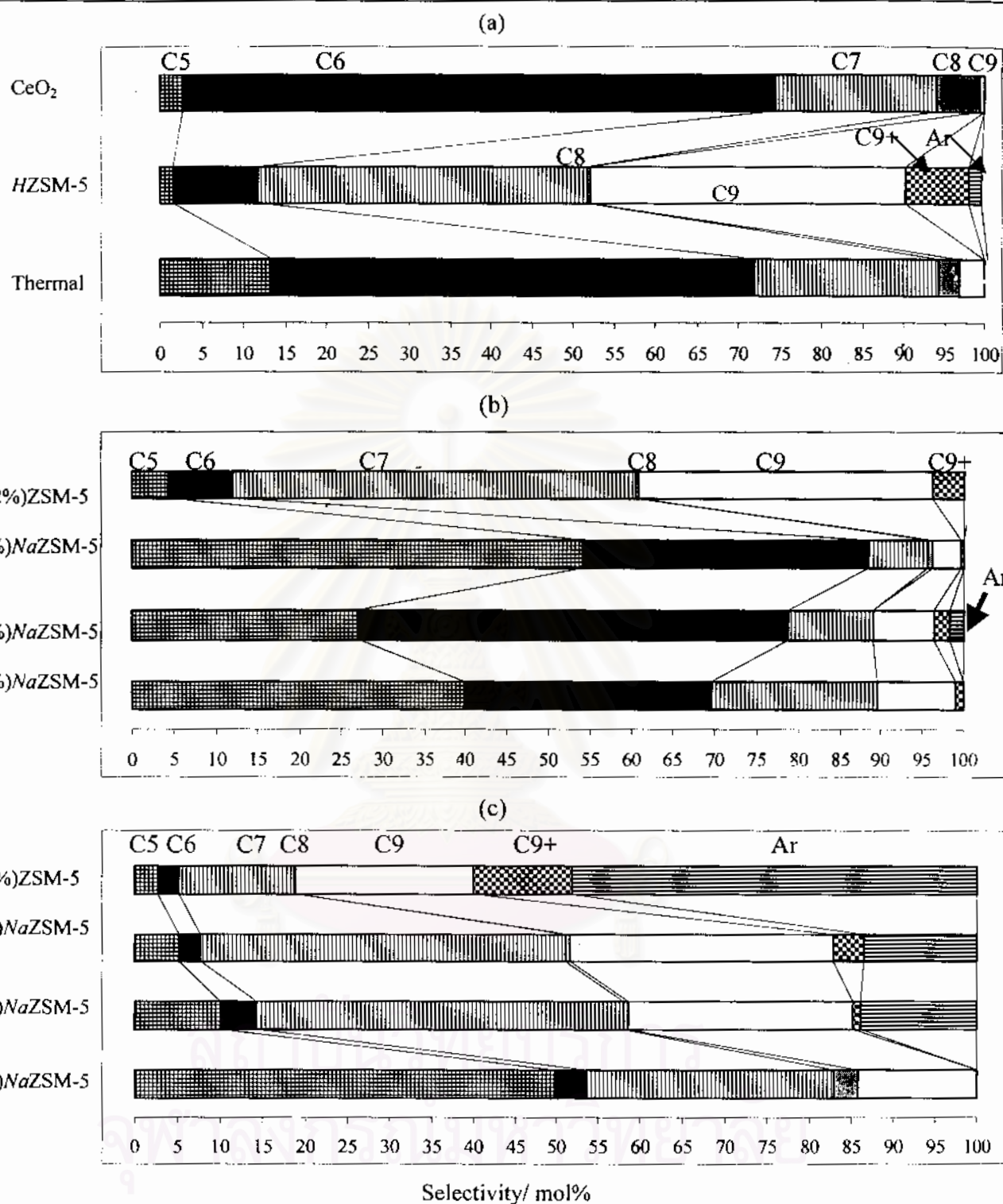


**Figure 4.8** Liquid products selectivity (mol%) from various catalysts: thermal reaction, HZSM-5, CeO<sub>2</sub> (a); and CeM ZSM-5 ( $M=\text{Na}^+$  or  $\text{H}^+$ ) with various Ce<sup>3+</sup> ion exchange levels calcined in air (b), or N<sub>2</sub> (c). Key: C<sub>n</sub> and C<sub>n</sub>+: paraffin with n and more than n carbon atoms; Ar: aromatics, including benzene, toluene, xylene, ethylbenzene, 1,2,3-trimethylbenzene and 1,2,4,5-tetramethylbenzene.

Light olefins are produced commercially mainly by thermal reaction of either single- or multicomponent feedstocks at 750-900°C.<sup>1,2</sup> Pyrolysis of *n*-hexane was therefore studied first, however, *at the temperature for catalytic reaction*. It is found that conversion at 500°C is very low, *i.e.*, 4.5%. Clearly low reaction temperature is not adequate for an acceptable *n*-hexane conversion. Products are formed both in gaseous and liquid state. Unfortunately, the proportion of each phase cannot be determined accurately. This is due to difficulties in measuring conversion and in adjusting flow rate in the presence of only quartz wool. Therefore, this proportion is not reported in Figure 4.6. Considering selectivity in gaseous products formed from thermal reaction (without catalyst), Fig 4.7(a), total selectivity to light olefins (ethylene, propylene, and butenes) as high as 45.7% was obtained.

Though there were many reports on the use of CeO<sub>2</sub> as a catalyst for light olefins production from light alkanes such as ethane,<sup>5-7</sup> propane,<sup>8-10</sup> and isobutane,<sup>11</sup> no such a report on larger molecules such as *n*-hexane is available. It is found in this work that *n*-hexane conversion of 14.5% (Figure 4.5) is obtained over CeO<sub>2</sub>. This is higher by a factor of *ca.* 3 to that of thermal reaction. Upon thermal treatment, disorder in CeO<sub>2</sub>, *i.e.*, formation of oxygen vacancies, is known to form easily.<sup>15</sup> Such anion vacancies were also observed in the 1CeO<sub>2</sub>/2CeF<sub>3</sub> catalyst.<sup>8</sup> It may be these vacant sites that enhance *n*-hexane conversion.

A controversy on the role of CeO<sub>2</sub> as a true catalyst, however, still exists. By considering product phase distributions, Figure 4.6(a), *n*-hexane converts into 7.1% and 5.7% gaseous and liquid products, respectively. Major part, 87.2%, is uselessly transformed to coke. Close inspection of Figure 4.7(a) shows that gaseous product distributions from CeO<sub>2</sub> are indeed almost identical to those from pyrolysis. In the above cases,<sup>5-11</sup> olefin formation from light reactants was performed in the presence of gaseous O<sub>2</sub>. The anaerobic condition used in this work is therefore one of the reasons why CeO<sub>2</sub> does not operate well as a catalyst. In a study of *n*-hexane combustion, Garrido Pedrosa *et al.*<sup>12</sup> stated that CeO<sub>2</sub> was not able to catalyze the combustion in the absence of O<sub>2</sub>. However, they did not report product distributions.



Also, distribution of liquid products from thermally- and  $\text{CeO}_2$ -catalyzed reactions are quite similar, Figure 4.8(a). Major portion has 6 carbon atoms, largely skeleton isomers of *n*-hexane. Selectivity to heavier products than *n*-hexane are not higher than 25%. Aromatics are not found. This result is in agreement with that of Greensfelder *et al.*<sup>76</sup>

There were reports supporting the use of *HZSM*-5 as an olefins-production catalyst as previously mentioned in Chapter I. *HZSM*-5 was tested, and 97.1% *n*-hexane conversion, almost complete, is obtained as shown in Figure 4.5. Product phase distribution in Figure 4.6(a) illustrates that 66.0 and 33.4% of *n*-hexane converted are in gaseous and liquid phases, respectively, whereas only 0.56% are wasted and ended up as coke in *HZSM*-5. Although 23.0% selectivity to light olefins, Figure 4.7(a), is lower than those obtained thermally and over  $\text{CeO}_2$ , high conversion, high gas yield, and low coke formation make *ZSM*-5 an attractive catalyst. Besides, *HZSM*-5 yields only 23.1% undesired methane, whereas thermal reaction and  $\text{CeO}_2$  yield 41.5 and 37.4% methane, respectively.

For liquid portion, heavier products than *n*-hexane account for more than 85%. In agreement with Greensfelder *et al.*,<sup>76</sup> aromatics are also found from the reaction of *n*-hexane over acidic silica-zirconia-alumina catalysts. However, the result is in contrast to that obtained over thermally- or  $\text{CeO}_2$ -catalyzed reactions. A gallium-containing *ZSM*-5 zeolite catalyst has been used in the Cyclar process<sup>1</sup> to aromatize light hydrocarbons, *e.g.*, propane, to aromatics. Heavier products than  $\text{C}_6$ ,<sup>39,40</sup> or aromatics,<sup>29,32,39,40,41</sup> were obtained from *n*-hexane cracking catalyzed by *HZSM*-5 reported earlier.

*(Na,H)ZSM*-5 was not tested, as it is well known that an active site in protolytic cracking and protolytic dehydrogenation is proton. Lack of proton makes *(Na,H)ZSM*-5 inactive. For example, Baba *et al.*<sup>77</sup> reported *n*-hexane conversion of 20, 6, and 0% respectively for *HZSM*-5 with 0, 20, and 40%  $\text{Na}^+$  ion exchange level. Nicolaidis *et al.*<sup>78</sup> found a decrease in *n*-hexane conversion from *ca.* 52 to 9% for *HZSM*-5 and 50% *K*-ion exchanged *HZSM*-5, respectively. *(Na,H)ZSM*-5 in this study with 70-100%  $\text{Na}^+$  occupation (as shown by elemental analysis in Section 4.3) will certainly not active, and any conversion observed would certainly occur thermally. However, as mentioned previously that acidity

usually results in poor selectivity to olefins in olefins production from catalytic cracking,  $(Na,H)ZSM-5$  is an ideal base catalyst for modification with  $Ce^{3+}$ .

#### 4.9.2 Air-Calcined Cerium-Containing ZSM-5

$CeMZSM-5$  ( $M=Na^+$  or  $H^+$ ) catalysts with various  $Ce^{3+}$  ion exchange levels were tested in *n*-hexane cracking. These catalysts were air-calcined to facilitate the movement of  $Ce^{3+}$  into inner position inside ZSM-5 cavity. Results are shown in Figure 4.5 to 4.8.

For  $(Na,H)ZSM-5$  with 23, 40, and 65% cerium ion-exchange level, *n*-hexane conversion of 30.6, 32.7, and 63.7%, respectively, are observed, Figure 4.5. An increase in cerium content results in increased *n*-hexane conversion. Cerium cations therefore increase activity of  $(Na,H)ZSM-5$  greatly, though they may or may not be the true active sites themselves. Similar trend of conversion as a function of rare earth content in Na-zeolite was found before for reaction of *n*-heptane over  $Pr^{3+}$ -exchanged  $NaY$ ,<sup>79</sup> and  $Ce^{3+}$ -exchanged  $NaZSM-20$ .<sup>80</sup> In this work, for  $Ce(65\%)NaZSM-5$  and  $HCe(62\%)ZSM-5$  with similar cerium content (65 vs 62%) but with different acidity ( $Na^+$  vs  $H^+$ ), conversion of 63.7 and 88.6% are obtained. The presence of proton *additionally* enhances *n*-hexane conversion. This result is in agreement with the generally accepted concept on the role of  $H^+$  as an active species.

The beneficial effect of ZSM-5 also manifests itself in product yields as shown in Figure 4.6(b). Gas yield of 55.5 to 64.8%, and liquid yield of 31.7 to 42.8% are obtained. The results are more or less similar to those on  $HZSM-5$ , Figure 4.6(a). Coke contents are in the range of 0.57 to 1.8wt%. These values are, if not equal to, slightly higher than of  $HZSM-5$  (0.56wt%), and are much better than those from  $CeO_2$  (87.2wt%).

Selectivity to various gaseous products is shown in Figure 4.7(b). Light olefins selectivities of 53.9, 51.2, 46.2, and 35.0% are observed over  $Ce(23\%)NaZSM-5$ ,  $Ce(40\%)NaZSM-5$ ,  $Ce(65\%)NaZSM-5$ , and  $HCe(62\%)ZSM-5$ , respectively. Though they remain relatively constant at cerium ion exchange degree of 23-40%, and decrease continuously beyond 40%, the presence of cerium clearly exerts a positive role on selectivity

to light olefins compared to *HZSM-5*, with only 23.0% selectivity, Figure 4.7(a). Selectivity to methane (12.8 to 15.3%) is highly improved from *HZSM-5* (23.1%). The beneficial effect of  $RE^{3+}$  in preferring to light olefins formation was reported before in *n*-hexane transformation over  $La^{3+}$ -exchanged *HZSM-5*.<sup>81</sup> Selectivity to olefinic products of 6.7 and 8.1wt% was obtained over, respectively,  $La(15\%)HZSM-5$  and  $La(58\%)HZSM-5$ , compared to that of 6.2wt% by *HZSM-5*.<sup>81</sup> A decline in olefins selectivity as cerium content increases should better be explained by the presence of  $H^+$ , proportions of which are continuously added up by hydrolysis of cerium. Indeed a decrease of olefins selectivity is significant over  $Ce(65\%)NaZSM-5$  and  $HCe(62\%)ZSM-5$  with similar cerium content but with different acidity.

Concerning composition of gaseous products in all cases, however, ethylene is major, followed by propylene and butenes. Possibly as conversion increases, propylene and butenes progressively transform to ethylene, as seen in Figure 4.7(b) where the decrease in propylene and butenes contents are accompanied by the increase in ethylene contents.

For products in liquid portion, C5 and C6 products are major and their selectivity is *ca.* 70-85%, Figure 4.8(b). Heavier products are formed in small quantities, *i.e.*, 15-30% selectivity. However, their formation is greatly enhanced when  $Na^+$  ions in  $Ce(65\%)NaZSM-5$  are replaced by  $H^+$  ions in  $HCe(62\%)ZSM-5$ . The result obtained over  $HCe(62\%)ZSM-5$  are quite similar to those over *HZSM-5*, and supporting the role of  $H^+$  as an active site responsible for oligomerization and aromatization.

Although  $Ce^{4+}-O^{2-}Ce^{4+}$  was suggested by Tempere *et al.*<sup>65</sup> in  $O_2$  calcined CeX zeolite, the presence of such species, e.g.,  $CeO_2$ , is not observed in  $Ce(65\%)NaZSM-5$  and  $HCe(62\%)ZSM-5$  with highest cerium loading as shown in Figure 4.4. There are no diffraction peaks characteristics of  $CeO_2$ , for example,  $2\theta$  of 28.6 and 47.5°.

#### 4.9.3 N<sub>2</sub>-Calcined Cerium-Containing ZSM-5

During preparation of air-calcined CeMZSM-5, color change of samples was observed in some cases. The zeolite turns from white (NaZSM-5 and Ce(23%)NaZSM-5) to pale yellow (Ce(40%)NaZSM-5), and to deep yellow (Ce(65%)NaZSM-5 and HCe(62%)ZSM-5). Yellow color is widely accepted as characteristic of Ce<sup>4+</sup>.<sup>15</sup> The formation of Ce<sup>4+</sup>-O<sup>2-</sup>Ce<sup>4+</sup> was described by Tempere *et al.*<sup>59</sup> in O<sub>2</sub>-calcined Ce<sup>3+</sup>-exchanged zeolite X. CeO<sub>2</sub> is yellow as well. Therefore, N<sub>2</sub>-calcined Ce\*MZSM-5 zeolites were prepared in order to compare the role of Ce<sup>3+</sup> and Ce<sup>4+</sup> species in a catalyst. Actually the preparation procedures for air- and N<sub>2</sub>-calcined Ce\*MZSM-5 were almost identical, except that whenever calcination was required, this was done in a quartz boat inside a split-tube furnace continuously flow with N<sub>2</sub>.

Using this method, *partial* reservation of Ce<sup>3+</sup> is possible, compared to the materials calcined in air. Unfortunately, spectroscopic determination of Ce<sup>3+</sup>/Ce<sup>4+</sup> is not available, and therefore cerium oxidation state has to be directly observed by eyes. However, it is believed that this observation was *semi-quantitatively* adequate. For example, 1- and 2-time Ce<sup>3+</sup> exchanged samples are still white, 3-time exchanged samples changes from deep to pale yellow, and a proton form of 3-time Ce<sup>3+</sup> exchanged is not as yellow as that calcined in air. Similarly, Dyer *et al.*<sup>65</sup> reported an observation that air-calcined CeX and CeY zeolites attained the yellow/cream colour, whereas those N<sub>2</sub>-calcined did not show this colour. Velu *et al.*<sup>74</sup> also observed color change from white to yellow in uncalcined and air-calcined CeY zeolites. Since the atmosphere in calcination will effect the oxidation state of cerium only but not its content, an elemental analysis of these samples are not performed, but are believed to be similar to those calcined in air.

Catalytic transformation of *n*-hexane catalyzed by these samples is investigated. *n*-Hexane conversion is shown in Figure 4.5. As in air-calcined catalysts, an increase in cerium content results in increased *n*-hexane conversion. However, when catalyzed by N<sub>2</sub>-calcined Ce\*NaZSM-5, conversion increases by a factor of 2 is observed, at

least at cerium ion exchange degree of 23% (30.6 vs 51.3 %conversion) and 40% (32.7 vs 58.8 %conversion). However, the enhancement is diminished at high cerium loading, *i.e.*, conversion of 63.6, 67.8%, 88.6 and 94.9% are obtained on Ce(65%)NaZSM-5, Ce\*(65%)NaZSM-5, HCe(62%)ZSM-5 and HCe\*(62%)ZSM-5, respectively, where Ce\* represents for a catalyst calcined in N<sub>2</sub>.

Selectivities to gaseous, liquid, and solid (coke) products on N<sub>2</sub>-calcined Ce\*MZSM-5 ( $M = \text{Na}^+$  or  $\text{H}^+$ ) are shown in Figure 4.6(c). The trend of gas selectivity as a function of cerium content is similar to that from air-calcined samples. For example, it changes from 34.1 to 67.5, 42.4, and 61.3wt% over Ce\*(23%)NaZSM-5, Ce\*(40%)NaZSM-5, Ce\*(65%)NaZSM-5, and HCe\*(62%)ZSM-5, respectively. Gas yield is generally lower than the corresponding samples calcined in air, with one exception on Ce\*(40%)NaZSM-5. The difference between gas and liquid products are more pronounced in N<sub>2</sub>-calcined Ce\*MZSM-5. Liquid yields are in the range of 38.1 to 64.9wt%, generally higher, if not equal to, the corresponding samples calcined in air. An advantage of N<sub>2</sub>-calcined catalysts over those of air-calcined is that *coke yield was greatly reduced, i.e., 0.57-0.93wt% vs 0.57-1.81wt%*. Coke yield on HZSM-5 is 0.56wt%.

Figure 4.7(c) shows the gaseous products selectivity. Light olefins selectivity of 53.7, 47.6, 44.6, and 27.3% over N<sub>2</sub>-calcined catalysts should be compared to the values of 53.9, 51.2, 46.2, and 35.2% of their counterparts. Clearly, lower selectivity to olefins is observed in N<sub>2</sub>-calcined catalysts. Selectivity to methane by Ce\*ZSM-5 (10.3 to 11.9 wt%) is lower than that by CeZSM-5 (12.8 to 15.3 wt%), with one exception on HCe\*(62%)ZSM-5 (18.5 wt%), which is still improved compared to methane selectivity in HZSM-5 (23.1%).

Product distributions in liquid phase are shown in Figure 4.8(c). At the same cerium content, Ce\*NaZSM-5 catalysts give higher amount of products with more than 6 carbon atoms than CeNaZSM-5 catalyst does, *i.e., 55 vs 30% for Ce(23%)NaZSM-5; 85 vs 22% for Ce(40%)NaZSM-5; and 90 vs 10% for Ce(65%)NaZSM-5*. Formation of aromatics is also enhanced by N<sub>2</sub>-calcined Ce\*MZSM-5. Besides, replacing Na<sup>+</sup> ions in Ce\*(65%)NaZSM-5 with H<sup>+</sup> ions in HCe\*(62%)ZSM-5 further enhances selectivity to

aromatics notably. Aromatic formation was reported earlier in  $\text{La}^{3+}$ -exchanged *HZSM-5* catalysts.<sup>81</sup>

#### 4.10 Active Sites in *CeMZSM-5*: $\text{H}^+$ vs $\text{Na}^+$

Catalytic activity of zeolites, especially with saturated hydrocarbons such as *n*-hexane, is usually explained in term of Brønsted acidity.<sup>20-23</sup> It is generally accepted that rare earth cations, which Lewis acidity property, withdraw electron density from nearby Brønsted acid sites, thereby making the associated proton more acidic.<sup>71</sup> Lemos *et al.*<sup>58,80</sup> found that at 350°C, the relative absorbance of IR band characteristic of  $\text{H}^+$ -bound pyridine of *HY* and  $\text{Ce}^{3+}$ *HY* zeolite decreased by 74 and 64%, respectively, of the original value at 150°C. Brønsted acid sites in *CeHY* zeolite was therefore stronger than those in unmodified *HY* zeolite. The *n*-heptane cracking activity varied in the same way as the Brønsted acidity, *i.e.* *CeHY* was more active than *HY*.<sup>58,80</sup> However, there was no direct relation between the activity and the Lewis acidity (as probed by the relative absorbance IR band characteristic of Lewis-bound pyridine).<sup>80</sup>

In this work, *n*-hexane conversion increases from 4.5 (thermal reaction) to 30.6% (over  $\text{Ce}(23\%)\text{NaZSM-5}$ ). However, the *strength* of  $\text{H}^+$  should be considered together with the *number* of  $\text{H}^+$ . Though proton in cerium-containing *CeNaZSM-5* is stronger than that in *HZSM-5*, the number in the former is less than that in the latter. As a result, highest conversion obtained over cerium-containing (*Na,H*)*ZSM-5* is *ca.* 63.7%. When  $\text{H}^+$  was introduced into  $\text{Ce}(65\%)\text{NaZSM-5}$  by ammonium ion exchange, conversion increases to 88.6%. *n*-Hexane conversion over *HZSM-5* is 97.1%. The increase in ionic field inside a zeolite caused by  $\text{Ce}^{3+}$  introduction, thereby favoring acidic O-H bonds dissociation, was also used to explain the results for *n*-heptane cracking in  $\text{Ce}^{3+}$ -exchanged *NaZSM-20* zeolites,<sup>80</sup>  $\text{Pr}^{3+}$ -exchanged *MY* zeolites ( $M=\text{Na}^+, \text{H}^+$ ),<sup>79</sup> and for *n*-hexane cracking in  $\text{La}^{3+}$ -exchanged *HZSM-5* zeolites.<sup>81</sup>

The presence of  $H^+$  in  $CeNaZSM-5$  and  $Ce^*NaZSM-5$  can be best described by a change in pH value of the zeolite slurry as shown in Figure 4.9. Zeolite, *i.e.*, parent, calcined  $(Na,H)ZSM-5$ , or 1-, 2-, and 3-time  $CeNaZSM-5$ , was soaked with deionized water (1 g zeolite per 37.5 mL water). It is believed that this information is at least *semi-quantitatively* valuable in the absence of results from more thoroughly sophisticated techniques such as IR,  $^1H$ -MASNMR spectroscopy, or acidity titration.

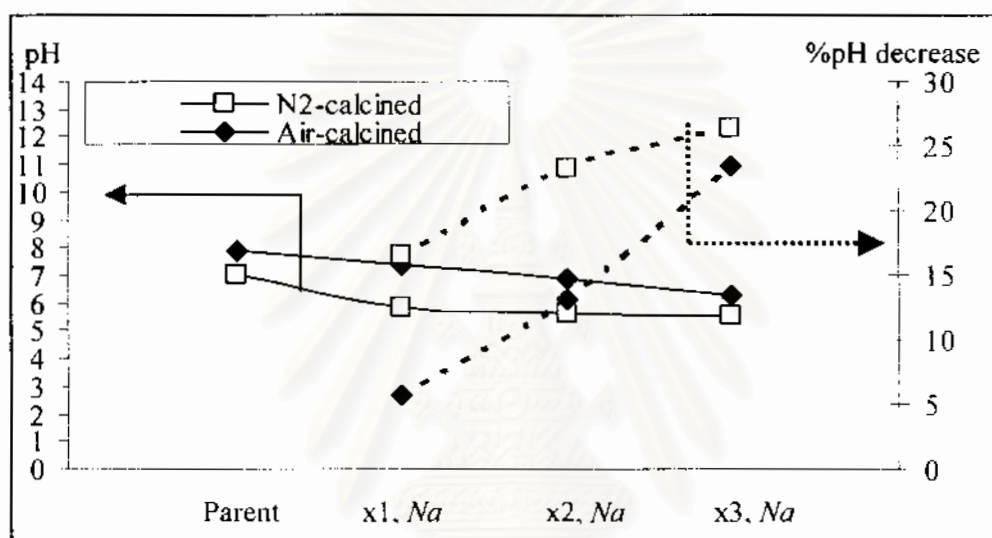


**Figure 4.9** Acidity of parent and cerium-containing ZSM-5. Change in pH value of the zeolite slurry. (x1,Na is denoted for parent, calcined  $(Na,H)ZSM-5$  ion exchanged once with  $Ce^{3+}$ , and others are assigned similarly.)

A pH value of the slurry gradually decreases as numbers of cerium ion exchange increases.  $(Na,H)ZSM-5$  and 3-time  $Ce^{3+}$  exchanged slurry had a pH value of 7.9 and 6.2, (7.0 and 5.5) for air- ( $N_2$ )-calcined samples. This *semi-quantitatively* indicates that Brønsted acidity increased continuously. One might argue that lower pH in  $N_2$ -calcined samples was caused by the lower initial pH. However, %decrease in pH value supports the above discussion. Protons are created as a result of cation hydrolysis shown in Figure 2.5, where  $Ce(H_2O)^{3+}$  dissociates to form  $Ce(OH)^{2+}$  and  $H^+$ . The divalent complex is able to dissociate more to  $CeO^+$  and another  $H^+$ . Rare earth hydrolysis inside a zeolite is confirmed by various techniques such as IR spectroscopy,<sup>57-61</sup>  $NH_3$  temperature programmed desorption ( $NH_3$ -

TPD),<sup>62</sup> neutron diffraction,<sup>63</sup> and elemental analysis.<sup>64</sup> Therefore conversion increases monotonically from when cerium content increases.

The last topic to be discussed in this section is the dependence of proton on olefins selectivity. It is found that selectivity to olefins decreases as cerium contents increase, *i.e.*, 53.9, 51.2, 46.2, and 35.2%; and 53.7, 47.6, 44.6, and 27.3% for 1-, 2-, 3-, and H<sup>+</sup>-containing 3-time cerium ion exchanged ZSM-5, respectively, activated in air and N<sub>2</sub>. In the author's opinion, loss in selectivity to olefins is not caused by cerium, but instead by proton. Because there are higher proton concentrations as cerium content increases due to cerium hydrolysis, less olefins selectivity is obtained over high cerium ZSM-5. Also, because there are higher proton contents in Ce\*ZSM-5 (activated in an anaerobic condition) than CeZSM-5 (activated in an aerobic condition), olefins selectivity in the former is lower than that in the latter. Olefins selectivity of 46.2 (44.6) drops to 35.2% (27.3%) when Ce(65%)NaZSM-5 (Ce\*(65%)NaZSM-5) is replaced by HCe(62%)ZSM-5 (HCe\*(62%)ZSM-5), respectively. HZSM-5 with highest proton contents gives the lowest selectivity to olefinic products, 23.0%. Other cerium-containing ZSM-5 catalysts give 27.3-53.9% selectivity.

The detrimental effect of H<sup>+</sup> in destroying olefins selectivity agrees with the results over both commercial alumina based catalysts and zeolitic based catalysts mentioned in Section 1.3. For example, Wang *et al.*<sup>41</sup> reported light olefins yield from *n*-hexane cracking of 32.9 and 46.1% for HZSM-5 without and with 0.5wt% K, respectively.

#### 4.11 Effect of Cerium Loading and Oxidation State (Ce<sup>3+</sup> vs Ce<sup>4+</sup>)

The transformation of Ce<sup>3+</sup> to Ce<sup>4+</sup> by air oxidation is supported by specific surface area data as shown in Figure 4.10. For air-calcined catalysts, surface area remains relatively unchanged for (Na,H)ZSM-5 and Ce(40%)NaZSM-5, but decreases significantly for Ce(65%)NaZSM-5. The amount of cerium in Ce(65%)NaZSM-5 is high enough such that Ce<sup>3+</sup> air oxidation, with the simultaneous formation of O<sup>2</sup>-Ce<sup>4+</sup>-O<sup>2</sup> bridge, reduces the pore volume inside a zeolite and consequently reduces the space available for N<sub>2</sub> adsorption.



Therefore, the specific surface area of  $\text{Ce}(65\%)\text{NaZSM-5}$  is low. For  $\text{Ce}^*(65\%)\text{NaZSM-5}$  with the same cerium content, air oxidation and incorporation of oxygen is prevented by calcination in  $\text{N}_2$ , hence its specific surface area insignificantly decreases. After ammonium exchange, the specific surface area of  $H$ -form of cerium-containing catalysts (for both air- and  $\text{N}_2$ -calcined samples) becomes higher than that of  $\text{Ce}(65\%)\text{NaZSM-5}$  because  $\text{H}^+$  ions leave more space inside ZSM-5 cavities compared to the larger  $\text{Na}^+$  ions.

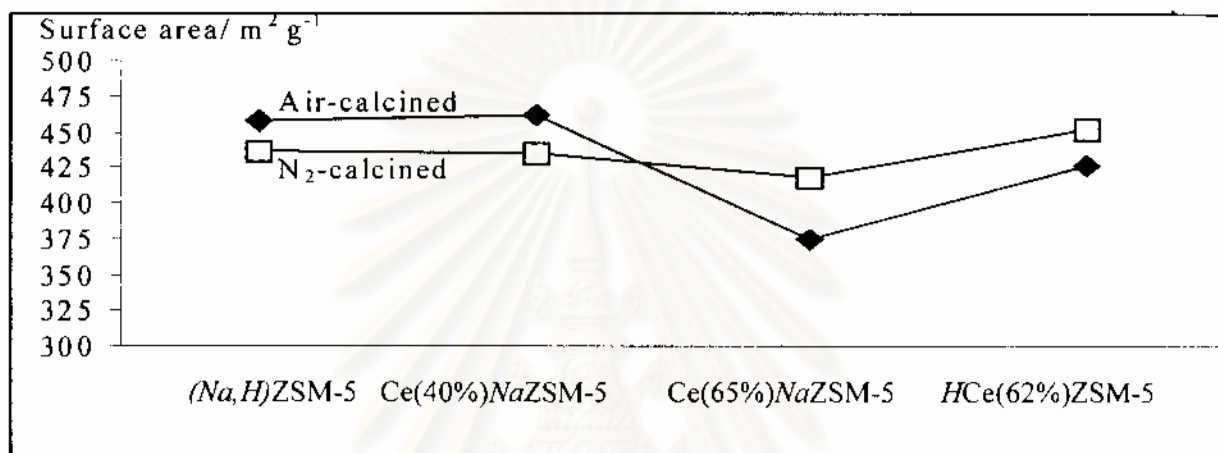


**Figure 4.10** Specific surface area (Langmuir) of air- and  $\text{N}_2$ -calcined  $\text{CeM/ZSM-5}$  ( $M = \text{Na}^+$  or  $\text{H}^+$ ).

In the present study,  $\text{Ce}^{3+}$  alone as judged by color observation, e.g.,  $\text{Ce}(23\%)\text{NaZSM-5}$  and  $\text{Ce}^*(23)\text{NaZSM-5}$ , already exhibit catalytic activity in  $n$ -hexane cracking. However, olefins synthesis over bulk  $\text{Ce}^{3+}$  has never been reported. Zhang *et al.*<sup>8</sup> found that melting of  $\text{CeF}_3$  into  $\text{CeO}_2$  produced an active and olefins-selective  $\text{CeO}_2/\text{CeF}_3$  catalyst for oxidative dehydrogenation of propane.  $\text{Ce}^{3+}$  in  $\text{CeF}_3$  might migrate into, or exchange with  $\text{Ce}^{4+}$  in,  $\text{CeO}_2$ , therefore, there would be both  $\text{Ce}^{3+}$  and  $\text{Ce}^{4+}$  in a catalyst. They reported<sup>8</sup> that  $\text{CeF}_3$  had no activity in propane oxidative dehydrogenation. The presence of both  $\text{Ce}^{3+}$  and  $\text{Ce}^{4+}$  was found by others as well.<sup>5,6,9</sup> It is found in this work that having higher proportion of cerium in 3+ instead of 4+ state is advantageous, since the increase in conversion by a factor of 2 is obtained, at least at low cerium content, Figure 4.5.

The question is why does anaerobic activation of  $\text{Ce}^*\text{ZSM-5}$  enhances  $n$ -hexane conversion. The concept in Section 4.10 above is also useful. Calcination in  $\text{N}_2$  atmosphere

partially blocks  $\text{Ce}^{3+}$  species from losing electron to form  $\text{Ce}^{4+}$ , therefore there is higher amount of  $\text{Ce}(\text{H}_2\text{O})^{3+}$  to be dissociated, hence higher active proton concentrations. This yields higher *n*-hexane conversion compared to a corresponding catalyst calcined in air. Once  $\text{Ce}^{4+}$  is from, its high charge-to-volume ratio makes charge neutralization by remote framework negative charge difficult. Because  $\text{Ce}^{4+}$  is highly oxophilic,  $\text{O}_2$  from air is trapped. The formation of  $\text{Ce}^{4+}-\text{O}^{2-}-\text{Ce}^{4+}$  bridge was suggested before by Tempere *et al.*<sup>59</sup> The role of  $\text{Ce}^{3+}/\text{Ce}^{4+}$  was discussed before in  $\text{NO}_x$  reduction<sup>62</sup> and benzyl alcohol oxidation,<sup>83,84</sup> but not in alkane transformation. Due to the difference in nature of a catalyst, *i.e.*, bulk vs porous, the influence of  $\text{Ce}^{3+}/\text{Ce}^{4+}$  in ZSM-5 differs from that in cerium-based catalysts reported in the literature.<sup>5,6,9</sup> Also an increase in *n*-hexane conversion by  $\text{Ce}^{3+}/\text{Ce}^{4+}$  couple was not similar to that by  $\text{Cr}^{6+}/\text{Cr}^{3+}$  couple in propane dehydrogenation over Cr-based catalysts.<sup>43</sup>

Interestingly, *n*-hexane conversion greatly enhances at relatively low (23-40%)  $\text{Ce}^{3+}$  ion exchange only. At higher (>65%) ion exchange degree, this enhancement is less observable. Recent theoretical calculation by Yang *et al.*<sup>85</sup> on  $\text{La}^{3+}$ -exchanged ZSM-5 ( $\text{Si}/\text{Al}=19$ ) shows that when the exchange degree,  $(3\text{La}/\text{Al}) \times 100$ , reaches 40%, lanthanum dimers have already taken up about half of all the lanthanum species. When the exchange level approaches 60%, the lanthanum ions should be *completely* in the form of dimers, *e.g.*,  $[\text{La}(\text{O}_2)\text{La}]^{2-}$  or  $[(\text{OH})\text{La}(\text{OH})_2\text{La}(\text{OH})]^{2-}$ . It may be possible that at high cerium content,  $\text{N}_2$  calcination is not strong enough to prevent dimer formation. Formation of bulky complexes after calcination such as  $[\text{Ce}(\text{O}_2)\text{Ce}]^{2+}$ ,  $[\text{Ce}_2(\text{OH})_2]^{2+}$ , and  $[\text{La}_2(\text{OH})_2]^{4+}$  are frequently cited in the literature.<sup>73</sup> Calcination at higher temperature (>540°C), at a longer time (>5 h), or even calcination in reducing condition should be further investigated.

## 4.12 Reaction Mechanism

Transformation of *n*-hexane in this work can be categorized into 2 pathways. *n*-Hexane reacted thermally or catalytically (protolytic decomposition) as shown in Figure 4.11<sup>25</sup> and 4.12,<sup>35</sup> respectively.

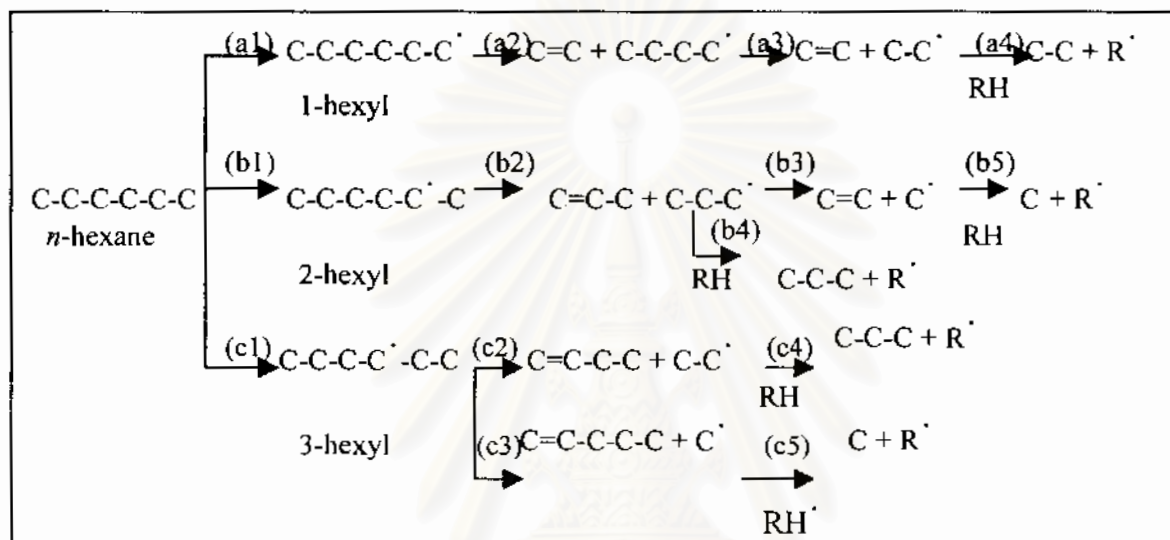


**Figure 4.11** Thermal or radical decomposition of *n*-hexane.<sup>25</sup> Hydrogen atoms in this figure are omitted for convenience.

The radical decomposition of *n*-hexane<sup>25</sup> can be described by the reaction shown in Figure 4.11. *n*-Hexane forms 1-, 2-, and 3-hexyl radicals by reaction (a1), (b1), and (c1), respectively. 1-Hexyl radical undergoes  $\beta$ -scission (a2) to form ethylene and 1-butyl radical. Poutsma and Schaffer<sup>25</sup> suggested that the latter was cleaved (a3) to ethylene and ethyl radical as indicated by the absence of *n*-butane product. *n*-Butane is not observed in thermally- and  $\text{CeO}_2$ -catalyzed *n*-hexane cracking in this work also. The ethyl radical abstracts hydrogen from RH, e.g., *n*-hexane, to form ethane by pathway (a4). The 2-hexyl radical cleaves (b2) to form propylene and propyl radical. The observed methane and propane require a hydrogen abstraction, (b3) to (b5). The 3-hexyl radical has available two  $\beta$  C-C cleavage, (c2) and (c3), producing respectively 1-butene and 1-pentene. Ethane and methane are also formed by

pathway (c4) and (c5), respectively. It is found that 1-butene is the only C<sub>4</sub>-olefins observed in thermal reaction, in agreement with Poutsma and Schaffer,<sup>25</sup> though CeO<sub>2</sub> additionally gives *trans*-2-butene.

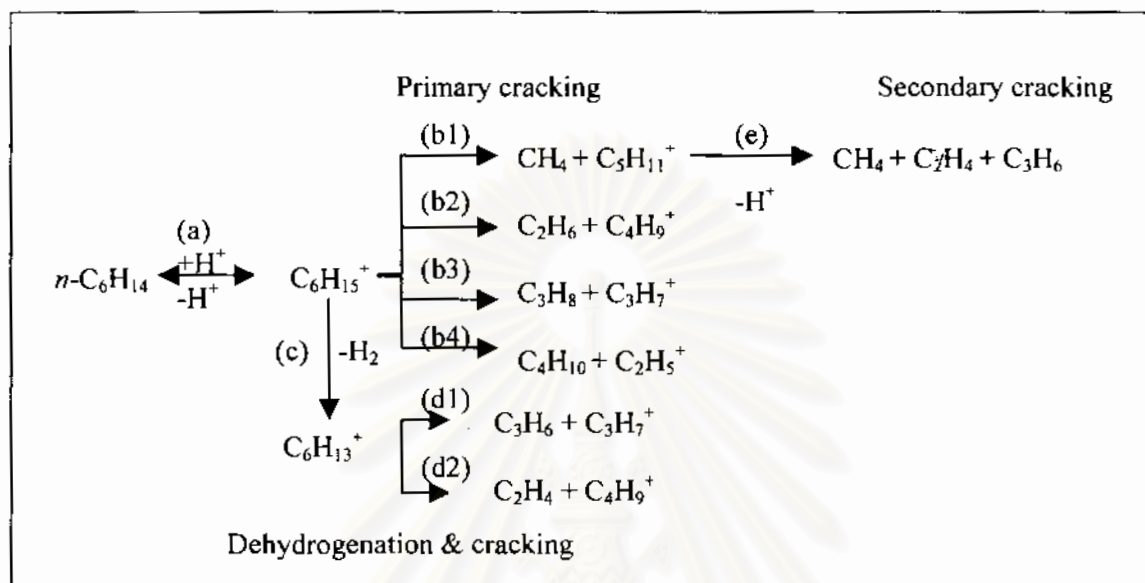


**Figure 4.12** Catalytic or protolytic decomposition of *n*-hexane.

Reaction networks taken place on ZSM-5 catalysts can be divided into 3 types as shown in Figure 4.12,<sup>35</sup> including primary cracking, dehydrogenation and cracking, as well as secondary (multiple) cracking. The scheme was proposed<sup>35</sup> for the reaction over SAPO5, MgAPO5 and CoAPO5, but can be applied to the present cerium-containing ZSM-5 as well.

Brønsted acid sites of a zeolite attack *n*-hexane as shown in reaction (a), resulting in a positively charged species  $\text{C}_6\text{H}_{15}^+$ . This species loses proton to form equimolar concentrations of methane and pentyl carbenium ion (b1), ethane and butyl carbenium ion (b2), propane and propyl carbenium ion (b3), and butanes and ethyl carbenium ion (b4). The excess of unsaturated hydrocarbons is suggested by a dehydrogenation step forming  $\text{C}_6\text{H}_{13}^+$ , reaction (c), prior to the cleavage of the carbon-carbon bond to small olefins, reaction (d1) and (d2). Pentyl carbenium ion  $\text{C}_5\text{H}_{11}^+$  do not desorb but instead reacts further by reaction (e) forming a mixture of  $\text{CH}_4$ ,  $\text{C}_2\text{H}_4$ , and  $\text{C}_3\text{H}_6$ .

Insights into reaction network illustrated in Figure 4.9 was provided by kinetic measurement provided by Lukyanov *et al.*<sup>86</sup> and Narbeshuber *et al.*<sup>87</sup> If the relative rate of

reaction (c), *e.g.*, transformation *via* dehydrogenation, is taken as 1, primary cracking according to (b2) and (b3) has relative rate 1.66 and 1.39, respectively; and therefore occurred faster. On the other hand, primary cracking according to reactions (b1) and (b4) has a relative rate of 0.20 and 0.54, respectively, and occurs slower. Similar sequence of relative rates in various steps were obtained by Narbeshuber *et al.*<sup>87</sup> also.

Besides, Narbeshuber *et al.*<sup>87</sup> showed that once  $C_6H_{13}^+$  was formed by dehydrogenation reaction, it could dissociate into two molecules of propylene at the same rate. This is the reason why hexenes are rarely observed in zeolite-catalyzed dehydrogenation. Nayak *et al.*<sup>88</sup> reported that, at 375-425°C, besides *n*-hexane cracking to smaller products, HZSM-5 (Si/Al=36) also catalyzed the dehydrogenation reaction, giving hexenes selectivity of ~8 and ~1% at 10 and 80% *n*-hexane conversion, respectively. Temperature had an effect on hexenes selectivity, *i.e.*, the higher the temperature, the lower hexenes products.<sup>88</sup> Similar observation was noted for *n*-hexane dehydrogenation over HZSM-48 zeolite,<sup>89</sup> where initial selectivity to  $C_6$ -olefins of 3.34, 1.96, and 1.64% were reported at reaction temperatures of 420, 450, and 500°C, respectively. Recently, using hydrogen form of ultrastable Y (HUSY) zeolite in the reaction of *n*-hexane, Reyniers *et al.*<sup>90</sup> found that at 450°C, selectivity to hexenes was only 1.73%. Also, pentyl carbocation ( $C_5H_{11}^+$ ) was not stable and dissociates into a mixture of methane, ethylene, and propylene by relative rate of 0.44.<sup>88</sup>

#### 4.13 Effect of Catalyst Types on Olefins Yields

The efficiency of the prepared catalysts in producing light olefins is evaluated by comparing two values. The first is the gaseous olefins yields, and the latter is the degree of coke formation. The former is shown in Figure 4.13, and the latter in Figure 4.14.

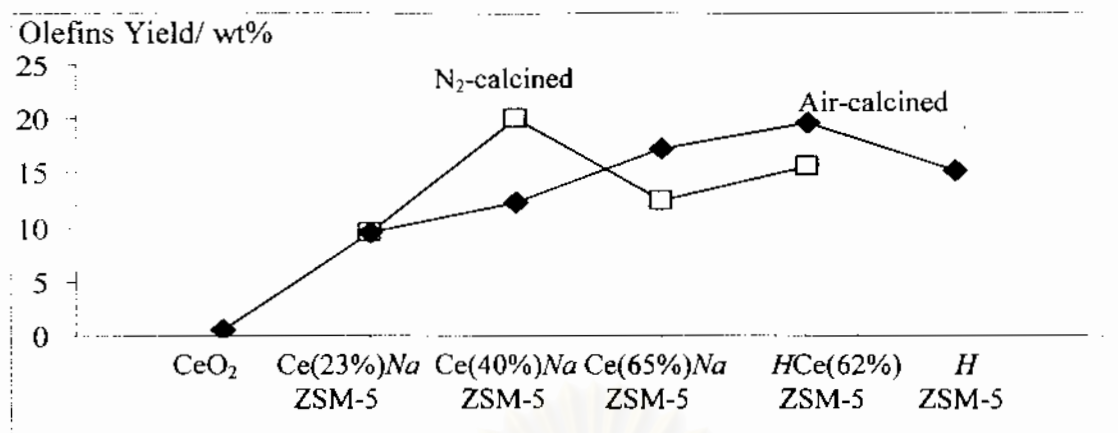


**Figure 4.13** Light olefins yields obtained over various catalysts studied.

Gaseous olefins yield is a function of three variables: conversion, gas yield, and selectivity to olefins. It is a measurement of (1) how much *n*-hexane is converted (%conversion); (2) in a fraction of *n*-hexane converted, how much is converted into gaseous products (gas yield); and (3) within the gaseous products, what is the selectivity to the desired products, ethylene, propylene, and butenes (%selectivity). Clearly CeO<sub>2</sub> is not suitable for use as an olefins-formation catalyst at the condition studied, since the olefins yield is only 0.58%. Although CeO<sub>2</sub> exhibits high selectivity to olefins (46.3%, Figure 4.7), its low gas yield (7.1%, Figure 4.6) and low conversion (14.5%, Figure 4.5) make it unsuitable.

For CeZSM-5 activated in an aerobic condition, olefin yields continuously increases from 9.6 (Ce(23%)NaZSM-5) to 19.7% (HCe(62%)ZSM-5). Ce(65%)NaZSM-5 and HCe(62%)ZSM-5 gives higher olefins yields than HZSM-5 (15.3%). An advantage of performing calcination under an anaerobic condition is visible. For Ce\*ZSM-5 activated in N<sub>2</sub>, olefins yield reaches its maximum, 20.1%, over Ce\*(40%)NaZSM-5. This value is the highest one obtained in this study. Also, by N<sub>2</sub>-calcination the optimum is reached much earlier than that by air-calcination, *i.e.*, Ce\*(40%)NaZSM-5 vs HCe(62%)ZSM-5. This means N<sub>2</sub>-calcined catalysts are economically preferable.

*n*-Heptane conversion over various rare earth containing zeolites, *e.g.*, CeHY,<sup>58,82</sup> LaHY,<sup>81</sup> PrNaY and PrHY,<sup>79</sup> and CeHZSM-20,<sup>80</sup> was reported before. However, products were mainly paraffinic. On the contrary, Tsuchiya<sup>91</sup> briefly reported enhancement of olefins formation from CeHY zeolite. A catalyst comprising cerium and an L zeolite was claimed in

the patent literature for *n*-hexane aromatization to C6-C8 aromatics.<sup>92</sup> Using CeZSM-5 and *n*-hexane in this work, olefins formation is possible.

Another important parameter is the degree of coke formation, Figure 4.14. This is calculated by dividing weight loss of a catalyst after regeneration, *i.e.* coke, by weight of a regenerated catalyst. The value is different from that mentioned previously, coke selectivity or coke yield, which is the tendency of a catalyst to convert *n*-hexane to coke. CeO<sub>2</sub> has the coke/catalyst ratio of 1.8 wt%. The ratios for N<sub>2</sub>-calcined Ce\*ZSM-5 and air-calcined CeZSM-5 lie in the range of, 3.0 to 9.4, and 0.2 to 4.9 wt%, respectively. HZSM-5 has the coke/catalyst ratio of 8.4 wt%. Almost all cerium-containing catalysts have higher coke resistance than HZSM-5 does. The amount of coke deposited on Ce\*(40%)NaZSM-5, however, is larger than that of HZSM-5. De la Puente *et al.*<sup>93</sup> found that the extent of hydrogen transfer, which ultimately led to coke formation, of RENaY catalysts (RE = La, Nd, Sm, Gd, and Dy), varied with the amount of Brønsted acid. This may be the reason why the amount of coke in Ce\*MZSM-5 is higher than that in CeMZSM-5, since the former has greater protons than the latter, Figure 4.10. Also the observation that coke deposition on HZSM-5 is the highest among all catalysts studied, with one exception on Ce\*(40%)NaZSM-5, can be explained by the same reason.

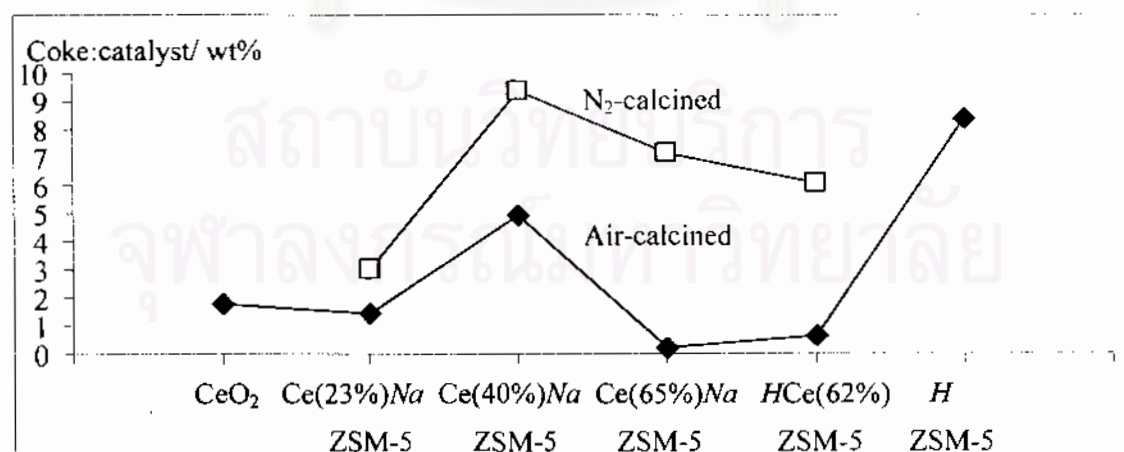


**Figure 4.14** Coke deposition over various catalysts studied.

## CHAPTER V

### CONCLUSIONS

The synthesis of ZSM-5 zeolite ( $\text{SiO}_2/\text{Al}_2\text{O}_3$  molar ratio of 40, or Si/Al of 20) was performed by the method developed in the laboratory using gel molar composition of  $1\text{SiO}_2: 0.36\text{Na}_2\text{O}: 0.025\text{Al}_2\text{O}_3: 0.10\text{TPABr}: 37.2\text{H}_2\text{O}$ . The gel was subsequently pH-adjusted to 10.5 using concentrated  $\text{H}_2\text{SO}_4$  and was crystallized at  $170^\circ\text{C}$  for 4 days. Product obtained is obtained as white solid having X-ray diffraction pattern characteristic of an MFI phase with orthorhombic symmetry. Different treatment, e.g., calcination, ammonium and cerium exchange, results in symmetry change to monoclinic, as observed by (1) shift in peak positions to lower  $2\theta$ ; (2) by a splitting of a peak at  $23.10^\circ 2\theta$ ; The synthesis is highly reproduced in term of either crystallinity of the obtained phase, or the chemical composition.

The calcined  $(\text{Na},\text{H})\text{ZSM-5}$  zeolite was converted into cerium-containing form by conventional ion exchange method, with the aim of introducing as high as possible cerium content into a zeolite. Two methods were compared, and the most effective one was that utilizing higher cerium concentration in the exchange solution, longer time, and more severe calcination conditions. Cerium-containing ZSM-5 having  $\text{H}^+$  as a counter ion was further prepared by  $\text{NH}_4^+$ -exchange of the resulting CeZSM-5, also with an intermediate calcination step. HZSM-5 was prepared similarly, but starting from  $(\text{Na},\text{H})\text{ZSM-5}$  instead of CeNaZSM-5.

The resulting materials were tested in *n*-hexane cracking at  $500^\circ\text{C}$ , GHSV of  $2000\text{ h}^{-1}$ , and time-on-steam of 30 min. Comparative studies were also performed with thermal reaction and commercial  $\text{CeO}_2$ . Pyrolysis of *n*-hexane hardly occurs at  $500^\circ\text{C}$ .  $\text{CeO}_2$  mainly



converts *n*-hexane to coke. *HZSM-5* gives high conversion, low coke yield, and acceptable selectivity to light olefins (ethylene, propylene, and butenes). Modification of *ZSM-5* typed zeolite by  $\text{Ce}^{3+}$  shows that activity of (*Na,H*)*ZSM-5* is greatly increased by cerium cations. Selectivity to olefins (35.0 to 53.9%) and methane (12.8 to 15.3%) are satisfactorily increased and decreased, respectively, by cerium-containing *ZSM-5*, better than *HZSM-5* (olefins, 23.0%; methane, 23.1%). Gas, liquid, and coke yields over cerium-containing *ZSM-5* are more or less similar to those over *HZSM-5*.

It is found that an anaerobic activation under  $\text{N}_2$  prevented cerium from forming dimers. Consequently cerium hydrolysis takes place with the simultaneous formation of active proton; this results in enhanced conversion by a factor of two. However, the enhancement is diminished at high cerium loading. Selectivity to olefins obtained from  $\text{N}_2$ -calcined  $\text{Ce}^*M\text{ZSM-5}$  ( $M = \text{Na}^+$  or  $\text{H}^+$ ) is lower than that obtained over the corresponding  $\text{Ce}M\text{ZSM-5}$  ( $M = \text{Na}^+$  or  $\text{H}^+$ ) catalysts calcined in air. Gas yield and liquid yield are generally (with one exception on  $\text{Ce}^*(40\%)\text{NaZSM-5}$ ) lower and higher, respectively, than those obtained over the corresponding samples calcined in air. Interestingly, *coke yield is greatly reduced* by  $\text{N}_2$ -activation.

Finally, improvement of olefins yields by cerium ion exchange is found promising. The highest olefins yield is achieved over  $\text{Ce}^*(40\%)\text{NaZSM-5}$ , followed by  $\text{HCe}(62\%)\text{ZSM-5}$ . These two catalysts provides higher yield than unmodified *HZSM-5*.

#### Suggestion for future work

1. Spectroscopic determination of  $\text{Ce}^{3+}/\text{Ce}^{4+}$  should be performed in order to understand the role of these species in catalytic cracking more clearly. Quantitative determination of proton concentration should be done as well by, for example, acidity titration or  $\text{NH}_3$ -TPD.

2. Ion exchange conditions, e.g., pH, solvent, atmosphere during ion exchange, should be varied. These parameters may affect cation hydrolysis inside a zeolite. Also, a study should include activation steps, e.g., temperature, time and type of gases ( $\text{H}_2$  or  $\text{H}_2\text{O}$  as examples).  $\text{Ce}^{4+}$  exchange should be carried out.

## REFERENCES

1. Olah, G. A. *Hydrocarbon Chemistry* New York: John Wiley & Sons, 1995, Chapter 1 to 3.
2. Kniel, L.; Winter, O.; Tsai, C. -H.; in *Ethylene*, Kirk-Othmer Encyclopedia of Chemical Technology, Vol. 9, Bushey, G. J.; Eastman, L. I.; Klingsberg, A.; Spiro, L., eds. New York: John Wiley & Sons, 1980.
3. Schoenberg, M. R.; Blieszner, J. W.; Papodolpoulos, C. G., in *Propylene*, Kirk-Othmer Encyclopedia of Chemical Technology, Vol. 19, Eastman, C. I.; Klingsberg, A.; Wachsman, G.; Wainwright, M., eds. New York: John Wiley & Sons, 1982.
4. Szostak, R. *Molecular Sieves: Principles of Synthesis and Identification* New York: Van Nostrand Reinhold, 1989.
5. Sugiyama, S.; Sogabe, K.; Miyamoto, T.; Hayashi, H.; Moffat, J. B. "Oxidative Dehydrogenation of Ethane on Rare Earth Oxides: Effects of Chlorine Additives in Gas and Solid Phase on the Oxidation over Cerium Oxide", *Catal. Lett.*, **1996**, *42*, 127-133.
6. Dai, H. X.; Ng, C. F.; Au, C. T. "SrCl<sub>2</sub>-Promoted REO<sub>x</sub> (RE = Ce, Pr, Tb) Catalysts for the Selective Oxidation of Ethane: A Study on Performance and Defect Structures for Ethene Formation", *J. Catal.*, **2001**, *199*, 177-192.
7. Sunter, J.; Ducarme, V.; Martin, G. A. "Influence of the Surface Area of Cerium Oxides on the Oxidative Dehydrogenation of Ethane", *Stud. Surf. Sci. Catal.*, **1994**, *81*, 125-130.

8. Zhang, W.; Zhou, X.; Tang, D.; Wan, H.; Tsai, K. "Oxidative Dehydrogenation of Propane over Fluorine Promoted Rare Earth-Based Catalysts", *Catal. Lett.*, **1994**, *23*, 103-106.
9. Jalowiecki-Duhamel, L.; Ponchel, A.; Lamonier, C.; D'Huysser, A.; Barbaux, Y. "Relationship between Structure of CeNi<sub>x</sub>O<sub>y</sub> Mixed Oxides and Catalytic Properties in Oxidative Dehydrogenation of Propane", *Langmuir*, **2001**, *17*, 1511-1517.
10. Boizumault-Moriceau, P.; Pennequin, A.; Grzybowska, B.; Barbaux, Y. "Oxidative Dehydrogenation of Propane on Ni-Ce-O Oxide: Effect of the Preparation Method, Effect of Potassium Addition and Physical Characterization", *Appl. Catal. A.*, **2003**, *245*, 55-67.
11. Moriceau, P.; Grzybowska, B.; Barbaux, Y.; Wrobel, G.; Hecquet, G. "Oxidative Dehydrogenation of Isobutane on Cr-Ce-O Oxide: I. Effect of the Preparation Method and of the Cr Content", *Appl. Catal. A*, **1998**, *168*, 269-277.
12. Garrido Pedrosa, A. M.; Souza, M. J. B.; Melo, D. M. A.; Araujo, A. S.; Zinner, L. B.; Fernandes, J. D. G.; Martinelli, A. E. "Systems Involving Cobalt and Cerium Oxides: Characterization and Catalytic Behavior in the C<sub>6</sub>-C<sub>7</sub> n-Alkanes Combustion", *Solid State Sci.*, **2003**, *5*, 725-728.
13. Araujo, A. S.; Aquino, J. M. F. B.; Souza, M. J. B.; Silva, A. O. S. "Synthesis, Characterization and Catalytic Application of Cerium-Modified MCM-41", *J. Solid State Chem.*, **2003**, *171*, 371-374.
14. Teschner, D.; Woosch, A.; Roder, T.; Matusek, K.; Paal, Z. "Ceria as a New Support of Nobel Metal Catalyst for Hydrocarbon Reactions: Chemisorption and Catalytic Studies", *Solid State Ionics*, **2001**, *141-142*, 709-713.
15. Trovarelli, A., ed. *Catalysis by Ceria and Related Materials* Singapore: Imperial College Press, 2002.
16. Trovarelli, A.; de Leitenburg, C.; Boaro, M.; Dolcetti, G. "The Utilization of Ceria in Industrial Catalysis", *Catal. Today*, **1999**, *50*, 353-367.

17. Cavani, F.; Trifiro, F. "The Oxidative Dehydrogenation of Ethane and Propane as an Alternative Way for the Production of Light Olefins", *Catal. Today*, **1995**, *24*, 307-313
18. Biswas, J.; Maxwell, I. E. "Recent Process- and Catalyst-Related Developments in Fluid Catalytic Cracking", *Appl. Catal.*, **1990**, *63*, 197-258.
19. Buchanan, J. S. "The Chemistry of Olefins Production by ZSM-5 Addition to Catalytic Cracking Units", *Catal. Today*, **2000**, *55*, 207-212.
20. Kissin, Y. V. "Chemical Mechanisms of Catalytic Cracking Over Solid Acidic Catalysts: Alkanes and Alkenes" *Catal. Rev.*, **2001**, *43*, 85-146.
21. Kotrel, S.; Knozinger, H.; Gates, B. C. "The Haag-Dessau Mechanism of Protolytic Cracking of Alkanes", *Microporous Mesoporous Mater.*, **2000**, *35-36*, 11-20.
22. Corma, A.; Orchilles, A. V. "Current Views on the Mechanism of Catalytic Cracking", *Microporous Mesoporous Mater.*, **2000**, *35-36*, 21-30.
23. Jentoft, F. C.; Gates, B. C. "Solid-Acid-Catalyzed Alkane Cracking Mechanisms: Evidence from Reactions of Small Probe Molecules", *Top. Catal.*, **1997**, *4*, 1-13.
24. Abbot, J.; Wojciechowski, B. W. "Catalytic Reactions of *n*-Hexane on HY Zeolite", *Can. J. Chem. Eng.*, **1988**, *66*, 825-830.
25. Poutsma, M. L.; Schafer, S. R. "Comparison of Thermal Cracking of the Isomeric Hexanes with That Catalyzed by Potassium Ion Exchanged Y Zeolite", *J. Phys. Chem.* **1973**, *77*, 158-166.
26. Rhodes, N. P.; Rudham, R.; Stanbridge, N. H. J. "Catalytic Studies with Dealuminated Y Zeolites. Part 3. *n*-Hexane Cracking", *J. Chem. Soc., Faraday Trans.*, **1996**, *92*, 2817-2823.
27. Anderson, M. W.; Klinowski, J.; Thomas, J. M.; Barlow, M. T. "Zeolites Treated with Silicon Tetrachloride Vapour. Part 5. Catalytic Cracking of *n*-Hexane", *J. Chem. Soc., Faraday Trans I*, **1989**, *85*, 1945-1962.
28. Bassir, M.; Wojciechowski, B. W. "The Protolysis of Hexanes over a USYH Zeolite", *J. Catal.*, **1994**, *150*, 1-8.

29. Abbot, J. "Cracking Reactions of C<sub>6</sub> Paraffins on HZSM-5", *Appl. Catal.*, **1990**, *57*, 105-125.
30. Santilli, D. S. "Mechanism of Hexane Cracking in ZSM-5", *Appl. Catal.*, **1990**, *60*, 137-141.
31. Nowak, A. K.; Wilson, A. E.; Roberts, K.; Datema, K. P. "Hexane Cracking in ZSM-5: *In Situ* <sup>13</sup>C Cross-Polarization Magic-Angle-Spinning NMR and Flow Reactor/ GC Experiments", *J. Catal.*, **1993**, *144*, 495-505.
32. Antia, J. E.; Tsrani, K.; Govind, R. "*n*-Hexane Cracking on Binderless Zeolite HZSM-5 Coated Monolithic Reactors", *Appl. Catal. A*, **1997**, *159*, 89-99.
33. Marchado, F. J.; Lopez, C. M.; Centeno, M. A.; Urbina, C. "Template-Free Synthesis and Catalytic Behaviour of Aluminium-Rich MFI-Type Zeolites", *Appl. Catal. A*, **1999**, *181*, 29-38.
34. Halik, C.; Chaudhuri, S. N.; Lercher, J. A. "Catalytic Activity of SAPO5 for Cracking of Butane and Hexane", *J. Chem. Soc., Faraday Trans I*, **1989**, *85*, 3879-3890.
35. Meusinger, J.; Vinek, H.; Lercher, J. A. "Cracking of *n*-Hexane and *n*-Butane Over SAPO5, MgAPO5 and CoAPO5", *J. Mol. Catal.*, **1994**, *87*, 263-274.
36. Jalil, P. A.; Al-Daous, M. A.; Al-Arfaj, A. -R. A.; Al-Amer, A. M.; Beltramini, J.; Barri, S. A. I. "Characterization of Tungstophosphoric Acid Supported on MCM-41 Mesoporous Silica Using *n*-Hexane Cracking, Benzene Adsorption, and X-ray Diffraction", *Appl. Catal. A*, **2001**, *207*, 159-171.
37. Farcasiu, D.; Lee, K. -H. "Isomerization of Hexane by Zeolite HZSM-5. The Effect of Cyclic Hydrocarbons", *J. Mol. Catal. A*, **2000**, *161*, 213-221.
38. Farcasiu, D.; Lee, K. -H. "The Liquid-Phase Reaction of Hexane on Acid Mordenite", *Catal. Commun.*, **2001**, *2*, 5-9.
39. Bhattacharya, D.; Sivasanker, S. "Aromatization of *n*-Hexane over H-ZSM-5: Influence of Promoters and Added Gases", *Appl. Catal. A*, **1996**, *141*, 105-115.
40. Borade, R. B.; Hegde, S. G.; Kulkarni, S. B.; Ratnasamy, P. "Active Centres over HZSM5 Zeolites for Paraffin Cracking", *Appl. Catal.*, **1984**, *13*, 27-38.

41. Wang, L.; Xie, M.; Tao, L. "Conversion of Light Paraffins for Preparing Small Olefins over ZSM-5 Zeolites", *Catal. Lett.*, **1994**, *28*, 61-68.
42. Talukdar, A. K.; Bhattacharyya, K. G.; Baba, T.; Ono, Y. "1-Hexene Isomerization and *n*-Hexane Cracking over HMCM-22", *Appl. Catal. A*, **2001**, *213*, 239-245.
43. Rombi, E.; Cutrufello, M. G.; Solinas, V.; De Rossi, S.; Ferraris, G.; Pistone, A. "Effects of Potassium Addition on the Acidity and Reducibility of Chromia/Alumina Dehydrogenation Catalysts", *Appl. Catal. A*, **2003**, *251*, 255-266.
44. Chang, Y., -F.; Somorjai, G. A.; Heinemann, H. "Oxydehydrogenation of Ethane over ZSM-5 Zeolite Catalyst. Effect of Steam", *Appl. Catal. A*, **1993**, *96*, 305-318.
45. Bulanek, R.; Novoveska, K.; Wichterlova, B. "Oxidative Dehydrogenation and Ammoxidation of Ethane and Propane over Pentasil Ring Co-Zeolites", *Appl. Catal. A*, **2002**, *235*, 181-191.
46. Katranas, T. K.; Vlessidis, A. G.; Tsiatouras, V. A.; Triantafylidis, K. S.; Evmirdis, N. P. "Dehydrogenation of Propane over Natural Clinoptilolite Zeolites", *Microporous Mesoporous Mater.*, **2003**, *61*, 189-198.
47. Argauer, R. J.; Landolt, G. R. "Crystalline Zeolite ZSM-5 and Method of Preparing the Same", *United States Patent*, **1972**, 3 702 886.
48. Dyer, A. *An Introduction to Zeolite Molecular Sieves*, John Wiley & Sons, Chichester, 1988.
49. Olson, D. H.; Kokotailo, G. T.; Lawton, S. L.; Meier, W. M. "Crystal Structure and Structure-Related Properties of ZSM-5", *J. Phys. Chem.*, **1981**, *85*, 2238-2243.
50. Kumar, R.; Mukherjee, P.; Pandey, R. K.; Rajmohanan, P.; Bhaumik, A. "Role of Oxyanions as Promoter for Enhancing Nucleation and Crystallization in the Synthesis of MFI-type Microporous Materials", *Microporous Mesoporous Mater.*, **1998**, *22*, 23-31.

51. Maluangnont, T.; Chaisuwan, A. "Maximizing Cerium Content in Cerium Exchanged ZSM-5" Abstracts: 29<sup>th</sup> Congress on Science and Technology of Thailand, Golden Jubilee Convention Hall, Khon Kaen University, Thailand, 20-22 October 2003, SC-229P, p.147. (Poster presentation).
52. Szostak, R.; Thomas, T. L. "Preparation of Ferrisilicate ZSM-5 Molecular Sieves", *J. Catal.*, **1986**, *100*, 555-557.
53. Ahmed, S.; El-Faer, M. Z.; Abdillahi, M. M.; Siddiqui, M. A. B.; Barri, A. I. "Investigation of the Rapid Crystallization for the Synthesis of MFI-Type Zeolites and Study of the Physicochemical Properties of the Products", *Zeolites*, **1996**, *17*, 373-380.
54. Van Grieken, R.; Sotelo, J. L.; Menendez, J. M.; Melero, J. A. "Anomalous Crystallization Mechanism in the Synthesis of Nanocrystalline ZSM-5", *Microporous Mesoporous Mater*, **2000**, *39*, 135-147.
55. Berry, F. J.; Marco, J. F.; Steel, A. T. "An Investigation by EXAFS of the Thermal Dehydration and Rehydration of Cerium- and Erbium-Exchanged Y Zeolite", *J. Alloys Comp.*, **1993**, *194*, 167-172.
56. Ciavatta, L.; Porto, R.; Vasca, E. "The Hydrolysis of the Cerium(III) Ion,  $Ce^{3+}$ , in Aqueous Perchlorate Solutions at 50°C", *Polyhedron*, **1988**, *7*, 1355-1361.
57. Christner, L. G.; Liengme, B. V.; Hall, W. K. "Studies of the Hydrogen Held by Solids. Part 15.-Cation Exchanged Zeolites", *Trans. Faraday Soc.*, **1968**, *64*, 1679-1692.
58. Lemos, F.; Ribeiro, F. R.; Kern, M.; Giannetto, G.; Guisnet, M. "Influence of the Cerium Content of CeHY Catalysts in Their Physicochemical and Catalytic Properties", *Appl. Catal.*, **1987**, *29*, 43-54.
59. Tempere, J. F.; Bozon-Verduraz, F.; Delafosse, D. "A Kinetic Study of the Oxidation of Cerium Ions in an X Zeolite", *Mater. Res. Bull.*, **1977**, *12*, 871-879.
60. Konya, Z.; Sugi, Y.; Kiricsi, I. "IR Spectroscopic Studies on the Surface Chemistry of Mordemites Modified by Ceria", *J. Mol. Struct.*, **2001**, *563-564*, 413-416.

61. Weyrich, P. A.; Holderich, W. F. "Dehydrogenation of  $\alpha$ -Limonene over Ce Promoted, Zeolite Supported Pd Catalysts", *Appl. Catal. A*, **1997**, *158*, 145-162.
62. Ito, E.; Hultermans, R. J.; Lugt, P. M.; Burgers, M. H. W.; van Bekkum, H.; van den Bleek, C. M. "Selective Reduction of  $\text{NO}_x$  with Ammonia over Cerium Exchanged Zeolite Catalysts: Toward a Solution for an Ammonia Slip Problem", *Stud. Surf. Sci. Catal.*, **1995**, *96*, 661-673.
63. Cheetham, A. K.; Eddy, M. M.; Thomas, J. M. "The Direct Observation of Cation Hydrolysis in Lanthanum Zeolite-Y by Neutron Diffraction", *J. Chem. Soc., Chem. Commun.*, **1984**, 1337-1338.
64. Li, Z.; Flytzani-Stephanopoulos, M. "On the Promotion of Ag-ZSM-5 by Cerium for the SCR of NO by Methane", *J. Catal.*, **1999**, *182*, 313-327.
65. Dyer, A.; Shesheniah, M.; Brown, J. G. "Some studies on Cerium Exchanged Synthetic Faujesites", *J. Inorg. Nucl. Chem.*, **1978**, *40*, 99-101.
66. Tempere, J. F.; Delafosse, D.; Contour, J. P. "An X-ray Photoelectron Spectroscopy Study on Zeolites", *Chem. Phys. Lett.*, **1975**, *33*, 95-98.
67. Hong, S. B. "Double 6-Ring as a Unique Site for the  $\text{Ce}^{3+}/\text{Ce}^{4+}$  Redox Couple in Zeolites", *J. Phys. Chem. B*, **2001**, *105*, 11961-11963
68. Zhang, Y.; Flytzani-Stephanopoulos, M. "Hydrothermal Stability of Cerium Modified Cu-ZSM-5 Catalyst for Nitric Oxide Decomposition", *J. Catal.*, **1996**, *164*, 131-145.
69. van Kooten, W. E. J.; Liang, B.; Krijnsen, H. C.; Oudshoorn, O. L.; Calis, H. P. A.; van den Bleek, C. M. "Ce-ZSM-5 Catalysts for the Selective Catalytic Reduction of  $\text{NO}_x$  in Stationary Diesel Exhaust Gas", *Appl. Catal. B*, **1999**, *21*, 203-213.
70. Weyrich, P. A.; Trevino, H.; Holderich, W. F.; Sachtler, W. M. H. "Characterization of Ce Promoted, Zeolite Supported Pd Catalysts", *Appl. Catal. A*, **1997**, *163*, 31-44.
71. Williams, B. A.; Babitz, S. M.; Miller, J. T.; Snurr, R. Q.; Kung, H. H. "The Roles of Acid Strength and Pore Diffusion in the Enhanced Cracking Activity of Steamed Y Zeolites", *Appl. Catal. A*, **1999**, *171*, 161-175.



72. Wu, E. L.; Lawton, S. L.; Olson, D. H.; Rohrman, A. Q., Jr.; Kokotallo, G. T. "ZSM-5-Type Materials. Factor Affecting Crystal Symmetry", *J. Phys. Chem.*, **1979**, *83*, 2777-2781.
73. Occelli, M. L.; Ritz, P. "The Effects of Na Ions on the Properties of Calcined Rare-Earths Y (CREY) Zeolites", *Appl. Catal. A*, **1999**, *183*, 53-59.
74. Velu, S.; Ma, X.; Song, C. "Selective Adsorption for Removing Sulfur from Jet Fuel over Zeolite-Based Adsorbents", *Ind. Eng. Chem. Res.*, **2003**, *42*, 5293-5304.
75. Yokoyama, C.; Misono, M. "Catalytic Reduction of Nitrogen Monoxide by Propene in the Presence of Oxygen over Cerium Ion-Exchanged Zeolites. I. General Characteristics of the Reaction and Effects of Alkaline Earth Metal Addition", *Bull. Chem. Soc. Jpn.*, **1994**, *67*, 557-562.
76. Greensfelder, B. S.; Voge, H. H.; Good, G. M. "Catalytic and Thermal Cracking of Pure Hydrocarbons. Mechanism of Reaction", *Ind. Eng. Chem.*, **1949**, *41*, 2573-2584.
77. Baba, T.; Inoue, Y.; Ono, Y. "Long-Range Interaction of Alkali Cations with the Acidic OH Groups in H-ZSM-5", *J. Catal.*, **1996**, *159*, 230-235.
78. Nicolaidis, C. P.; Wapiennik, M.; Weiss, K. I. G.; van den Akker, H.; van Zalk, B.; Wieleard, P. "Alkali Metal Cation Exchange of HZSM-5 and the Catalytic Properties of the Alkalized Zeolites", *Appl. Catal.*, **1991**, *68*, 31-39.
79. Lemos, F.; Lopes, J. M.; Ramoa Ribeiro, F. "Influence of Cation Content on the Catalytic Properties of PrHNaY Zeolites in the Cracking of *n*-Heptane", *J. Mol. Catal.*, **1989**, *53*, 265-273.
80. Lemos, F.; Lopes, J. M.; Ramoa Ribeiro, F.; Derouane, E. "Influence of Cerium on the Catalytic Properties of ZSM-20 Zeolites in the Cracking of *n*-Heptane: Comparison with Rare Earth Y Zeolites", *Appl. Catal.*, **1989**, *49*, 175-181.
81. Tynjälä, P.; Pakkanen, T. T. "Acidic Properties of ZSM-5 Zeolite Modified with Ba<sup>2+</sup>, Al<sup>3+</sup> and La<sup>3+</sup> Ion-Exchange", *J. Mol. Catal. A*, **1996**, *110*, 153-161.

82. Lemos, F.; Ramoa Ribeiro, F.; Kern, M.; Giannetto, G.; Guisnet, M. "Influence of Lanthanum Content of LaHY Catalysts on their Physico-Chemical and Catalytic Properties. Comparison with CeHY Catalysts", *Appl. Catal.*, **1988**, *39*, 227-238.
83. Kanada, A.; Idaka, N.; Nishiyama, S.; Tsuruya, S.; Masai, M. "Oxidation Activity of Cerium Supported on NaZSM-5 Zeolites with and without Added Alkali Metals in the Gas-Phase Catalytic Oxidation of Benzyl Alcohol", *Phys. Chem. Chem. Phys.*, **1999**, *1*, 373-381.
84. Idaka, N.; Nishiyama, S.; Tsuruya, S. "Role of Potassium Added to Ce/NaZSM-5 Catalyst in Partial Oxidation Activity of Benzyl Alcohol", *Phys. Chem. Chem. Phys.*, **2001**, *3*, 1918-1924.
85. Yang, G.; Wang, Y.; Zhou, D.; Zhuang, J.; Liu, X.; Han, X.; Bao, X. "On Configuration of Exchanged La<sup>3+</sup> on ZSM-5: A Theoretical Approach to the Improvement in Hydrothermal Stability of La-Modified ZSM-5 Zeolite", *J. Chem. Phys.*, **2003**, *119*, 9765-9770
86. Lukyanov, D. B.; Shtral, V. I.; Khadzhiev, S. N. "A Kinetic Model for the Hexane Cracking Reaction over H-ZSM-5", *J. Catal.*, **1994**, *146*, 87-92.
87. Narbeshuber, T. F.; Vinek, H.; Lercher, J. A. "Monomolecular Conversion of Light Alkane over H-ZSM-5", *J. Catal.*, **1995**, *157*, 388-395.
88. Nayak, V. S.; Moffat, J. B. "Catalytic Activity and Product Distribution in the Cracking of *n*-Hexane over Heteropoly Oxometallates and ZSM-5 Zeolite", *Appl. Catal.*, **1989**, *47*, 97-113.
89. Bhattacharya, D.; Tambe, S. S.; Sivasanker, S. "The Influence of Reaction Temperature on the Cracking Mechanism of *n*-Hexane over H-ZSM-48", *Appl. Catal. A*, **1997**, *154*, 139-153.
90. Reyniers, M. -F.; Beirnaert, H.; Marin, G. B. "Influence of Coke Formation on the Conversion of Hydrocarbons. I. Alkanes on a USY-Zeolite", *Appl. Catal. A.*, **2000**, *202*, 49-63.

91. Tsuchiya, S. "Acid-Base Properties of Some Zeolites and Their Activity in the Decomposition of *n*-Hexane", *Stud. Surf. Sci. Catal.*, **1995**, *100*, 535-542.
92. Wu, A. -H.; Drake, C. A. "Hydrocarbon Conversion with Dual Metal Promoted Zeolite". *United States Patent*, **2000**, 6 017 442.
93. De la Puente, G.; Souza-Aguiar, E. F.; Zotin, F. M. Z.; Camorim, V. L. D.; Sedran, U. "Influence of Different Rare Earth Ions on Hydrogen Transfer Over Y Zeolite", *Appl. Catal. A.*, **2000**, *197*, 41-46.



สถาบันวิทยบริการ  
จุฬาลงกรณ์มหาวิทยาลัย



**APPENDICES**

สถาบันวิทยบริการ  
จุฬาลงกรณ์มหาวิทยาลัย

## Appendix

### 1 ZSM-5 Synthesis

An example of calculation for ZSM-5 synthesis is shown in Table A-1.

**Table A-1.** Amounts of chemicals used in ZSM-5 synthesis.

Reactants	FW	Wt (g)	Wt%			Mole				
			SiO <sub>2</sub>	H <sub>2</sub> O	Na <sub>2</sub> O	Al <sub>2</sub> O <sub>3</sub>	SiO <sub>2</sub>	TPABr	H <sub>2</sub> O	Na <sub>2</sub> O
FW						101.96	60.08	266.18	18	62
NaAlO <sub>2</sub>	81.97	0.7868				0.0048				0.0048
Water glass		38.79	29.71	59.8	10.13		0.1918		1.289	0.0634
TPABr	266.18	5.11						0.01919		
H <sub>2</sub> O	18	105.26							5.85	
Sum		149.94				0.0048	0.1918	0.01919	7.136	0.0682
Reactant molar ratio						0.025	1.0	0.10	37.2	0.36

$$\begin{aligned} \text{\%Yield based on Si} &= (\text{wt. obtained zeolite} / \text{wt. Si in the gel}) \times 100\% \dots (\text{A-1}) \\ &= (11.09 / (38.79 \times 0.2971)) \times 100\% \\ &= 96\% \end{aligned}$$

$$\text{Molar ratio of TPA}^+ / (\text{TPA}^+ + \text{Na}^+) = (0.01919) / (0.01919 + (2 \times 0.0682)) = 0.12$$

Hydroxide concentration is calculated by summing up moles of OH<sup>-</sup> generated from Na<sup>+</sup>, and subtracting with moles of added acid, *i.e.*, Al<sub>2</sub>O<sub>3</sub>, which is considered to be equivalent to 2 moles of hydronium ions H<sub>3</sub>O<sup>+</sup>.

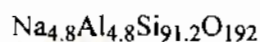
$$\text{Mol of OH}^- = (2 \times 0.0682) - (2 \times 0.0048) = 0.1268$$

$$\text{Molar ratio of OH}^- / \text{SiO}_2 = 0.1268 / 0.1918 = 0.66$$

$$\text{Molar ratio of H}_2\text{O} / \text{OH}^- = 7.136 / 0.1268 = 56.28$$

## 2 Ion Exchange Stoichiometry

For ZSM-5 zeolite (Si/Al=20) with the empirical formula of  $\text{Na}_n\text{Al}_n\text{Si}_{96-n}\text{O}_{192} \cdot 16\text{H}_2\text{O}$ ,  $(96-n)/n = 20$ , or  $n = 4.8$ . The dehydrated composition of



with formula weight of 5873.66 is obtained. An amount of 4.01 g of *NaZSM-5* will contain  $(4.8 \times 4.01)/5873.66 = 3.27 \times 10^{-3}$  mol of  $\text{Na}^+$ . If the exchange stoichiometry  $\text{Ce}^{3+}/\text{Na}^+$  molar ratio is kept constant at 0.9 (method L),

$$\text{Wt. Ce}(\text{NO}_3)_3 \cdot 6\text{H}_2\text{O} = 0.9 \times 3.21 \times 10^{-3} \times 434.23 = 1.27 \text{ g}$$

Calculation of method H can be performed similarly by substituting  $\text{Ce}^{3+}/\text{Na}^+$  molar ratio with 5.0. For ammonium ion exchange,  $\text{NH}_4^+/\text{Na}^+$  molar ratio with 50.0, and formula weight of 53.49 are used instead. All calculations in this work base on *parent NaZSM-5*.

สถาบันวิทยบริการ  
จุฬาลงกรณ์มหาวิทยาลัย

### 3 Tests for Nitrates and Chlorides \*

Nitrates were tested by brown ring method. A portion of 3 mL of freshly prepared saturated solution of  $\text{FeSO}_4$  was added into 2 mL of tested solution. Concentrated  $\text{H}_2\text{SO}_4$  of 3-5 mL was slowly poured down the side of the test tube so that the acid forms a layer beneath the mixture. A brown ring, the  $[\text{Fe}(\text{NO})]^{2+}$ , will form at the interface of the liquid layers.

Chlorides were tested by adding a few drops of  $\text{AgNO}_3$  solution into the tested solution.  $\text{AgCl}$  precipitates were formed.

All tests were compared to blank, deionized water, used in washing.



สถาบันวิทยบริการ  
จุฬาลงกรณ์มหาวิทยาลัย

\*From Svehla, G., *Vogel's Qualitative Inorganic Analysis*, Longman Singapore Publishers, Singapore, 1995.

## 4 Calculation on Catalysis

### 4.1 Vapor Pressure of *n*-Hexane\*

$$\log P = A - \{B/(t + C)\} \dots \dots \dots (A-2)$$

where P is vapor pressure, A, B, and C are constants. For *n*-hexane, A is 6.87776, B is 1171.530, and C is 224.366. Substituting these values into Equation (A-1) and also substituting temperature to 30°C gives,

$$P = 187 \text{ mmHg} \times (1 \text{ atm} / 760 \text{ mmHg}) = 0.246 \text{ atm}$$

Thus, at the atmospheric pressure of 1 atm and the temperature of 30°C, the *n*-hexane partial pressure of 0.25 atm generates the mixture of 24.6% *n*-hexane and the balancing gas.

\*From Dean, J. A., ed., *Lange's Handbook of Chemistry*, McGraw-Hill, New York, 1967.

### 4.2 Feed Flow Rate

The amount of catalyst used was 0.1000 g. Packed catalyst was loaded into a borosilicate tube reactor which has the radius of 0.27 cm. The average height of catalyst bed was 0.8 cm. Required gas hourly space velocity (GHSV) was 2000 h<sup>-1</sup> at STP.

$$\begin{aligned} \text{Volumetric flow rate (STP)} &= \text{GHSV} \times \text{Volume of catalyst} \dots \dots \dots (A-3) \\ &= 2000 \times \pi \times (0.27)^2 \times 0.8 \quad \text{mL/h} \\ &= 2000 \times \pi \times (0.27)^2 \times (0.8/60) = 6.11 \quad \text{mL/min} \end{aligned}$$

$$\begin{aligned} \text{Volumetric flow rate at } T \text{ (}^\circ\text{C)} &= \text{Volumetric flow rate (STP)} \times \{(273.15 + T)/273.15\} \\ &\dots \dots \dots (A-4) \end{aligned}$$



For example, at 30°C,

$$\text{Volumetric flow rate} = \frac{6.11 \times (273.15 + 30)}{273.15} = 6.78 \text{ mL/min, or } 8.84 \text{ s/mL}$$

#### 4.3 Weight of Reactant Feed

From the ideal gas equation,

$$PV = nRT \dots \dots \dots (A-5)$$

where  $P$  is partial pressure of  $n$ -hexane (atm),  $V$  is the volume of gas (L),  $n$  is the numbers of mole of  $n$ -hexane,  $R$  is a universal gas constant ( $0.082 \text{ atm} \cdot \text{L} \cdot \text{mol}^{-1} \cdot \text{K}^{-1}$ ), and  $T$  is the temperature at  $n$ -hexane reservoir (K).

At the reaction condition,  $P = 0.25 \text{ atm}$ ;  $V = 6.78 \times 10^{-3} \text{ L/min} \times 60 \text{ min} = 0.407 \text{ L}$ ;  $T = 303.15 \text{ K}$  (30°C), therefore,

$$n = \frac{PV}{RT}$$

$$n = \frac{0.25 \times 0.407}{0.082 \times 303.15}$$

Thus, mol of  $n$ -hexane = 0.00409 mol, or 0.3517 g.

#### 4.4 Calculation of Liquid, Coke, and Gas Yield

Percentage yield of liquid is determined by equation (A-6). An amount of coke is determined, after regeneration by air calcination as shown in Figure 3.3(d), by equation (A-7). Coke yield (per  $n$ -hexane converted) and coke deposition (per weight of a catalyst) are therefore calculated as shown in equations (A-8) and (A-9).

$$\% \text{ yield of liquid product} = \frac{\text{Wt. liquid product}}{\text{Wt. } n\text{-hexane converted}} \times 100\% \dots\dots(A-6)$$

$$\text{Wt. coke} = \text{Wt. used catalyst} - \text{Wt. regenerated catalyst} \dots\dots(A-7)$$

$$\text{Coke yield \%} = (\text{Wt. coke} / \text{Wt. } n\text{-hexane converted}) \times 100\% \dots\dots(A-8)$$

$$\text{Coke deposition \%} = (\text{Wt. coke} / \text{Wt. regenerated catalyst}) \times 100\% \dots\dots(A-9)$$

Yield of gas product can then be calculated as,

$$\% \text{ yield of gas product} = 100 - (\% \text{ yield liquid} + \% \text{ yield coke}) \dots\dots(A-10)$$

#### 4.7. Percentage Conversion of n-Hexane

Using peak areas obtained from GC analysis,

$$\% \text{ Conversion} = \frac{A_{\text{in}} - A_{\text{out}}}{A_{\text{in}}} \times 100\% \dots\dots(A-11)$$

Where  $A_{\text{in}}$  = Peak area of 1-hexene at the inlet of the catalyst reactor

$A_{\text{out}}$  = Peak area of 1-hexene at the outlet of the catalyst reactor

#### 4.8 Calculation of Percentage Selectivity to Gas Product

$$C_x = \frac{A_x \times C_{\text{std}} \times V_{\text{std}}}{A_{\text{std}} \times V_x} \dots\dots(A-12)$$

$$\% \text{ selectivity} = \frac{C_x \times 100}{C_{\text{total}}} \dots\dots(A-13)$$

When  $C_{\text{std}}$  = Concentration of the component of interest in the standard mixture  
(%mol)

$C_x$  = Concentration of the component in the sample (% mol)

$C_{total}$  = Concentration of the total component in the sample (% mol)

$A_{std}$  = Peak area of the component in standard mixture (a.u.)

$A_x$  = Peak area of the component in the sample (a.u.)

$V_{std}$  = Injected volume of the standard mixture ( $\mu\text{L}$ )

$V_x$  = Injected Volume of the sample ( $\mu\text{L}$ )



สถาบันวิทยบริการ  
จุฬาลงกรณ์มหาวิทยาลัย

## VITAE

Mr. Tosapol Maluangnont was born on December 29, 1979 in Bangkok, Thailand. He received a Bachelor Degree of Science in Chemistry from Chulalongkorn University in 2001. Since then, he has been a graduate student studying Inorganic Chemistry in the Faculty of Science, Chulalongkorn University. During his graduate studies towards the Master's degree, he also received a teaching assistantship from Department of Chemistry, the Faculty of Science in 2002, a research assistantship by the Materials Chemistry and Catalysis Research Unit, Department of Chemistry, in 2003, and a research grant from the Graduate School, Chulalongkorn University.



สถาบันวิทยบริการ  
จุฬาลงกรณ์มหาวิทยาลัย